

Distribution Agreement

In presenting this thesis or dissertation as a partial fulfillment of the requirements for an advanced degree from Emory University, I hereby grant to Emory University and its agents the non-exclusive license to archive, make accessible, and display my thesis or dissertation in whole or in part in all forms of media, now or hereafter known, including display on the world wide web. I understand that I may select some access restrictions as part of the online submission of this thesis or dissertation. I retain all ownership rights to the copyright of this thesis or dissertation. I also retain the right to use in future works (such as articles or books) all or part of this thesis or dissertation.

Signature:

Patricia Campbell

Date

Role of the M Segment in Influenza A Virus Transmission

By

Patricia Campbell
Doctor of Philosophy

Graduate Division of Biological and Biomedical Sciences
Microbiology and Molecular Genetics

John Steel, Ph.D.
Advisor

Eric Hunter, Ph.D.
Committee Member

Jackie Katz, Ph.D.
Committee Member

Anice Lowen, Ph.D.
Committee Member

Dave Steinhauer, Ph.D.
Committee Member

Elizabeth Wright, Ph.D.
Committee Member

Accepted:

Lisa A. Tedesco, Ph.D.
Dean of the James T. Laney School of Graduate Studies

Date

Role of the M Segment in Influenza A Virus Transmission

By

Patricia Campbell
B.S., University of Tennessee, 2003
M.S., Northern Arizona University, 2007

Advisor: John Steel, Ph.D.

An abstract of
a dissertation submitted to the Faculty of the
James T. Laney School of Graduate Studies of Emory University
in partial fulfillment of the requirements for the degree of
Doctor of Philosophy
in Microbiology and Molecular Genetics
2015

ABSTRACT

Role of the M Segment in Influenza A Virus Transmission

By Patricia Campbell

Influenza pandemics are caused by the emergence of antigenically distinct and highly transmissible influenza viruses within human populations. These viruses result from reassortment within an animal reservoir and likely adapt to productively transmit between humans. Recent studies suggested that the M segment contributes to the transmissibility of the 2009 pandemic H1N1 influenza virus [pH1N1], although the underlying mechanism(s) remain unknown. In addition, a balance between hemagglutinin (HA) receptor binding and neuraminidase (NA) receptor destroying activities was found to be important for pH1N1 transmission. The M segment encodes the matrix protein (M1) and the proton channel. M1 is a major determinant of virus morphology and interacts with the NA and HA glycoproteins. We hypothesized that the M segment could impact virus transmission by altering virus morphology and NA/HA balance. Using the guinea pig model, we demonstrated that introduction of the pH1N1 A/Netherlands/602/2009 (H1N1) [NL602] M segment into an otherwise non-transmissible A/Puerto Rico/8/34 (H1N1) [PR8] background significantly increased virus contact transmission, and when combined with its cognate HA+NA, recapitulated the high transmission efficiency of the wild-type pH1N1 strain. Evaluation of the morphology and NA activity of these reassortant viruses revealed a correlation between filamentous morphology, as well as NA activity, and transmission. In addition, a naturally-occurring M1 polymorphism (A41P), in the Eurasian avian-like swine [EAsw] strain, A/swine/Spain/53207/2004(H1N1) [SPN04], impacted replication and transmission of wild type SPN04- and PR8-based reassortant viruses, although no clear correlation with morphology or NA activity was established. Lastly, since the pH1N1 M segment originated within the EAsw lineage, and EAsw viruses do not readily transmit between humans, we hypothesized that pH1N1 M segment residues not present in the EAsw M segment would impact virus transmission. We demonstrated that PR8-based viruses harboring an EAsw M segment, or the NL602 M segment containing an EAsw M1 protein, did not replicate or transmit as well as the PR8/NL602 M virus, and transmission correlated with a filamentous morphology. Furthermore, all three residues that differed between the pH1N1 and EAsw M1 proteins individually decreased transmission of the PR8/NL602 M virus, although only one (N207S) was significant. Taken together, these results demonstrate that residues within the matrix protein can impact transmission of influenza A viruses and may concurrently alter virus morphology and NA activity, although neither is sufficient nor necessary for transmission.

Role of the M Segment in Influenza A Virus Transmission

By

Patricia Campbell
B.S., University of Tennessee, 2003
M.S., Northern Arizona University, 2007

Advisor: John Steel, Ph.D.

A dissertation submitted to the Faculty of the
James T. Laney School of Graduate Studies of Emory University
in partial fulfillment of the requirements for the degree of
Doctor of Philosophy
in Microbiology and Molecular Genetics
2015

ACKNOWLEDGEMENTS

This work could not have been completed without the support and participation of many individuals. In particular, I would like to thank my advisor, Dr. John Steel, for his guidance, willingness to let me learn through experience, and constant encouragement to rigorously solve any problem. I am a better scientist and researcher for having had him as a mentor. In addition, my PhD committee has my everlasting thanks for their continuous support, feedback, and expert advice that guided both my research and development. It was an honor and a pleasure to work with each of them. A particularly large thanks to Dr. Liz Wright and the EM Core staff, especially Hong Yi, for their above-and-beyond assistance with everything electron microscopy and for serving as my lab home away from home.

In addition to all of the professional contributions to this work, my friends and family served as constant pillars of support and encouragement. First, I'd like to thank my parents, who always emphatically told me that I could achieve any goal in life with enough hard work and enthusiasm – I count that message as one of the best gifts that I have received. My brothers, Tom and Geoff, have always championed me and remain two of my favorite people in the world. I have also had the pleasure of gaining a great friend in Shamika Danzy, whose work helped to produce the data contained herein, and whose daily conversations kept life fun and served as an unwavering source of light. Thank you also to Nicolle Marshall, who besides being the best work wife that anyone could ask for, traveled the world, shared countless therapeutic glasses of wine, and graciously shared a brain with me throughout my

time at Emory. Also, a huge thank you to my lifelong friend, Carter, who has been by my side through thick and thin, never once wavering in her support, and gave me the best godson in the world.

Last, but certainly not least, all of the thanks in the world to my husband, Bob, who endured the constant sacrifices and demands of graduate school with grace and never lost sight of the end goal. His patience, faith, and positive attitude were indispensable throughout this endeavor and will never be forgotten. After nine years together, I am pleased to say that he is still my best friend and I certainly would not be where I am today without his love and support.

TABLE OF CONTENTS

Abstract

Acknowledgements

Table of Contents

List of Figures and Tables

Introduction

Influenza Virus Classification and Host Range.....	1
Influenza A Virus Life Cycle.....	2
Influenza A Virus Matrix Protein.....	5
Influenza A Virus: Human Disease and Pandemics.....	7
History of North American and European Swine Influenza.....	10
Influenza A Virus Structure and Morphology.....	15
Influenza A Virus Transmission and Host Adaptation.....	19

Chapter 1: The M Segment of the 2009 Pandemic Influenza Virus Confers

Increased Neuraminidase Activity, Filamentous Morphology, and Efficient

Contact Transmissibility to A/Puerto Rico/8/1934-Based Reassortant Viruses

Abstract.....	28
Importance.....	29
Introduction.....	29
Materials and Methods.....	33
Results.....	38
Discussion.....	51

References.....	57
-----------------	----

Chapter 2: Residue 41 of the Eurasian avian-like swine influenza A virus matrix protein modulates virion filament length and efficiency of contact transmission

Abstract.....	69
Importance.....	70
Introduction.....	70
Materials and Methods.....	72
Results.....	77
Discussion.....	89
References.....	95

Chapter 3: Reassortant viruses harboring the 2009 pandemic influenza virus matrix protein have replication and transmission advantages over those containing a matrix protein from the pandemic precursor Eurasian avian-like swine lineage

Abstract.....	103
Introduction.....	104
Materials and Methods.....	107
Results.....	112
Discussion.....	126
References.....	131

Chapter 4: Conclusion

Collective introduction of pH1N1 M, NA, and HA segments into an otherwise non- transmissible virus reproduces the 100% transmission efficiency of wild-type pH1N1 in the guinea pig model	138
A single amino acid change within the IAV matrix protein can simultaneously alter virus morphology, NA activity, and transmission efficiency in the guinea pig model	140
The pH1N1 M segment confers transmissibility to an otherwise non-transmissible recombinant virus through functions encoded by its matrix protein	142
Novel swine H3N2v viruses contain the pH1N1 M segment, transmit more readily to humans than other swine-origin IAVs, and can cause limited human- to-human transmission	144
Overall Conclusions.....	145
References.....	146

LIST OF FIGURES AND TABLES

Chapter 1

Figure 1: Schematic, plaque phenotype and growth kinetics of rescued influenza viruses in MDCK cells.....	40
Figure 2: Growth kinetics of reassortant influenza viruses in differentiated HTBE cells.....	41
Figure 3: Growth kinetics and contact transmission of reassortant influenza viruses in guinea pigs.....	43
Figure 4: Growth kinetics and contact transmission of reassortant influenza viruses in guinea pigs.....	44
Table 1: Virions possessing the PR8 M segment have lower V_{max} , but not K_m , of NA interaction with MUNANA than virions possessing NL602 M.....	47
Figure 5: PR8 and NL602 viruses display distinct virion morphologies.....	48
Figure 6: PR8/NL M+NA+HA virus recapitulates the virion morphology of rNL602 virus.....	49
Figure 7: PR8/NL M+NA+HA recapitulates the virion morphology of rNL602 virus...50	
Table 2: Reassortant viruses differ in prevalence of filamentous virions.....	51

Chapter 2

Figure 1: Schematic diagram of recombinant viruses.....	78
Figure 2: Characterization of recombinant viruses in HTBE and MDCK cells.....	80
Figure 3: A proline at residue 41 of matrix protein increases filament length of recombinant viruses.....	85

Table 1: <i>Reassortant viruses, measured using TEM, differ in the prevalence of filamentous virions.....</i>	86
Figure 4: <i>A proline at residue 41 of matrix protein increases neuraminidase activity of select recombinant viruses in vitro.....</i>	87
Figure 5: <i>A proline at residue 41 of matrix protein attenuates growth and transmission of recombinant viruses in guinea pigs.....</i>	90

Chapter 3

Figure 1: <i>Wild-type, M1/M2 chimeric, and mutant M segments were used in a plasmid-based reverse genetics system to generate a panel of recombinant PR8 viruses.....</i>	113
Figure 2: <i>PR8 viruses harboring NL602 and EAsw M segments replicated similarly in vitro, while the single M248I (M2 C19Y) mutation reduced growth of the PR8/ NL602 M virus in MDCK cells.....</i>	115
Table 1: <i>PR8/ NL602 M1 residues differentially alter virus morphology.</i>	117
Figure 3: <i>Introduction of the EAsw matrix protein reduced the filamentous morphology of the PR8/ NL602 M virus.....</i>	118
Figure 4: <i>EAsw matrix protein 30G, 207S, and 248I (M2 19Y) residues differentially impacted PR8/ NL602 M virus morphology.....</i>	119
Figure 5: <i>PR8 virions harboring PR8 and EAsw M segments have higher V_{max}, but not K_m, against MUNANA than those with NL602 and EAsw M1+NL602 M2 (M2 C19Y) M segments.....</i>	121
Table 2: <i>PR8 viruses with the PR8 and EAsw M segments have fewer defective particles and higher V_{max}, but not K_m, against MUNANA compared to the PR8/ NL602</i>	

M virus.....122

Figure 6: *PR8 viruses harboring the EAsw M1 protein, or the single NL602 M1 N207S mutation, have reduced transmission efficiency, but not reduced growth, compared to the PR8/ NL602 M virus in the guinea pig model*.....125

INTRODUCTION

Influenza Virus Classification and Host Range

Influenza viruses belong to the negative-sense single-stranded RNA virus family *Orthomyxoviridae*, which contains six genera: *Influenzavirus A*, *Influenzavirus B*, *Influenzavirus C*, *Isavirus*, *Quaranjavirus*, and *Thogotovirus*. In addition, an “*Influenzavirus D*” genus has been proposed based on the identification of a novel virus circulating in US cattle and swine with 50% sequence homology to *Influenzavirus C* (1). The influenza virus A, B, and C genera are separated based on distinct antigenic reactivity between their nucleoprotein and matrix proteins (2). *Influenzavirus A* (IAV) has a primarily avian reservoir and has established multiple distinct, persistent, lineages within human, porcine, canine, and equine hosts (3). Influenza B viruses circulate in humans and possibly seals (4), while influenza C viruses only infect humans. Bats have also recently been identified as IAV carriers, however all of the bat influenza viruses isolated to date are phylogenetically distinct from previously identified influenza strains (5, 6). In addition to the circulating lineages, IAV is known to infect a number of other mammals, including: ferrets, mice, guinea pigs, seals, whales, dogs, cats, tigers, leopards, and minks (7-16).

Of the influenza viruses, only IAV is further separated into numbered serotypes based on differences in the antigenicity of the viral surface glycoproteins, hemagglutinin (HA) and neuraminidase (NA). Currently, there are 18 HA subtypes and 11 NA subtypes, where H17N10 and H18N11 are unique to bats (5, 6). Each of the H1 to H16 and N1 to N9 subtypes are known to circulate in aquatic birds within

the avian reservoir. Within the human population, the H1N1, H2N2, and H3N2 subtypes have caused pandemics and seasonal epidemics. In addition, unique combinations of the H5, H6, H7, H9 and H10 subtypes with the N1, N2, N3, N7, N8, and N9 subtypes have been associated with self-limiting human infections from the avian reservoir (17-21). Within the swine population, H1N1, H3N2, and H1N2 serotypes form genetically distinct endemic lineages (22, 23). Lastly, H7N7 and H3N8 subtypes have caused outbreaks in horses while the H3N8 and H3N2 viruses cause canine infections (14, 15, 24-26).

Of the less well studied members of the influenza virus family, strains of the *Isavirus* genus infect and cause disease in salmon, while *Thogotovirus* and *Quarantavirus* genera comprise arthropod vector borne viruses (27-30). *Thogotovirus* spp. infect metastriate tick species and have vertebrate hosts including cattle, camels, bats, man, and likely other ruminants (30). *Quarantavirus* spp. also infect ticks and only one species, the *Quarantavirus*, has caused mild febrile illness in humans (27).

Influenza Virus Life Cycle

IAV primarily infect epithelial cells of the respiratory tract in mammals and the gastrointestinal tract of birds. Irrespective of host, infection begins with attachment of the viral HA binding protein to ubiquitously expressed host cell sialic acids (SA). The interaction between HA and terminal glycan SA (linked to galactose on glycan chains or glycoproteins extending from the host cell surface) is influenced by the geometry and charge of the HA binding site, as well as the orientation of the

SA-glycan bond (31). Additionally, the HA globular head can be altered through amino acid substitutions and changes in glycosylation. These alterations can lead to changes in the affinity and specificity of the HA binding site for the SA receptor and recognition by HA-specific host cell antibodies (31).

Once bound, the virus can enter the host cell through clathrin-mediated endocytosis, clathrin-independent endocytosis, and / or macropinocytosis (32-39). Within the cell, trafficking of endosomes toward the nuclei leads to acidification of the endosomal interior. The decrease in endosomal pH triggers structural changes in virion-associated HA protein, allowing for fusion of the viral and endosomal membranes. Acidification of the interior of the virion also occurs within the endosome, as the virally encoded M2 protein act as a proton-selective ion channel to mediate transport of protons into the virion (40, 41). As the interior of the virion becomes more acidic, the matrix protein (M1) dissociates from the viral ribonucleoprotein (vRNP) complex (42), allowing vRNP to diffuse into the cytoplasm. Nuclear localization signals (NLS) on the vRNP-associated nucleoprotein (NP) and polymerase complex proteins (PB1, PB2, and PA) are recognized and bound by the cellular adaptor protein, importin- α , which exists in multiple isoforms (43). Mammalian PB2 and NP proteins require the importin- α 7 isoform for nuclear import, while avian PB2 and NP proteins are transported by the importin- α 3 isoform (44). Once bound to the vRNP, importin- α can then bind to the nuclear transport receptor, importin- β , to translocate the importin + vRNP complexes through the nuclear envelope and into the nucleus (43, 45, 46).

Once inside the nucleus, the negative-sense viral RNA can be transcribed by the viral RNA-dependent RNA polymerase into capped mRNAs and subsequently replicated into positive-sense complementary RNAs (cRNA), which serve as a template for genomic RNA replication (47, 48). mRNA transcription begins with “cap snatching,” whereby the viral PB2 protein binds the host pre-mRNA 5' cap and the PA protein then cleaves the cap using its endonuclease activity (49). The cap is subsequently used as a primer for transcriptional activation and elongation by the PB1 protein (50-52). Transcription ends when the polymerase stutters along the terminal poly-U sequence to form a 3' poly-A tail (53, 54). Once transcribed, the mRNA is exported from the nucleus to the cytoplasm and translated by host cell machinery.

Once translated and properly folded, the NP and polymerase complex proteins enter the nucleus through the importin pathway. Inside the nucleus, the NP coats the cRNA and associates with the polymerase subunits to provide the template for replication of nascent vRNA. The negative-sense nuclear vRNA is also coated with NP and associates with the viral polymerase to form new vRNP complexes. At later stages of the replication cycle, newly synthesized cytoplasmic M1 and non-structural protein 2 (NS2 or NEP) proteins are imported into the nucleus where M1 associates with the vRNPs in an NS2-dependent manner (55). The vRNP-M1-NS2 complexes are then transported from the nucleus through interactions of the cellular export machinery and two nuclear export signals on the viral NS2 protein (55-57).

On the ER-associated ribosomes, the viral membrane proteins HA, NA, and M2 are translated and translocated into the ER where they undergo oligomerization, glycosylation (HA and NA), and palmitoylation (HA and M2) as they traffic through the Golgi complex to the plasma membrane. The nascent vRNP-M1-NS2 complexes that have exited the nucleus associate with Rab11-positive recycling endosomes within the cytoplasm and are transported along microtubules and actin filaments to the plasma membrane (58-61). Once at the plasma membrane, HA and NA associate with cholesterol and sphingolipid-rich lipid rafts and their cytoplasmic tails bind vRNP-associated M1 (62-64). HA, NA, M1 and M2 have all been associated with viral budding, while the M2 protein mediates membrane scission for virus release (33, 65-71). Lastly, the NA glycoprotein serves as a receptor-destroying enzyme by cleaving sialic acid from the virus and host cell surfaces, allowing for efficient release of progeny virions from the cell.

Influenza A Virus Matrix Protein

Matrix Protein Structure

Influenza A virus M1 is the most abundant protein in the virion (72). M1 is the major structural component of the virion, underlying the cell-derived plasma membrane and interacting with the vRNP complexes, the M2 proton channel, and the cytoplasmic tails of both HA and NA. The M1 protein is composed of 252 amino acids encoded by segment 7 of the influenza genome. The M1 crystal structure has been solved for amino acids 2 through 158 under both acidic (pH 4.0) and neutral conditions and this fragment of the protein is composed of nine alpha helices joined

by eight loop regions (73, 74). Each complete M1 monomer has three domains, comprising the N-terminal domain (N), the middle domain (M) and the C-terminal domain (C). The N and M domains are each composed of four alpha helix bundles (H1 to H4 and H6 to H9, respectively) connected by an alpha helix linker (H5) (73, 74). The C domain has not been crystallized due to protease sensitivity of the M-C linker; however, *in silico* analysis and tritium bombardment data suggest that the C domain may also fold into alpha helices (73-76).

M1 monomers oligomerize to form a helical protein ribbon under the plasma membrane that provides structure and rigidity to the virion (75, 77-80). The outer face of the M1 ribbon interacts with the plasma membrane through electrostatic interactions while the charged inner face of the ribbon interacts with the vRNP complexes (73, 74, 80). At low pH, which occurs during acidification of the virion interior within the endosome, the M1 monomers undergo structural changes that lead to dissociation of the M1 protein layer from the plasma membrane, release of the vRNP complexes, and the formation of a stable multilayered M1 coil structure (74, 75, 79). The M1-plasma membrane dissociation may help facilitate fusion by releasing unconstrained sections of lipid bilayer to become part of HA-mediated fusogenic complexes (79). Additionally, release of the vRNP complexes from the virion structure allows for vRNP nuclear trafficking and genome replication.

Matrix Protein Function

In addition to forming the structure of the influenza virion, M1 also participates in nuclear export of vRNP complexes from the nucleus, vRNP trafficking

to the plasma membrane, and virion budding. Once synthesized in the cytoplasm, the M1 nuclear localization sequence (RKLKR) in the M domain is bound by cellular importin- α and the M1 protein is transported via the importin pathway into the nucleus (81). Once inside the nucleus, the M domain of the M1 protein binds vRNP complexes and inhibits viral replication at early stages of transcriptional activation through functions presumably encoded by the C domain (82-85). The M1 nuclear localization sequence is then bound by NS2 and the vRNP-M1-NS2 complex is exported to the cytoplasm by host cell nuclear export machinery (55-57, 86, 87). The complexes then associate with Rab11-positive recycling endosomes and are trafficked to the plasma membrane along the host cell cytoskeletal network (59, 60). M1 protein then associates with the host cell membrane and the cytoplasmic tails of HA, NA and M2 (62, 80, 88-92). Mutations or deletions of the HA, NA, and M2 cytoplasmic tails have been shown to affect their interactions with M1 and impact virion budding, assembly, and morphology (90, 93-97). Oligomerization of M1 at the plasma membrane may help facilitate budding by enhancing membrane curvature and / or exerting an outward membrane force through the oligomerization process (33, 79). However, only the M1 from the 2009 pandemic H1N1 virus has been shown to be sufficient for viral budding in an *in vitro* transfection model (98, 99). Since both HA and NA have been shown to independently generate virus-like particles, any role M1 plays in viral budding most likely occurs in conjunction with one or both glycoproteins (98, 100, 101).

Influenza A Virus: Human Disease and Pandemics

Human Disease

Influenza virus infection leads to respiratory disease in humans, which ranges from mild to severe and is usually limited to the respiratory tract. Infection of the respiratory epithelium leads to an immune response (including cytokine release and increased mucus production), which can result in respiratory inflammation, headache, malaise, runny nose, coughing, sore throat and fever. Clinical symptoms usually appear after a two-day incubation period and last for approximately 7 to 10 days. However, severe influenza disease is possible, involving viral pneumonia and possible death if viral replication spreads from the bronchial space to the alveoli of the lower respiratory tract. Disease severity can be attributed to the virulence of the infecting virus and the immune competence and exposure history of an infected individual. Some influenza viruses, such as the H5N1 and H7N9 avian strains, can cause severe disease in humans by inducing high levels of proinflammatory cytokines that result in increased tissue damage and fluid accumulation in the lungs (102-104). Additionally, young children, persons 65 years of age or older, those with chronic medical conditions (i.e.: asthma, diabetes, heart disease), and pregnant women are all considered to be high risk for severe influenza illness due to their potentially compromised immune response to viral infection (105).

Influenza Pandemics

The segmented nature of the influenza virus RNA genome allows for the

packaging and release of novel progeny from a cell infected with two or more genetically distinct viruses, a process known as reassortment. Reassortment drives pandemics through introduction of viruses possessing antigenically novel HA and/or NA subtypes into an immunologically naïve population. The first documented influenza pandemic occurred in 1918 with the introduction of a novel H1N1 virus into the human population that killed an estimated 50 million people worldwide (106). Recent phylogenetic evidence suggests that the virus may have been the reassortant progeny of avian and human H1N1 parental lineages (107, 108) This pandemic was characterized by high morbidity and mortality in young adults as well as the immunologically disadvantaged young (<5 years old) and elderly (>65 years old) populations (109). The unique mortality distribution has been attributed to 1) the high pathogenicity of the 1918 virus that lead to an elevated immune response, which resulted in a 'cytokine storm' in young adults, and 2) the preexisting immunity of individuals age 18 to 43 that were infected in the 1880s or 1890s by a presumably antigenically related virus (110-113). After the 1918 pandemic, the H1N1 lineage became endemic in both humans and swine (107, 114).

The next influenza pandemic (known as the "Asian" influenza pandemic) occurred in 1957 with the introduction of a novel H2N2 virus into the human population in China (115). The H2N2 virus resulted from reassortment between the circulating H1N1 virus (PB2, PA, NP, M, NS segments) and an avian H2N2 (HA, NA, and PB1 segments) virus (116, 117). Comparatively, this second pandemic had greatly reduced global mortality from the 1918 pandemic, with an estimated excess of influenza-associated deaths of 69,800 people in the United States (115).

In 1968 there was another reassortment event in Hong Kong between an avian virus (H3 subtype HA and PB1 segments) and the circulating human H2N2 (remaining segments) virus (117). The resultant H3N2 virus caused fewer excess influenza-associated deaths than the previous pandemics (33,800 within the US), which might be attributed to the conservation of the circulating NA protein in the pandemic virus, whereby those previously-infected with the H2N2 virus had preexisting immunity against the H3N2 N2 protein (115).

Lastly, the most recent pandemic began in Mexico with the emergence of the 2009 pandemic H1N1 influenza virus (pH1N1), which spread rapidly within the human population and caused up to 400,000 US hospitalizations within its first year of circulation (118, 119). The pH1N1 virus is presumed to be the result of genetic reassortment between the Eurasian avian-like swine (EAsw) H1N1 lineage (M and NA segments) and the North American triple reassortant swine H3N2 lineage (remaining segments) in swine (118). Recent phylogenetic evidence suggests that this reassortment event may have occurred in pigs between 1998 and 2009 but gone undetected by swine surveillance efforts (120). Notably, although human infections have occurred with viruses belonging to both parental lineages, none of the documented infections lead to the sustained human-to-human transmission that characterized the 2009 pandemic (121-123).

History of North American and European Swine Influenza

Swine influenza (SI) was first described in China and the US in 1919, based on clinical symptoms and disease progression that differed from previously-

recognized swine illnesses (124, 125). According to the USDA inspector, Koen, the disease first appeared in the pig herds of Iowa in 1918 (124). The flu-like illness continued to circulate and cause high morbidity but low mortality in North American swine throughout the 1920s (126, 127). However, influenza virus was not proven to be the causative agent of the disease until its isolation by Shope in 1931 (128). Shope went on to demonstrate that SI viruses could infect other mammals, including mice and ferrets, and that human sera from influenza-infected individuals had cross-reactivity to isolated swine viruses, suggesting a close antigenic relationship with human strains (8, 107, 129). Although swine viruses were known to circulate in swine herds, and the viruses were recognized as being antigenically similar to human strains, there was no direct evidence of swine-to-human transmission until the 1970s, when a swine influenza virus was cultured directly from the lungs of an infected boy (130). Further infrequent zoonoses involving SI viruses of the influenza A viruses have been reported, however, to date, the only recorded swine virus to successfully transmit from human-to-human was the 2009 pandemic H1N1 virus (121-123, 131).

North American Swine Influenza

In North America, the H1N1 lineage, closely related to the virus that caused the 1918 pandemic in humans, became known as 'classical swine H1N1' and continued to circulate in swine herds through the 1990s (132, 133). This classical swine lineage remained largely genetically conserved through the 1980s (134-136). In fact, not until 1991 were significant antigenic variants isolated in the US and

Canada (137-139). In addition to the H1N1 variants, the 1990s saw the emergence of novel reassortant H3N2 and H1N2 influenza virus strains in US swine herds (22, 23, 140, 141). Of three H3N2 genotypes identified in 1997 and 1998, the most prominent was the North American triple reassortant swine (NAtr) lineage, which resulted from reassortment between human H3N2 (HA, NA, and PB1 segments), classical swine (M, NP, NS segments), and avian (PA and PB2 segments) viruses (142, 143). Within two years of its identification, viruses belonging to the NAtr lineage were isolated from pigs in nine states and, according to the USDA, accounted for 27% of all North American swine isolates (22, 142-144). In 1999, a secondary reassortment event between a classical swine H1N1 virus (HA segment) and a NAtr virus (all remaining segments) gave rise to the novel H1N2 lineage (145). All three swine subtypes (H1N1, H3N2, and H1N2) continue to circulate and reassort within the North American swine population (23, 146, 147). Additionally, a recent H3N2 variant virus (H3N2v) was identified in the US in 2011 (148). The H3N2v virus contains the M segment from a human 2009 pandemic H1N1 virus and the remaining segments from the NAtr H3N2 virus and was responsible for 343 confirmed human infections from 2011 to 2014, including 18 hospitalizations and one death (149-151).

European Swine Influenza

The first potential report of swine influenza (SI) in European pigs was published by Köbe in Germany in 1933, wherein he described a similar illness as Koen's American "hog flu" but only occurring in piglets (152). Unfortunately,

although Köbe isolated the virus, it was lost before it could be confirmed as an influenza virus. However, reports of influenza-like illness continued throughout the 1930s and 1940s in Ireland and England (153, 154). By 1941, three swine influenza strains were isolated and later studies demonstrated that all three were more closely related to concurrent circulating human H1N1 strains than to those of the North American classical swine H1N1 lineage (133, 155-157). However, once the classical H1N1 lineage was isolated in Europe in 1950 it spread rapidly to other European countries and continued to circulate at very low levels until its last isolation in 1993 (158-160).

In 1979, a novel “Eurasian avian-like swine H1N1” (EAsw) lineage was identified in the pigs of Belgium (161, 162). Recent phylogenetic evidence suggests that the virus may have been a triple reassortant containing the PB1 and PB2 segments from one H3N2 avian clade, the PA and NS segments from a separate H3N2 avian clade, and the remaining segments from an avian H1N1 group (163). The EAsw viruses spread rapidly and remain endemic in all of the pig producing countries of Europe with seasonal prevalence values ranging from approximately 40-80% (158, 159, 164). Subsequent reassortment between an EAsw virus (internal segments) and a human seasonal H3N2 (HA and NA segments) virus in 1982 gave rise to the first “human-like H3N2” European swine infection (165-167). Although this first H3N2 infection did not lead to sustained transmission among pigs, another virus differing in the sequence of its parental HA and NA segments, was introduced in 1984 and led to a widespread and stable human-like swine H3N2 lineage (168, 169). The human-like H3N2 viruses remain endemic in European

swine but at a much lower prevalence than those of the EAsw lineage (164, 170). Importantly, the HA proteins of modern H3N2 swine viruses have undergone significant antigenic drift compared to the initial isolates and this antigenic diversity has been implicated in an increase in zoonotic outbreaks (171). Additionally, the drifted H3N2 HA proteins no longer share antigenic cross-reactivity with modern human H3N2 HAs, suggesting that young individuals will lack preexisting immunity to these proteins and may therefore be susceptible to zoonotic infections with modern H3N2 swine lineage viruses (172).

In addition to the human-like H3N2 viruses, a distinct “human-like H1N2” swine lineage emerged in England in 1994 (173). This novel lineage presumably arose from multiple reassortment events between the EAsw H1N1 (internal segments), human seasonal H1N1 (HA segment), and human seasonal H3N2 (NA segment) viruses (174). By 1997, the human-like H1N2 viruses were isolated in 5 mainland European countries, however, similar to the human-like H3N2 viruses, prevalence in the swine population remains low (<3 – 35%) (164, 169).

Lastly, due to the continued circulation of EAsw H1N1, human-like swine H3N2, and human-like swine H1N2 within European swine and the opportunity for these swine strains to reassort with human seasonal viruses, multiple reassortant strains have been isolated throughout Europe. Reassortants harboring differing combinations of swine lineage HA and NA segments have been identified, however, none of the reassortants have led to sustained transmission within the swine population (159, 175, 176). Reassortant viruses containing either 1) seasonal human H3N2 HA and NA segments with the internal segments from the EAsw

lineage or 2) a seasonal human H3N2 NA segment and all other segments from the human-like swine H1N2 lineage have also been isolated (165, 177). However, as was the case for the wholly swine lineage reassortants, none of these human-swine variants have established a stable lineage in pigs. Lastly, a unique swine H1N7 virus was identified in England in 1994 that contained the NA and M segments from an equine influenza virus with all remaining segments from a human seasonal H1N1 virus (178). However, no further isolates of the unusual reassortant have been reported to date.

Influenza A Virus Structure and Morphology

Influenza viruses are pleomorphic enveloped RNA viruses that range from spherical (80 - 300nm in diameter) to filamentous (>300nm in length) in shape. The viral envelope is derived from the cellular lipid bilayer and is studded with the viral glycoproteins, HA and NA, as well as the M2 proton channel. The matrix (M1) protein provides the virion with structural stability by oligomerizing into a continuous helical layer that lies beneath the exterior envelope. The M1 protein therefore interacts directly with the cytoplasmic tails of the HA and NA proteins, the M2 proton channel, and the nucleoprotein that coats each of the eight viral RNA segments (89).

Laboratory-adapted influenza strains are regularly passaged *in vitro* and can be spherical while primary and low-passage clinical isolates are characterized by the presence of filaments (179-181). It was recently found that the spherical, laboratory-adapted A/Puerto Rico/8/34 (H1N1) virus became filamentous upon

multiple passages within the guinea pig, demonstrating that filaments can be selected for in an animal host (182). Passage of the filamentous isolate A/Georgia/M5081/2012 (H1N1) in embryonated chicken eggs also resulted in a decrease in filament prevalence and increased growth *in vitro* (182). The selection of filaments *in vivo* suggests that they provide a functional advantage over spheres; however, the exact nature of the advantage remains unknown.

Viral Proteins that Impact Influenza Virus Morphology

As the primary structural component of the virion, the matrix protein is a major determinant of influenza virus morphology. Evidence that the M segment could be linked to changes in virus morphology was first presented in 1998, when a single M1 amino acid change (Ala41Val) was found to eliminate the formation of filamentous virions in the context of the A/Udorn/301/72 (H3N2) [Udorn] virus gene constellation (183). Additional studies demonstrated that introduction of an M segment, and more specifically the M1 coding region, from a filamentous strain into a spherical virus genome, could confer a filamentous virion phenotype to otherwise spherical viruses and vice versa (181, 184). Comparison of M1 protein sequences between the spherical and filamentous strains identified several amino acid differences, and showed that polymorphisms at positions 41, 95, 204, and 218 were associated with altered virus morphology (181, 184). A separate study identified specific amino acid residues at positions 98, 101, and 102 in M1 as important for virus morphology (185). Interestingly, the Ala41Val mutation in the Udorn M1 protein resulted in a loss of filamentous virions when included in the

A/Victoria/3/75 (H3N2) background but did not affect filament production when included in the A/WSN/33 (H1N1) (WSN) background (181, 184). These data highlight the importance of genetic background and interaction between the M1 and other viral proteins in virion assembly. Additionally, recent cryoelectron tomography data demonstrated a difference in M1 helix curvature for spherical versus filamentous virions and suggested that single amino acid exchanges within the matrix protein can affect M1 polymerization and virion curvature (79).

Other viral proteins also impact influenza virus morphology, including the HA and NA glycoproteins, the M2 proton channel, and the NP. In particular, deletion of the single NA, or HA and NA, cytoplasmic tail(s) has been shown to increase filament production, while deletion of the HA cytoplasmic tail alone did not alter morphology of the virion in the WSN background (95, 96). The M2 proton channel cytoplasmic tail has been implicated in M1/M2 interactions and virus budding. Investigations into the role of M2 in virion assembly and budding showed that partial deletion of the M2 cytoplasmic tail could result in 1) filament loss in an otherwise filamentous virus (WSN with an Udorn M segment; 17 amino acid deletion) and 2) filament production in the otherwise spherical WSN background (22 - 44 amino acid deletion) (91, 92). The M2 protein also has a membrane proximal amphipathic helix that is involved in membrane scission and virion release from the host cell (66, 67). Recent studies demonstrated that the amphipathic helix is also important for filament production, as disruption of the helix by the replacement of two or more hydrophobic amino acids with alanine residues abrogated Udorn filament formation (66, 186). Lastly, the NP protein is known to

directly associate with the M1 protein on the inside of the virion. A recent study utilized site-directed mutagenesis to demonstrate that amino acid changes at NP positions 214, 217, and 253 can inhibit filament formation in the context of an otherwise filamentous reassortant virus (WSN + A/Aichi/2/68 (H3N2)), presumably by altering NP-M1 interactions, although the exact mechanism remains unknown (187).

Cellular Proteins that Impact Virus Morphology

The host cell type, cytoskeletal network, and proteins can all affect influenza virus morphology. Influenza viruses are capable of budding from both polarized and non-polarized epithelial cells, however, when non-polarized cells were infected with the filamentous Udorn virus, virions were determined to be almost exclusively spherical by electron microscopy (188). Cell polarity is, in part, dependent upon cytoskeletal components and dynamics for protein sorting and membrane trafficking. Although previous studies found that disruption of the cytoskeleton did not decrease virus titers for spherical viruses, a later study found that filament formation was ablated when cells were treated with the actin polymerization inhibitor, cytochalasin D, but was not affected by disruption of the microtubule inhibitor, nocodazole (188-190). The prevention of filament formation was therefore found to be dependent upon the actin network and was also independent of viral replication, as titers were unaffected by cytochalasin D treatment (188). Further work demonstrated that distribution of HA, NP, and M1 is altered in cells treated with drugs that disrupt proper actin filament assembly and disassembly

(191). This research suggests that actin-lipid raft interactions may be required for filaments to efficiently bud from lipid raft sites in the plasma membrane (191). In addition to the cytoskeleton, Rab11-positive endosomes involved in membrane trafficking were determined to be important in influenza virus membrane assembly. A recent study demonstrated that Rab11 was required for influenza virus budding, while both Rab11 and the Rab11 Family-Interacting-Protein 3 (FIP3), which binds Rab11 and directs it to cholesterol-rich regions of the plasma membrane, were required for filament formation through an as yet unknown mechanism (192).

Influenza A Virus Transmission and Host Adaptation

Influenza viruses may be transmitted by respiratory droplets or direct contact with either an infected host and/ or contaminated surface (fomite) (193, 194). Coughing, sneezing, talking, and heavy breathing can all generate aerosols that contain influenza viruses (195, 196). Although debated, expelled droplets of <5-10um are considered by some to be associated with respiratory aerosol transmission of influenza viruses, as they are small enough to remain airborne for longer periods of time and travel further than larger droplets (197). When inhaled, the smaller (<5um) droplets are thought to travel further down the respiratory tract, while larger (5-10um) droplets are thought to deposit more often in the upper respiratory tract due to their larger mass (197). Exhaled droplets that are larger than 10um in diameter are thought to drop out of suspension at a faster rate, thereby potentially contributing to contact transmission through surface contamination (195).

Environmental conditions also contribute to influenza virus transmission, as is seen with the seasonal nature of influenza epidemics. Low temperatures (approximately 5°C) and low humidity (20-35% relative humidity) were determined to be optimal for respiratory droplet transmission of influenza viruses between infected and naïve guinea pigs (198, 199). These conditions are in agreement with the observed seasonality of influenza virus transmission (200). However, the mechanism(s) by which temperature and humidity affect aerosol transmission of influenza viruses remain(s) unclear, but virus stability, host susceptibility, and potential effects on exhaled droplets have all been proposed as potential factors (200).

Viral Factors Involved in Influenza Virus Transmission and Host Adaptation

In order to cause productive infection within a host, influenza viruses must be able to bind to appropriate host cells, enter and replicate efficiently, and produce progeny virions that can then be released and transmitted to a new cell (or host). The first step in the lifecycle is therefore recognition and binding of the viral HA protein to terminal sialic acids on the host cell surface that serve as the viral receptors. The amino acid composition and glycosylation state of a particular HA protein determines whether or not it recognizes sialic acid residues displayed with an α -2,3 linked (predominant in the avian gastrointestinal tract) or α -2,6 linked (predominant in the human respiratory tract) conformation relative to the preceding sugar moiety (201). Efficient binding to the appropriate host-specific sialic acid receptor is critical to productive infection and replication of the virus

within a novel host. The respiratory tracts of swine contain both α -2,3 and α -2,6-linked sialic acid species, which has led to the proposal that pigs may serve as potential “mixing vessels” for both avian and human viruses (202-204). Changes in the receptor binding specificity of the 1918 H1N1, 2009 pandemic H1N1, and H5N1 viruses, were shown to be associated with cross-species transmission events (205-208). Changes in the H5N1 receptor specificity were also shown experimentally to increase transmission efficiency of highly pathogenic avian influenza viruses in the ferret model (205, 206).

In addition to changes in receptor binding, alterations in HA stability can also impact virus transmissibility. Since the HA protein mediates membrane fusion, and pH-dependent changes in HA conformation are required for fusion to occur, molecular changes that alter the optimal value of pH at which the HA fusion peptide is released impact virus fitness in the host environment. Human influenza viruses have experimentally-determined lower optimal pH values for fusion (pH 5.5 to 5.6) than avian viruses (pH 4.9 to 5.4), which may facilitate an appropriate conformational change of HA in the naturally acidic environment of the human respiratory tract (209, 210). This relationship between host and the pH of hemagglutinin activation is additionally supported by data which demonstrate that HA mutants that activate at increased pH values replicate to higher titers in ducks than in mice, while those with decreased pH values could only replicate in mice (211, 212).

Subsequent to host cell attachment and entry, an influenza virus must

replicate its genome in the nucleus. Amino acid changes at positions 627 and 701 of the viral polymerase subunit, PB2, alter the optimal temperature for viral replication and binding of the polymerase to host factors, respectively (213). In particular, the Glu627Lys substitution has been shown to allow for efficient viral replication in mammals, presumably by altering the optimal replication temperature from the avian host body temperature of 39-41°C to that of the mammalian host upper respiratory tract: 33°C (214-217). The PB2 Asp701Gln change adapts the polymerase for increased replication in mammalian cells and, in combination with a concurrent change in the NP, increases affinity of the polymerase + NP complex for importin- α , leading to increased transport of the viral genome to the nucleus (218, 219).

Once viral replication and virion assembly are complete, nascent virus is efficiently released from the host cell through cleavage of the SA receptors by the viral NA protein. Since the HA protein and the NA enzyme both share SA as a substrate and have counteracting functions, a balance between their functions must be reached in order for the virus to both productively infect (bind) and release (cleave) from a cell. Recent studies have demonstrated that transmission of the human 2009 pandemic H1N1 strain was partially dependent upon the presence of HA and NA proteins with functionally matched activities, while such a balance was not required for swine isolates to transmit efficiently between swine (220, 221). For the first time, the M segment was also found to impact the transmission efficiency of influenza virus, however, the mechanism underlying this phenotype remains unknown (222-224).

Mammalian Models for Influenza Virus Transmission

Several animal models have been developed for investigation of influenza virus infection, transmission, disease progression, and pathogenicity. The ferret was the first animal adopted for influenza research (9). Influenza A and B strains readily infect the ferret respiratory tract without adaptation, replicate sufficiently to produce human-like disease symptoms (coughing, and fever, as well as sneezing), and transmit between animals by both the direct contact and aerosol transmission routes (225-228). Ferrets can be productively infected with a range of influenza A (including H1N1, H2N2, H3N2, H5N1, and H7N9) subtypes from the human, porcine, and avian reservoirs as well as influenza B strains (129, 179, 225, 226, 229-236). Distribution of virus within the lungs is comparable between humans and ferrets, where seasonal human H1N1 and H3N2 strains primarily infect the upper airways, while viruses of the H5N1 subtype infect and replicate primarily within the lower respiratory tract (207, 225, 237, 238). Virus transmissibility is also comparable between ferrets and humans, with the human H1N1 and H3N2 subtypes transmitting more readily than avian viruses. However, ferrets can be difficult to house and are more expensive than smaller mammals used for research purposes, which can limit the number of animals, and therefore statistical significance of results, for each study.

An alternative to the ferret model is the smaller and more cost effective guinea pig (7). Guinea pigs are also infected with influenza virus (without prior adaptation) via the respiratory route, are characterized by productive viral replication in the nasal passages and lungs, and transmit virus by both contact and

aerosol routes (7, 222, 239, 240). Similar to ferrets, guinea pigs are naturally susceptible to infection with seasonal human H1N1 and H3N2 subtypes, as well as avian and swine strains (7, 194, 199, 239, 241-243). Moreover, similar to humans, swine and avian influenza viruses generally replicate to lower titers than human viruses in the guinea pig airways. Interestingly, despite being susceptible to influenza virus infection and displaying significant airway histopathology as a result of viral replication, guinea pigs do not show overt influenza-like signs of illness, making them a weaker model for viral pathogenesis than the ferret (7, 239, 242, 244, 245). However, guinea pigs do serve as a suitable model for influenza virus contact and aerosol transmission. Importantly, lineage-specific differences in guinea pig transmission are comparable to those seen in humans, with human H1N1 and H3N2 strains transmitting more efficiently than viruses from the swine reservoir, while avian viruses typically do not transmit among guinea pigs (194, 198, 241, 246).

In order to investigate viral pathogenesis, virulence, and immunological responses surrounding influenza infection, the mouse model is frequently utilized (247-250). Mice are cost effective, can be genetically engineered, and are accompanied by a comprehensive range of immunological reagents. However, influenza strains do not readily transmit between mice, and human derived strains are typically genetically adapted by serial passage to elicit productive infection and overt pathogenicity. The lack of mouse infectivity with human influenza strains may be partially due to the predominance of α -2,3-linked sialic acid receptors in the mouse respiratory tract, as opposed to the α -2,6 linkage that is predominant in the

upper human airway (251, 252). In addition, although mice exhibit clinical signs of disease that can be measured for determination of strain pathogenicity, mouse disease progression and signs do not reflect those of infected humans. For example, influenza viruses typically infect and replicate within the upper airways of humans, resulting in coughing, fever, and malaise, while mouse-adapted influenza strains infect and replicate in the lower lungs of mice and result in primary pneumonia, hypothermia instead of fever, weight loss, and mortality (251-254). However, despite their increased disease severity and differing clinical signs, the quantifiable nature of their disease symptoms and mortality make mice a tractable model for the study of pathogenesis and assessment of antiviral therapies (255-257).

In the following chapters, we investigate the impact of the influenza virus M segment on virus transmission. We utilize the guinea pig model to determine the *in vivo* replication kinetics and transmission efficiencies of reassortant viruses that contain differing (1) M, NA, and HA segments, (2) M1 and M2 proteins, and (3) M1 protein sequences. We demonstrate that although the M and NA segments from a 2009 pandemic H1N1 virus confer transmissibility to an otherwise non-transmissible influenza virus, the two must be combined with their cognate HA segment to achieve optimal NA / HA balance and recapitulate the wild type pH1N1 transmission efficiency. We suggest that the M+NA+HA segment combination allows for optimized interaction between M segment products and the cognate glycoproteins and may also provide a functional balance between the HA (binding) and NA (release) activities. In addition, by introducing chimeric M segments that differ in their M1 and M2 proteins into a non-transmissible background, we show

that the M1 protein can independently impact virus transmissibility. Lastly, we utilize *in vitro* electron microscopy and neuraminidase activity assays to demonstrate that different M segments, M1 proteins, and single M1 amino acid changes can differentially alter virion morphology and neuraminidase activity levels. Our results suggest that functions encoded by the influenza virus M segment, and specifically by the M1 matrix protein, can affect virus transmissibility.

CHAPTER 1

The M Segment of the 2009 Pandemic Influenza Virus Confers Increased Neuraminidase Activity, Filamentous Morphology, and Efficient Contact Transmissibility to A/Puerto Rico/8/1934-Based Reassortant Viruses

Patricia J. Campbell, Shamika Danzy, Constantinos S. Kyriakis, Martin J. Deymier,
Anice C. Lowen, and John Steel

This work was published in 2014 in the *Journal of Virology*.

Article Citation:

Campbell PJ, Danzy S, Kyriakis CS, Deymier MJ, Lowen AC, Steel J. 2014. The M Segment of the 2009 Pandemic Influenza Virus Confers Increased Neuraminidase Activity, Filamentous Morphology, and Efficient Contact Transmissibility to A/Puerto Rico/8/1934-Based Reassortant Viruses. *J Virol* 88(7):3802.

ABSTRACT

The 2009 H1N1 lineage represented the first detection of a novel, highly transmissible influenza A virus genotype: six gene segments originated from the North American triple-reassortant swine lineage; two segments, NA and M, derived from the Eurasian avian-like swine lineage. As neither parental lineage transmits efficiently between humans, the adaptations and mechanisms underlying the pandemic spread of the swine-origin 2009 strain are not clear. Toward identifying determinants of transmission, we used reverse genetics to introduce gene segments of an early pandemic isolate, A/Netherlands/602/2009 [H1N1] (NL602), into the background of A/Puerto Rico/8/1934 [H1N1] (PR8) and evaluated the resultant viruses in a guinea pig transmission model. Whereas the NL602 virus spread efficiently, the PR8 virus did not transmit. Swapping of the HA, NA and M segments of NL602 into the PR8 background yielded a virus with indistinguishable contact transmissibility to the wild-type pandemic strain. Consistent with earlier reports, the pandemic M segment alone accounted for much of the improvement in transmission. Toward understanding how the M segment might affect transmission, we evaluated neuraminidase activity and virion morphology of reassortant viruses. Transmission was found to correlate with higher neuraminidase activity and a more filamentous morphology. Importantly, we found that introduction of the pandemic M segment alone resulted in an increase in the neuraminidase activity of two pairs of otherwise isogenic PR8-based viruses. Thus, our data demonstrate the surprising result that functions encoded by the influenza A virus M segment impact

neuraminidase activity and, perhaps through this mechanism, have a potent effect on transmissibility.

IMPORTANCE

Our work uncovers a previously unappreciated mechanism through which the influenza A virus M segment can alter the receptor destroying activity of an influenza virus. Concomitant with changes to neuraminidase activity, the M segment impacts the morphology of the influenza A virion and transmissibility of the virus in the guinea pig model. We suggest that changes in NA activity underlie the ability of the influenza M segment to influence virus transmissibility. Furthermore, we show that co-adapted M, NA, and HA segments are required to provide optimal transmissibility to an influenza virus. The M-NA functional interaction we describe appears to underlie the prominent role of the 2009 pandemic M segment in supporting efficient transmission, and may be a highly important means by which influenza A viruses restore HA / NA balance following reassortment or transfer to new host environments.

INTRODUCTION

The 2009 influenza pandemic was caused by an H1N1 subtype influenza A virus that originated in the swine reservoir. Although swine influenza viruses, including H1N1 subtype strains, are occasionally detected in humans who have had direct contact with pigs, these are most often isolated events which do not lead to sustained human-to-human spread (1-6). Clearly, the 2009 pandemic H1N1

influenza A viruses transmit with significantly greater efficiency among humans than do swine influenza isolates. Given that all eight gene segments of the pandemic strain derive from influenza A viruses that have been circulating in swine for at least 10 years, this raises the important question of what viral factors permit efficient human-to-human transmission. One novel feature of the 2009 pandemic virus which appears to play a role is the presence of two gene segments from the avian-like Eurasian swine lineage in the context of a North American triple reassortant swine virus background (7-12).

Efforts over the last several years to identify the viral factors required for spread of influenza A virus between mammals have revealed that transmissibility is a complex, multi-genic trait. The receptor binding specificity (13, 14) and the acid stability (15, 16) of the hemagglutinin (HA) glycoprotein appear to be important factors, and the viral polymerase complex has been seen to contribute to the transmission phenotype (17, 18). Nevertheless, it has also been shown that neither an HA protein which binds human type receptors nor viral replication machinery (as encoded by the 6 internal genes) adapted to growth in human cells is sufficient to support transmission of influenza viruses between ferrets (19). To date, the set of viral traits sufficient to give rise to a fully transmissible phenotype in humans has yet to be identified. Previous studies on the 2009 pandemic strain suggest that determinants residing in the M segment (9, 11, 12), which encodes the matrix (M1) and proton channel (M2) proteins, as well as the NA gene (10-12), which encodes the neuraminidase (NA) protein, may contribute to transmissibility.

The matrix protein forms a structural layer under the viral envelope through

interaction with the viral glycoproteins HA and NA (20, 21) and is thought to subsequently recruit the viral ribonucleoprotein (vRNP) complexes during assembly (20-22). M2 is a transmembrane channel protein that is involved in (i) membrane scission during viral egress (23); (ii) acidification of the virion during viral entry, which leads to release of vRNPs from the M1 protein (24-27); and (iii) preventing premature conformational change of specific hemagglutinin proteins in the Golgi complex, mediated through control of the pH within this organelle (24, 25, 27). Both M1 and M2 have been identified as determinants of influenza virion morphology (28-33), and point mutations in either protein can convert an exclusively spherical influenza virus (approximately 200nm diameter) to one that produces a mixture of spheres and filaments (which can be greater than 1 μm in length), and vice versa (28-34). As clinical isolates of influenza A virus overwhelmingly include some percentage of filamentous virions, and lab adaptation frequently results in the generation of strains with an exclusively spherical morphology (29, 34), an understanding of the biological relevance of filamentous influenza A virus particles has long been sought.

Hemagglutinin mediates attachment to host cells via binding to glycans possessing terminal sialic acid moieties and, following virion endocytosis, fusion between host and virion membranes (35). Neuraminidase has a complementary function to HA in that it is the receptor-destroying enzyme. NA cleaves sialic acids from host and virion surfaces to facilitate release of progeny virus (35). NA is also presumed to act on sialic acid-rich mucins that line target epithelia, which would otherwise prevent infection by competing with cellular receptor for the HA binding

site (36). Due to their opposing functions, the HA and NA proteins encoded by a given influenza virus are required to be in balance to achieve high viral fitness (37). A loss of HA / NA balance can occur through i) reassortment involving either, but not both, of these genes (38); ii) infection of a new tissue or host species, where sialic acids on cells or mucins may differ in type and distribution (39); iii) a change in HA affinity / avidity due to the acquisition of antibody escape mutations (37, 40-42) or iv) the presence of pharmaceutical neuraminidase inhibitors in the host (43). In each of these cases, studies have demonstrated that selective pressure on the virus can result in realignment of HA and NA functions such that viral attachment and release are not compromised. Typically, this realignment is achieved through direct modification of HA or NA. Observation of reassortant viruses suggests a greater level of complexity exists, however alternative mechanisms for modulating HA-NA balance have not been explored in detail.

The HA and NA proteins have been found to be important to influenza virus transmission in a number of contexts (10, 44). Unexpectedly, the M segment was also found to be highly important to the transmissibility of the 2009 pandemic strain (9, 11, 12). We therefore formed the hypothesis that M1 and / or M2 proteins can alter HA / NA balance through effects on one or both glycoproteins. We tested this hypothesis through the examination of PR8-based viruses carrying combinations of the HA, NA and/or M segments of the A/NL/602/09 (NL602) pandemic isolate. We confirmed that the M and NA gene segments of the NL602 virus contribute to transmissibility, and also found a requirement for a cognate HA segment for optimal transmissibility. Among the reassortant viruses tested, efficient

transmission among guinea pigs was found to correlate with increased neuraminidase activity. Surprisingly, changes to the M segment were sufficient to alter neuraminidase activity markedly, suggesting a mechanism by which M1 and/or M2 may affect transmission. Finally, our data implicate changes to virion morphology as a mechanism by which M1 and/or M2 affect the functionality of NA.

MATERIALS AND METHODS

Ethics statement

This study was performed in accordance with the recommendations in the Guide for the Care and Use of Laboratory Animals of the National Institutes of Health. Animal husbandry and experimental procedures were approved by the Emory University Institutional Animal Care and Use Committee (IACUC protocol 2001001 071214GA).

Cells

Madin-Darby Canine Kidney (MDCK) cells were maintained in minimum essential medium (MEM) supplemented with 10% FBS and penicillin-streptomycin. 293T cells were maintained in Dulbecco's MEM supplemented with 10% FBS. Human tracheo-bronchial epithelial (HTBE) cells were purchased from Lonza and cultured on transwell filters at an air-liquid interface with basal epithelial growth medium (BEGM) supplied to the basolateral chamber, essentially as directed by the manufacturer.

Guinea pigs

Female Hartley strain guinea pigs weighing 300 to 350 g were obtained from Charles River Laboratories. Prior to intranasal inoculation, nasal lavage or CO₂ euthanasia, guinea pigs were sedated with a mixture of ketamine and xylazine (30 mg/kg of body weight and 2 mg/kg, respectively). Inoculation and nasal lavage were performed as described previously (45), with PBS as the diluent/ collection fluid in each case.

Viruses

A/Puerto Rico/8/1934 (H1N1) [PR8] and A/Netherlands/602/2009 (H1N1) [NL602] based viruses were recovered by reverse genetics following standard procedures (18, 46). Briefly, 8 plasmid rescue systems based on pDZ for PR8 and pHW for NL602 (47, 48) (a kind gift of Ron Fouchier) were used to transfect 293T cells. The pHW NL602 reverse genetic-derived clones were identical to the consensus sequence present in the original clinical specimen of virus (48). One day after transfection, 293T cells and associated medium were collected and injected into 9-11 day old embryonated hens' eggs. Stock titers were determined by plaque assay on MDCK cells.

Immunostaining of plaques

Characterization of plaque phenotypes on MDCK cells was performed as described previously (49). For immunostaining, polyclonal guinea pig anti-PR8 serum (raised in-house) was used as the primary antibody, horseradish peroxidase-

linked anti-guinea pig IgG (Invitrogen) was used as the secondary antibody and TruBlue (KPL) peroxidase substrate was used for staining.

Multicycle growth experiments

MDCK cells were infected at a multiplicity of infection (MOI) of 0.002 PFU/cell. Following a 45 min incubation at 37°C, inoculum was removed and monolayers were washed with PBS. Dishes were then incubated at 37°C and samples of growth medium collected at 1, 12, 24, 48 and 72 h postinfection (hpi). Titers were determined by plaque assay on MDCK cells.

HTBE cells were washed with PBS to remove mucus, then infected at an MOI of 0.001 PFU/cell by adding virus in a 100 ul volume of PBS to the apical surface and incubating at 37°C for 45 min. The inoculum was then removed and the cells washed with PBS. At 1, 12, 24, 48 and 72 hpi, virus was collected from the apical surface of the cells by adding 200 ul PBS, incubating at 37°C for 30 min and then transferring the 200 ul PBS to a tube. Titers were determined by plaque assay on MDCK cells.

Transmission experiments

To evaluate transmission, four guinea pigs were inoculated intranasally with 10^3 , or 10^2 PFU of virus in 300 μ l PBS. At 24 h postinoculation, each infected animal was placed in the same cage with one naïve guinea pig. The four cages were then placed within an environmental chamber (Caron 6040) set to 20% relative humidity and 10°C. Standard rat cages with wire tops were used. Nasal washes were collected from all eight guinea pigs on days 2, 4, 6, and 8 postinfection, as previously

described (50).

Electron microscopy

(i) Transmission and scanning electron microscopy. For imaging of virions, MDCK cells were infected at MOI of 5. Eighteen hours post-infection, cells were fixed with 2.5% glutaraldehyde, post-fixed with 1% OsO₄ and 1.5% potassium ferrocyanide, rinsed with distilled water, and dehydrated through a series of ethanol washes. For transmission electron microscopy (TEM), monolayers were embedded in Eponate 12 resin, thin sectioned at 70nm, and stained with 5% uranyl acetate and 2% lead citrate at the Emory Robert P. Apkarian Integrated Electron Microscopy Core. After sample preparation, grids were imaged using a Hitachi H-7500 transmission electron microscope and attached CCD.

For scanning electron microscopy (SEM), the chips underwent critical point drying in a Polaron E-3000 unit, were fixed to aluminum stubs, coated with 20nm of chromium, and imaged using a Topcon DS130F scanning electron microscope.

Alternatively, to obtain negative stained images of virions, 10-day-old embryonated eggs were infected with 1,000 PFU of the relevant virus. Forty-eight hours postinfection allantoic fluid was collected, and following sucrose cushion purification, virions were dialyzed and stained with 1% aqueous methyl tungstate at the Emory Robert P. Apkarian Integrated Electron Microscopy Core. After sample preparation, grids were imaged using a Hitachi H-7500 transmission electron microscope and attached CCD.

(ii) TEM particle counts. Virions within TEM fields were counted at a magnification of 30,000 to 40,000X. For each virus between 178 and 845 virions (negatively stained TEM samples) and 53 and 239 virions (cell associated virion TEM) were counted. Filaments were defined as being equal to or greater than 300 nm in length, and no more than 200 nm in cross section, along 90% of the virion length. Virions shorter than 300 nm in length were defined as spheres. From these counts, the percentage of spherical and filamentous virions was calculated. The difference in proportions test was used to determine if the proportion of virions that were filamentous was significantly different than that of the wild type. Results were considered significant if $P < 0.05$.

Neuraminidase activity

To assess the neuraminidase activity associated with each virus, enzyme kinetic data on each virus was obtained essentially as described by Peiris and co-workers (10). Briefly, neuraminidase kinetics were determined by incubation of virus preparations with the fluorogenic sialoside, MUNANA, at final concentrations of 1.12 to 150uM in a total volume of 100 ul. Fluorescence was detected using a BioTek Synergy H1 plate reader every minute for 1 h, and the linear slopes of the resultant fluorescence curves were fit to the Michaelis-Menten non-linear regression algorithm for enzyme kinetics modeling. Virus input concentrations were normalized to PFU and confirmed to be of approximately equal number of virions by NP RNA copy number, as determined by quantitative reverse transcription-PCR (RT-qPCR) of extracted viral RNA.

RESULTS

In vitro characterization of recombinant viruses

Using reverse genetics, a set of seven reassortant viruses was generated. The set comprised the recombinant wild-type PR8 (rPR8) and NL602 viruses and five reassortants thereof: PR8 NL602 M, PR8 NL602 NA, PR8 NL602 M+NA, PR8 NL602 HA+NA and PR8 NL602 M+NA+HA (**Fig. 1A**). Initial characterization of these viruses was performed in MDCK cells. Plaque assays showed clear plaques for all of the recombinant viruses: those carrying the NL602 HA segment (including the wild-type rNL602 virus) were found to form smaller plaques than viruses carrying the PR8 HA segment (**Fig. 1B**). All recombinant viruses also replicated well in multicycle growth experiments in MDCK cells (**Fig. 1C**). Mirroring the trend in plaque morphologies, the rPR8 virus grew to the highest titers and the rNL602 virus grew to the lowest titers from low multiplicity of infection (MOI). Although the differences among the reassortant strains were small, the MDCK growth phenotypes appeared to map to the HA segment. To confirm that the recombinant NL602 virus was not attenuated due to artifactual errors in the genome, its growth in MDCK cells was compared to that of the biological NL602 isolate (**Fig. 1D**). The results indicated similar growth for rNL602 and biological NL602 viruses, with the titers of the biological NL602 being slightly lower (perhaps due to some components of this quasispecies).

Viral growth was then assessed in a more relevant substrate: fully differentiated human tracheo-bronchial epithelial (HTBE) cells cultured at air-liquid interface. In this system, the rNL602 virus showed very robust growth (peaking at

1.4x10⁸ PFU/ml after 48 h) and the lab adapted rPR8 strain showed relatively poor growth (100 to 1,000 fold lower titers than rNL602 virus) (**Fig. 2**). The growth of the PR8-NL602 reassortant viruses bracketed that of rPR8 virus: of this group, the PR8/NL602 M+NA+HA virus showed the most efficient growth and the two strains carrying the NL602 NA but the PR8 HA grew very poorly, presumably due to an HA-NA imbalance. It is interesting to note, however, that the inclusion of the NL602 M with the NL602 NA enhanced growth over the single gene reassortant with only the NL602 NA segment.

Growth and contact transmission in the guinea pig model

In the guinea pig model the wild type rNL602 virus transmits with high efficiency (**Fig. 3A and 4A**) (51, 52), while the wild-type rPR8 strain does not transmit (**Fig. 3B and 4B**) (9). With the aim of understanding the contribution of the pandemic M, NA and HA segments to the transmissible phenotype of rNL602 virus, the transmissibility of the five PR8-NL602 reassortant viruses was evaluated in a guinea pig contact model. As shown in Fig. 3C, at an inoculum dose of 1,000 PFU, the fully transmissible phenotype of rNL602 virus was recapitulated by inclusion of the pandemic M, NA and HA segments in the PR8 background. Consistent with the previous report of Chou et al. (9), we found that inclusion of only the NL602 M segment in the PR8 background also led to a marked improvement in transmission: with an n of 16 transmission pairs, this virus transmitted to 75% of contact guinea pigs (**Fig. 3E to F**). A critical role for the NL602 M segment was further confirmed by the efficient transmission of the PR8-based virus containing M and NA segments

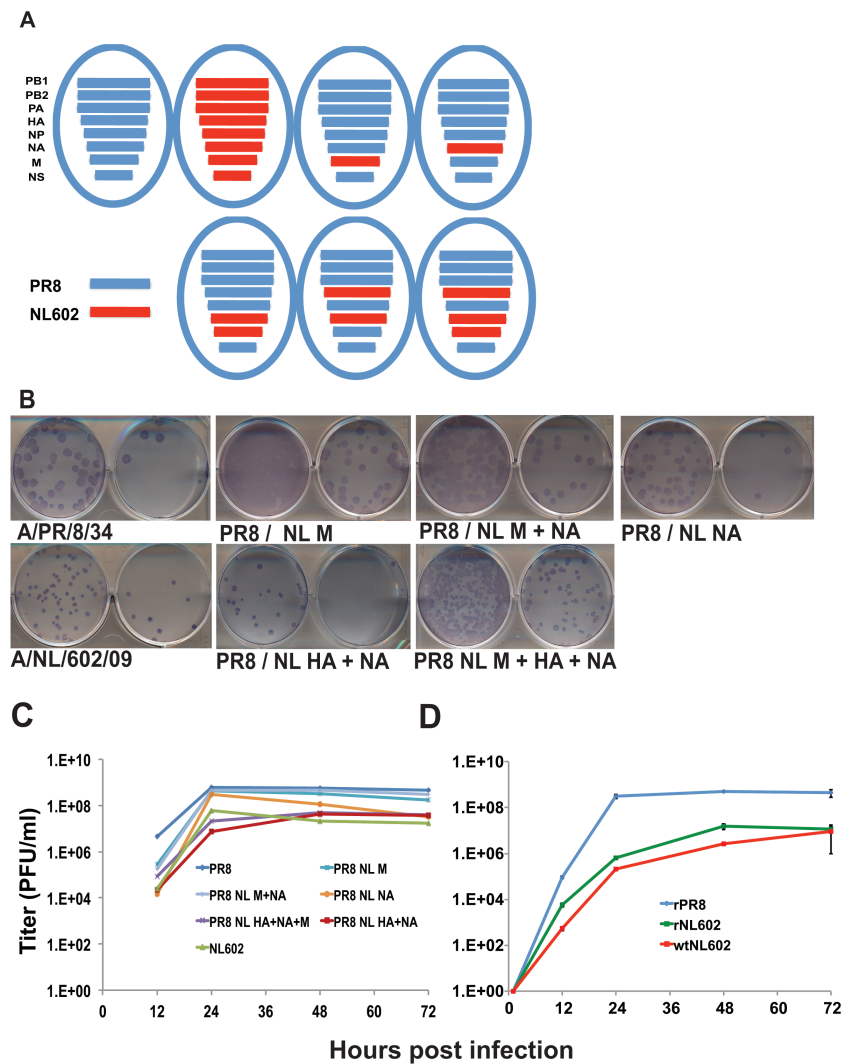


Figure 1. Schematic, plaque phenotype and growth kinetics of rescued influenza viruses in MDCK cells. (A) Virus genotypes. Blue and red bars represent genes from A/PR/8/34 and A/NL/602/09 (NL602), respectively, as indicated. **(B)** Plaque phenotype of each virus (as indicated) was visualized at 48h postinfection by immunostaining of infected MDCK cells. A polyclonal guinea pig serum reactive to PR8 virus was used to stain viral plaques. **(C)** MDCK cells were infected at a low MOI (0.002) with recombinant PR8, NL602, or PR8/ NL602 reassortant viruses as indicated, and incubated at 37°C in 5% CO₂ for 72 h. Released virus was enumerated by plaque assay of collected supernatants at indicated time points. **(D)** MDCK cells were infected at a low MOI (0.002) with recombinant and wild type NL602 viruses as indicated, and treated as described for panel C.

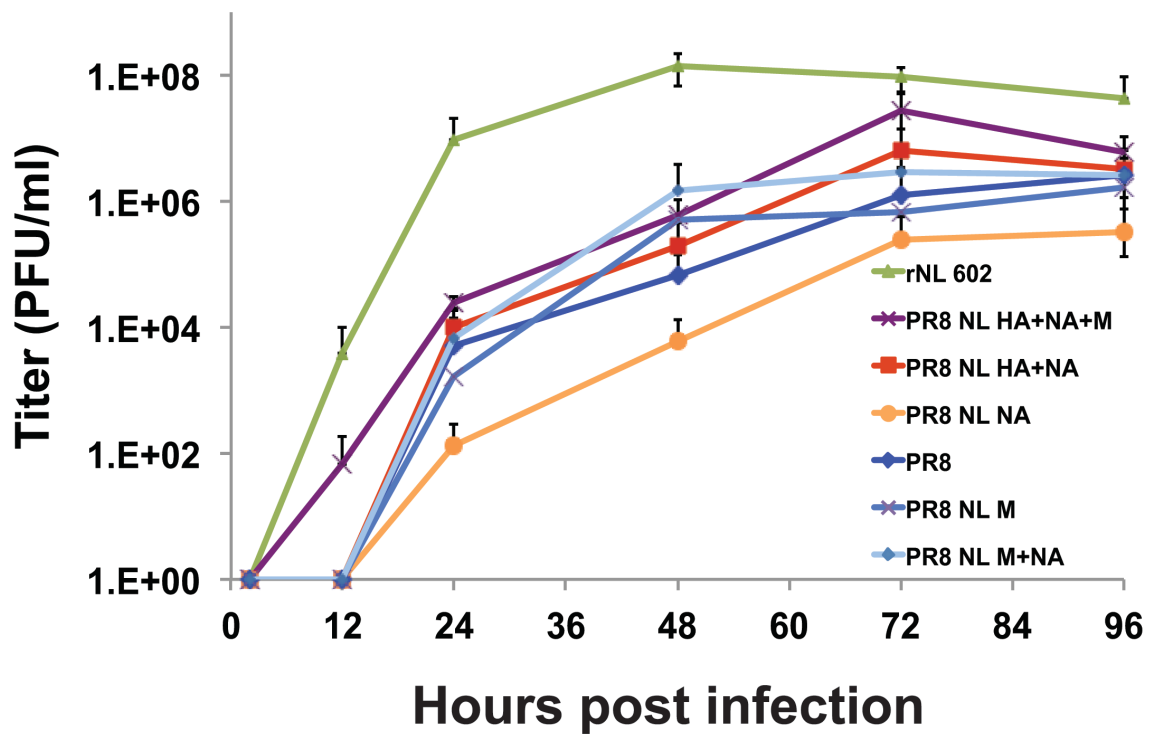


Figure 2. Growth kinetics of reassortant influenza viruses in differentiated HTBE cells. HTBE cells were infected at a low MOI (0.001) with recombinant PR8, NL602, or PR8 / NL602 reassortant viruses (as indicated), and incubated at 37°C in 5% CO₂ for 96 h. Released virus was collected from the apical surface of differentiated cells and enumerated by plaque assay at indicated time points.

from NL602, which transmitted to eight out of twelve contact animals (Figure 3D), as well as by the poor transmission of the PR8 and PR8 NL602 HA+NA viruses (**Fig. 3B and 3H**). The PR8 NL602 NA virus transmitted to four out of eight animals (**Fig. 3G**). In addition to increased transmissibility, the inclusion of the pandemic M segment, or NA segment, or both segments significantly improved growth ($P>0.05$) of the PR8-based viruses (as assayed on day two post infection) relative to the parental rPR8.

The ability of the viruses to transmit from a lower inoculation dose of 100 PFU was examined in the guinea pig model. Under these more stringent conditions, the PR8 NL602 M+NA+HA virus was again found to transmit efficiently (**Fig. 4C**), while the PR8 NL602 M+NA, PR8 NL602 M, and PR8 NL602 NA viruses each retained the ability to replicate and transmit (**Fig. 4D and E**), albeit with reduced efficiency relative to the PR8 NL602 M+NA+HA virus. In contrast, the PR8 and PR8 NL602 HA+NA viruses failed to transmit at this inoculum dose (**Fig. 4B and 4G**).

Neuraminidase activity of reassortant viruses

As neuraminidase activity has been reported to be important to the transmissibility of influenza virus in guinea pigs (53, 54), we wished to test whether the NA activity of the transmissible viruses differed from those of the non-transmissible strains. Since the M segment is central to the transmissible phenotype, we focused on viruses that differ genetically only in the M segment. Two subsets of viruses, each possessing the same NA segment were compared: (i) PR8 versus PR8 NL602 M virus, and (ii) PR8 NL602 HA+NA, versus PR8 NL602 M+NA+HA virus. In each case,

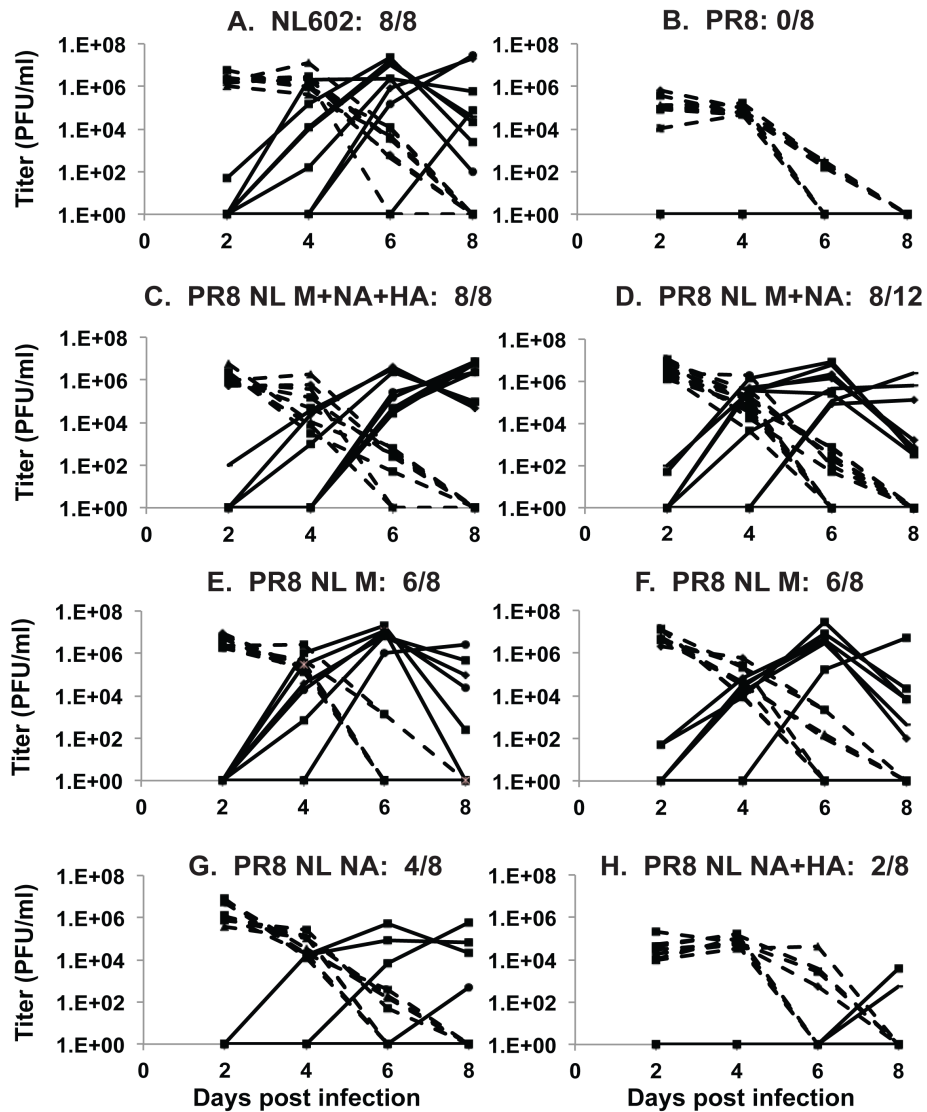


Figure 3. Growth kinetics and contact transmission of reassortant influenza viruses in guinea pigs. Guinea pigs were inoculated with 1,000 PFU of PR8, NL602, or PR8 NL602 reassortant viruses, as indicated, and viral titers in nasal wash, collected every 2 days post infection from either inoculated (dashed lines) or contact exposed (solid lines) animals, were determined by plaque assay. Each graph represents data from duplicate experiments, conducted at 10°C and 20% relative humidity, except one experiment in panel C, which was performed at 10°C and 75% relative humidity; in this case all 4 exposed animals were infected on day 6 postinfection.

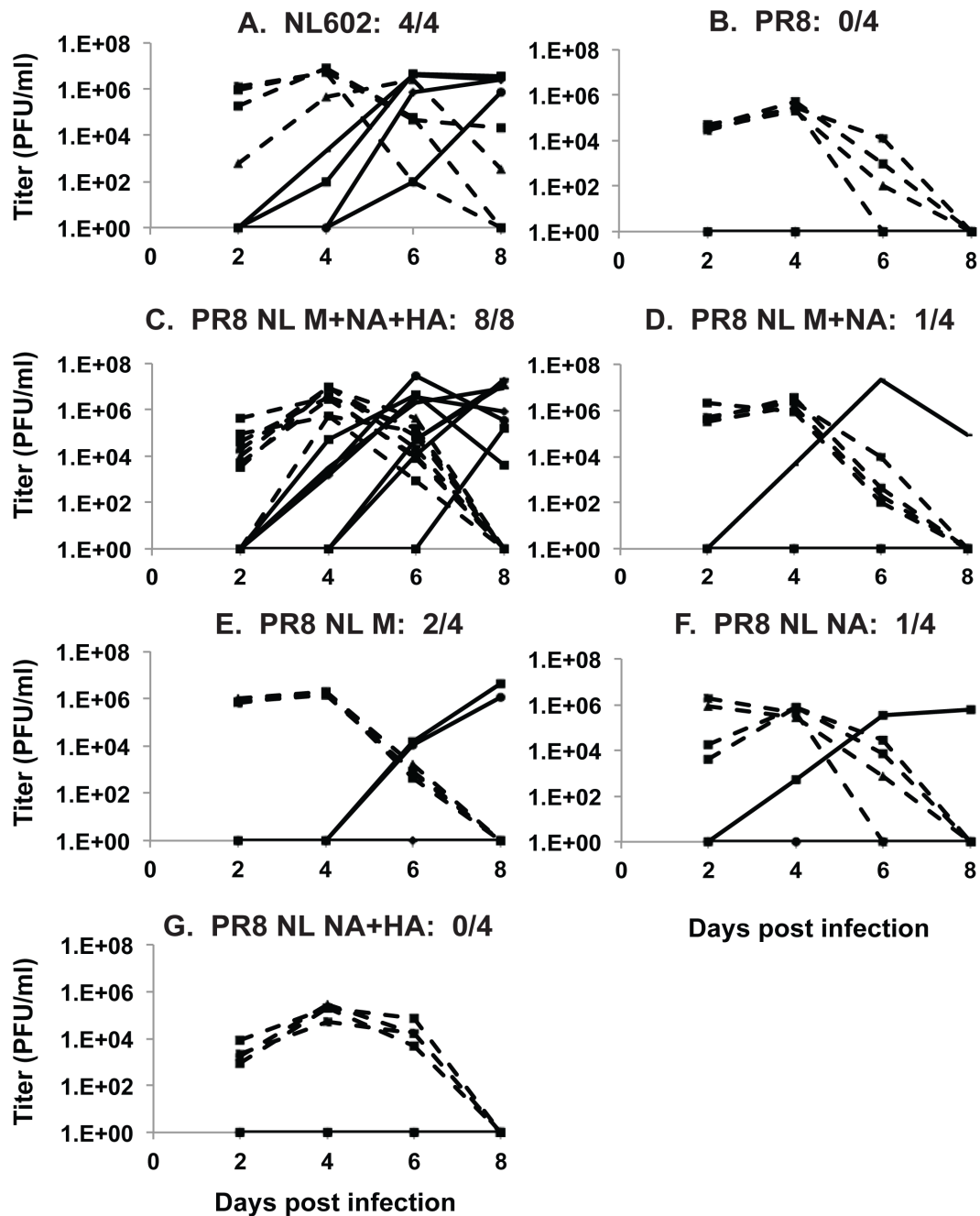


Figure 4. Growth kinetics and contact transmission of reassortant influenza viruses in guinea pigs. Guinea pigs were inoculated with 100 PFU of PR8, NL602, or PR8 NL602 reassortant viruses, as indicated, and viral titers in nasal wash, collected every 2 days post infection from either inoculated (dashed lines) or contact exposed (solid lines) animals, were determined by plaque assay.

inclusion of the pandemic M segment in place of the PR8 M segment was found to increase the neuraminidase activity associated with a standardized quantity of virions (**Table 1**). The sequence of each NA segment was verified to confirm that the observed changes in neuraminidase V_{\max} were not due to mutations that had arisen in the NA segment. In addition, while the V_{\max} of preparations possessing the pandemic M segment were increased relative to those possessing the PR8 M segment, the K_m was similar, suggesting no change in affinity of the neuraminidase protein for substrate. The increased V_{\max} of viruses possessing the pandemic M segment suggests a mechanism through which M1 and/or M2 could alter virus fitness and transmission.

Morphology of reassortant viruses

We next wished to address the mechanism by which M1 and/or M2 affects NA activity. Since spherical and filamentous virus particles differ greatly in the surface area of the (neuraminidase-containing) viral envelope, we hypothesized that changes to virion shape might be associated with changes to virion-associated neuraminidase activity; therefore, we examined the morphology of virus particles produced by each virus in our panel. As expected based on previous reports (29, 55), the rPR8 virus produced spherical or small ovoid particles almost exclusively (**Fig. 5C and D**). Also consistent with published data on 2009 pandemic strains (34, 56), the rNL602 virus was highly filamentous (**Fig. 5E and F**), particularly when imaged associated with a cell monolayer. Negative stain transmission electron microscopy of released rNL602 virus, concentrated through ultracentrifugation with a sucrose

cushion, revealed a wide range of virion shapes, including filaments and spheres (**Fig. 7A**). While it is typical, even for a filamentous influenza virus, to see spherical virions by this method (32), the larger spheres and irregular shapes observed are most likely cellular debris, and filaments that were damaged during preparation of the concentrated sample. Imaging of the PR8 NL602 M+NA+HA virus by cell associated transmission electron microscopy revealed robust filament formation, similar to that seen with the rNL602 virus (compare **Fig. 6A and B** to **Fig. 5E and F**). When the NL602 M segment alone was included in the PR8 background, filamentous virus particles were produced (**Fig. 6C and D**), but to relatively lower levels of prevalence compared to the PR8 NL602 M+NA+HA reassortant ($P>0.05$ by difference of proportions test). Interestingly, the NL602 NA alone was also found to confer a partially filamentous morphology to the PR8-based virus, PR8 NL602 NA (**Fig. 6E and F**). In contrast, while the PR8 HA+NA virus produced a number of filaments, these were typically shorter in length than the PR8 NL602 NA virus (**Fig. 6G and H, Table 2**).

The relative proportions of spherical (<300 nm), and filamentous (>300 nm) virions produced by each virus, as visualized by negative stain TEM of released virus (**Fig. 7**) and TEM of infected MDCK cells, is summarized in **Table 2**. The results of these size-based particle counts clearly show quantitative differences among the virus strains in the prevalence of filaments.

In summary, the NL602 M and NA segments individually, or in combination, conferred varying degrees of filamentous virion morphology to PR8 virus. The M, NA and HA segments from NL602 together generated a morphologic phenotype

TABLE 1 Virions possessing the PR8 M segment have lower V_{\max} , but not K_m , of NA interaction with MUNANA than virions possessing NL602 M

Virus and input ^a (PFU)	V_{\max} ^b (SE; 95% CI)	K_m (SE; 95% CI)
PR8		
1×10^6	1,798 (72.1; 1,645–1,950)	8.1 (1.4; 5.2–11.1)
	1,807 (55.7; 1,687–1,926)	9.9 (1.1; 7.5–12.2)
	1,908 (52.7; 1,794–2,021)	10.8 (1.1; 8.5–13.1)
PR8/NL M		
1×10^6	2,621 (67.3; 2,476–2,765)	10.8 (1.0; 8.7–12.9)
	2,568 (73.0; 2,411–2,724)	11.2 (1.1; 8.7–13.5)
	2,749 (73.1; 2,592–2,905)	11.6 (1.1; 8.9–13.4)
PR8/NL HA+NA ^c		
1×10^5	1,407 (31.4; 1,304–1,475)	28.2 (1.8; 24.4–32.0)
	1,472 (40.3; 1,386–1,556)	29.3 (2.2; 24.5–34.0)
	1,618 (22.1; 1,499–1,738)	22.1 (2.7; 16.3–27.8)
PR8/NL M+NA+HA ^c		
1×10^5	2,354 (75.5; 2,192–2,516)	24.7 (2.3; 19.8–29.7)
	2,296 (74.4; 2,136–2,455)	23.3 (2.2; 18.5–28.1)
	2,266 (90.9; 2,073–2,458)	18.8 (2.8; 13.0–24.7)

^a Presence of equal numbers of virions was confirmed by measuring NP RNA copy number using qRT-PCR. No significant difference in copy number was observed between PR8 and PR8/NL M virus preparations or between PR8/NL HA+NA and PR8/NL M+NA+HA virus preparations in independent experiments.

^b Enzyme kinetics data were fit to the Michaelis-Menten equation by nonlinear regression to determine the Michaelis constant (K_m) and maximum velocity (V_{\max}) of substrate conversion. CI, confidence interval. SE, standard errors. For each virus, data are presented from three independent experiments.

^c Note that the NA proteins of PR8 NL09 HA+NA and PR8 NL09 HA+NA+M differ from the NA carried by PR8 and PR8 NL09 M; thus, the NL09 NA-containing viruses should only be compared to each other.

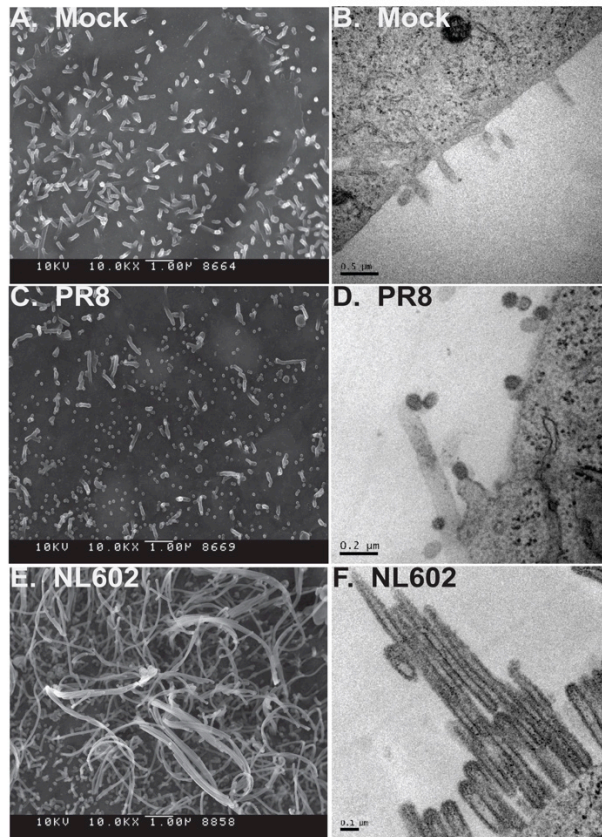


Figure 5. *PR8 and NL602 viruses display distinct virion morphologies.* Virion morphologies shown as SEM (A, C and E) or TEM (B, D and F) images of well-bound MDCK cells that were infected at MOI 5.0 and mock incubated, or incubated with virus for 16 h, before fixing and staining. Mock infected MDCK cells display distinctive filapodia (A and B). PR8 virus is visible as spherical virions of 100 to 200 nm diameter (C and D) while NL602 virus produced pleiomorphic virions, including highly filamentous examples (E and F).

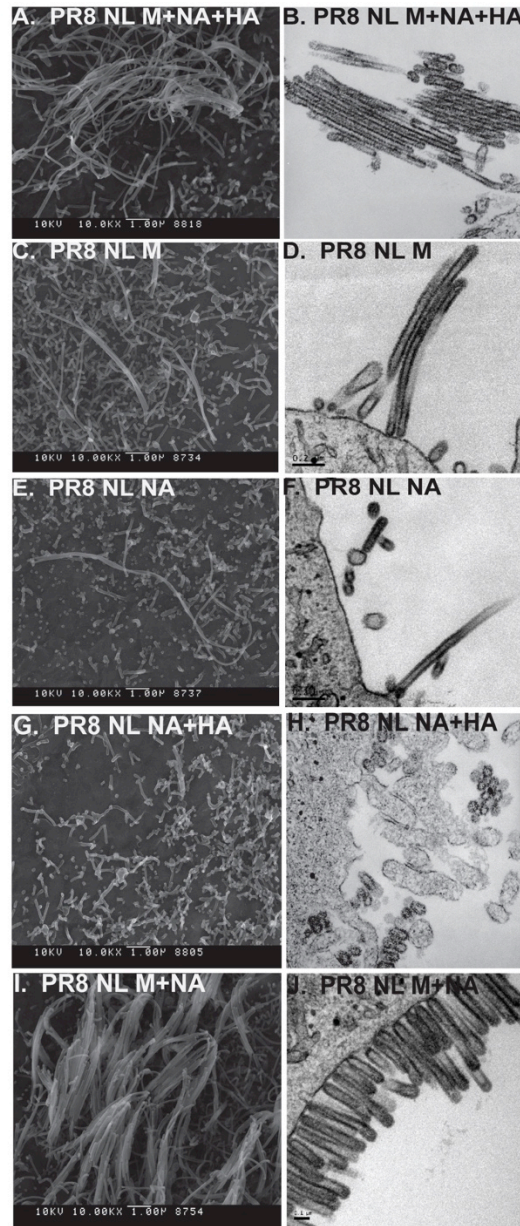


Figure 6. *PR8/NL M+NA+HA virus recapitulates the virion morphology of rNL602 virus.* Virion morphologies shown as SEM (A,C,E,G, and I) or TEM images (B, D,F,H, and J) of well-bound MDCK cells that were infected at MOI 5.0 and incubated with the indicated viruses for 16 h before fixing and staining. PR8 NL M+NA+HA virus exhibits long filaments, as well as spheres, similar to the rNL602 virus (compare A and B with Fig.5E and F). Other reassortant viruses display various rates of prevalence of filamentous particles.

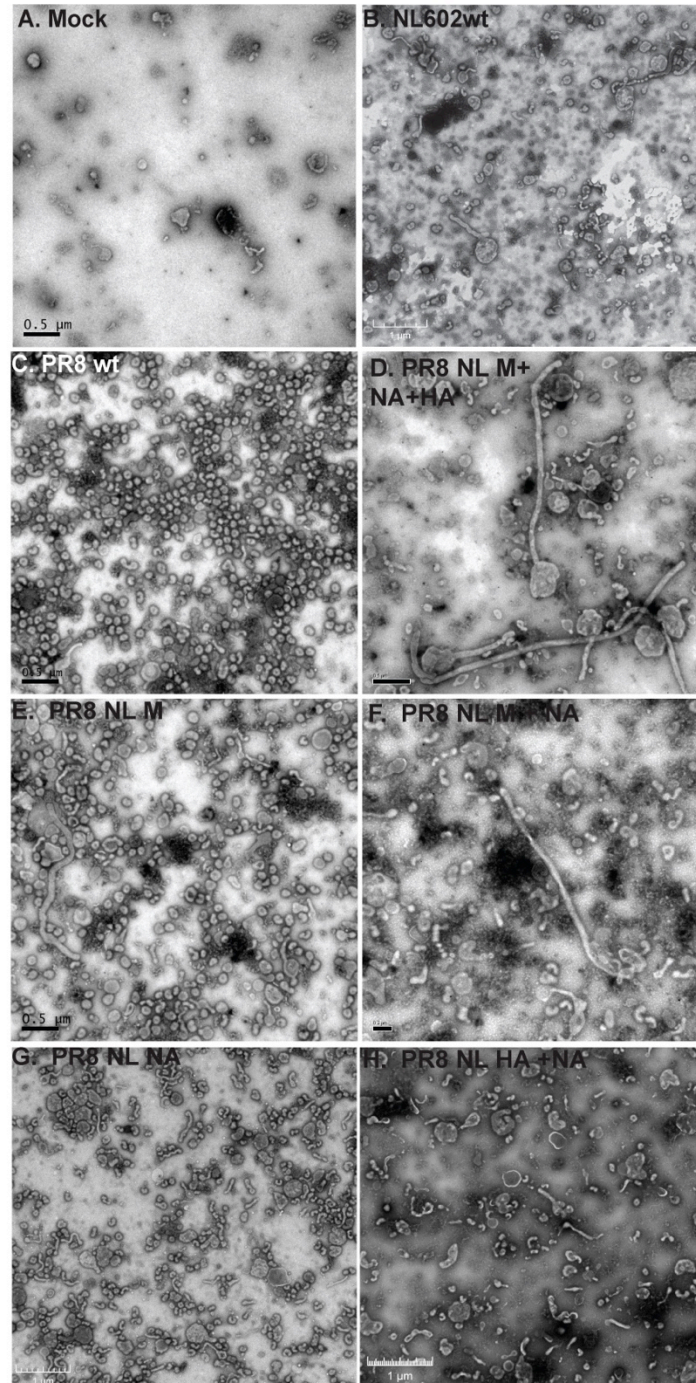


Figure 7. *PR8/NL M+NA+HA* recapitulates the virion morphology of *rNL602 virus*. Virion morphologies shown as negative stain images of influenza virions, as indicated, grown in embryonated chicken egg for 48h and concentrated through sucrose-cushioned centrifugation before fixing and staining.

TABLE 2 Reassortant viruses differ in prevalence of filamentous virions

Morphology and particle length (nm)	Virus prevalence ^a (%)													
	rPR8		PR8/NL HA+NA		PR8/NL NA		PR8/NL M+NA		PR8/NL M		PR8/NL M+NA+HA		rNL602	
	NS	TEM	NS	TEM	NS	TEM	NS	TEM	NS	TEM	NS	TEM	NS	TEM
Spherical														
<100	6.5	75.5	8.9	53.8	9.6	47.9	1.8	16.7	2.7	42.4	4.9	44.8	24.2	20.9
100–200	80.6	24.5	67.1	42.4	65.3	32.9	57.4	27.2	75.2	43.0	53.2	14.7	47.8	31.8
200–300	9.5	0	17.1	1.6	15.7	9.6	26.4	15.5	14.0	4.1	13.1	11.0	16.9	12.2
All sizes	96.6	100	93.0	100	90.6	90.4	85.6	59.4	91.9	89.5	71.1	70.6	88.8	64.9
Filamentous														
300–500	3.2	0	4.9	2.2	7.0	2.7	9.8	25.5	5.3	2.3	16.7	8.6	2.8	27.7
500–1,000	0.2	0	1.9	0	2.4	6.8	3.4	14.2	2.3	4.7	6.4	16.6	5.1	4.7
>1,000	0	0	0.2	0	0	0	1.2	0.8	0.5	3.5	5.8	4.3	3.4	2.7
All sizes	3.4 ^b	0	7.0 ^b	2.2 ^b	9.4 ^b	9.6 ^b	14.4 ^b	40.6	8.1 ^b	10.5 ^b	28.9	29.4	11.2 ^b	35.1
Total no. of particles	845	53	428	184	510	73	326	239	786	172	329	163	178	148
Total % transmission efficiency in GP ^c	0		17		42		56		70		100		100	

^a NS, negative-stain TEM of released virus; TEM, TEM of infected, sectioned MDCK cells.

^b Percentage of filamentous virions (>300 nm in length) is significantly different ($P > 0.05$) from that of PR8/NL M+NA+HA by difference of proportions test.

^c Combined results of contact transmission experiments involving guinea pigs (GP) inoculated at either 100 or 1,000 PFU and naive cagemates.

which was highly similar to the full wild type NL602 virus. Of significant interest, a strong correlation between the prevalence of filamentous particles greater than 300nm, and efficiency of contact transmission was observed (**Table 2**). Thus, our data suggest a model in which pandemic M1 and/or M2 lead to increased virion associated NA activity on a per virion basis, and therefore heightened transmissibility, by favoring the production of longer filamentous virions than the parental PR8.

DISCUSSION

We have shown that a recombinant PR8-based influenza virus, possessing the M, NA and HA gene segments from the pH1N1 strain A/NL/602/09, is capable of efficient contact transmission in the guinea pig model from low-dose inoculation. This transmission was indistinguishable from that of wild type recombinant A/NL/602/09 virus. Consistent with previously published data (9), our evaluation

of single-gene reassortants indicated the M segment of the pandemic strain is critical, and the NA segment of the pandemic strain contributes independently, to the transmission of a PR8-based virus in the guinea pig model. Interestingly, wild-type NL602 virus and the PR8 NL M+NA+HA virus retained optimally efficient transmission among guinea pigs upon reduction of the inoculation dose to 100 PFU. In contrast, the PR8 NL M, PR8 NL M+NA, and PR8 NL NA viruses demonstrated decreased transmission under these more stringent conditions, suggesting that each of the HA, NA, and M segments derived from NL602 contribute to the optimal transmission of the PR8-based virus. Neither the PR8 nor the PR8 NL HA+NA viruses transmitted from guinea pigs infected at 100 PFU. Examination of transmission from low dose is a valuable experimental tool for dissecting relative transmission efficiencies. In addition, we suggest that this assay is biologically relevant: the ability of a virus to transmit efficiently from a host infected at a low dose would be a highly advantageous biological trait, likely conferring an important selective advantage at a population level.

Of note, Ma and colleagues (12) have shown that, in a swine influenza virus background, strains individually possessing either the 2009 pandemic M or NA segment grew to lower titers than parental virus, either *in vitro* (in MDCK cells), or following intratracheal inoculation of swine at a dose of 10^6 EID₅₀. However, in each substrate, the reassortant strain containing both the M and NA segments replicated to higher titer than the parental swine virus. *In vivo*, the M+NA virus also subsequently transmitted among swine. A virus possessing pandemic M, NA, and HA segments in the parental background was not tested in that study.

The level of neuraminidase activity exhibited by particular influenza virus strains has been shown to affect transmission efficiency in both guinea pig and ferret models (57). In addition to the observation that HA/NA balance is critical for the transmission of the 2009 pandemic virus (10), a number of research groups have demonstrated that mutations that confer resistance to NA inhibitors, and reduce the NA activity of the virus, also resulted in decreased transmission (53, 54). These resistance mutations can affect both the replication and transmission of influenza viruses carrying them (58, 59). In some cases, however, viruses possessing NA inhibitor resistant phenotypes nonetheless transmit efficiently, and permissive changes elsewhere in the NA gene (60), as well as the overall gene constellation, appear to play a role in supporting transmission of these viruses (57).

We have also found that transmission correlates with increased NA activity. Interestingly, this trend is clear even between virus pairs that carry identical NA genes and differ only in their M segment. Thus, we have shown that the NA activity of influenza virus particles is dependent on the M segment. We suggest that this effect is mediated through virion morphology and that transmission, NA activity, and virion morphology are therefore linked.

It is not conclusive from our data that the observed increases in NA activity conferred by the inclusion of the NL602 M segment, in place of the PR8 M, are biologically relevant. It is possible that as the NA activity increases, presumably through increased incorporation of NA, a concomitant increase in HA molecules results in particles that maintain an overall balance between HA and NA. However, we have not assessed incorporation levels of HA or NA in the virions biochemically,

and our data do not allow us to assess whether levels of virion incorporated HA and NA increase proportionately as the virion length increases. It is furthermore possible that proportionate changes in the levels of HA and NA would not be “functionally colinear”, such that increases in avidity due to increased levels of virion associated HA occur at a different rate to increases in receptor cleavage efficiency. These aspects of the virion biology remain to be investigated.

Among the viruses on our panel, strains producing long filamentous virions tended to transmit more efficiently among guinea pigs. Wild-type A/PR/8/34 virus, which is almost exclusively spherical, did not transmit. PR8 NL HA+NA virus possesses mainly short filamentous or spherical virions and transmitted inefficiently. The inclusion of the NL602 M segment in the PR8 virus, which increased replication of the resultant virus *in vivo* and conferred 75% transmission at 1,000 PFU inoculum, also altered the proportion of virions longer than 1 μm from 0%, in PR8, to 3.5% in PR8 NL M, as assessed by measurement of TEM images. The largely filamentous PR8 NL M+NA+HA and wt NL602 virions possess 4.3% and 2.7% of filaments greater than 1 μm in length (as assessed by TEM), respectively, and both transmitted efficiently, even from an inoculation dose of 100 PFU. While we did not observe a strong correlation between shedding titers and transmission efficiency, those viruses that transmitted least efficiently (PR8 and PR8 NL NA+HA) were shed to markedly lower titers than the remaining viruses.

A recent report by Subbarao and colleagues (11) involving reassortant virus strains possessing pH1N1 M and NA segments also supports a role for morphological changes in determining transmissibility. In that study, replacement

of the pandemic M and NA segments with those from a swine adapted virus resulted in a loss of respiratory droplet transmissibility from ferrets inoculated intranasally at $10^{6.5}$ TCID₅₀. This non-transmissible strain also exhibited a spherical morphology. In trying to understand how the M segment impacts transmissibility, our data do not allow us to separate the effects of M on morphology and NA activity. Nevertheless, we favor a model in which changes to morphology allow modulation of NA activity and in turn, transmissibility over the alternative model in which virion shape is an independent determinant of transmission.

Several previous studies have demonstrated that the gene products of the M segment affect the morphology of the influenza virion (28, 29, 31, 32). Elleman and colleagues (29) reported that that differences in morphology between (i) the lab adapted strains A/PR/8/34 and A/WSN/33 and (ii) the human isolate A/Victoria/3/75 could be mapped to the matrix protein, and in particular M1 residues 41, 95, and 218. Similarly, Bourmakina and colleagues (28) identified M1 residues 95 and 204 as morphology determinants. Roberts and colleagues reported that amino acids in both the matrix and M2 proteins affect virion morphology (32), again including M1 residue 41.

The matrix proteins of PR8 and NL602 have 13 amino acid differences (95% identity), while the M2 proteins of the strains differ by 14 amino acids (86% identity). We have not mapped the specific residues that are responsible for the observed phenotypes in the present study, but among the changes, M1 residue 41, as well as residues 207, 209 and 214 (which map close to residue 218, also identified by Elleman and colleagues) differ between the PR8 and NL602 strains.

The NA protein of influenza virus has been reported to interact with the M1 protein through its cytoplasmic tail and transmembrane regions (61, 62). Furthermore, Mitnaul and colleagues (63) have shown that deletion of the NA cytoplasmic tail can alter the morphology of influenza virions, suggesting that NA-M1 interaction affects morphology. Notably, no amino acid differences exist in the NA cytoplasmic tail domains of PR8 and NL602, suggesting that amino acid residues in the transmembrane domain of NA may be responsible for the changes in morphology observed upon replacement of the PR8 NA with that of NL602. There are 8 amino acid polymorphisms between the two transmembrane domains, as well as additional differences present in the membrane proximal stalk region of the two proteins.

In sum, our data reveal a previously unappreciated mechanism through which the M segment can tune the receptor destroying activity of influenza virus. We suggest that M1 or M2 mediated changes to morphology could alter NA V_{\max} through alterations in NA incorporation, distribution or presentation at the virion surface. We also show that cognate (NL602) M, NA, and HA segments confer more efficient transmissibility than a matched (PR8) HA and NA combined with the NL602 M segment. The M-NA functional interaction we describe appears to underlie the prominent role of the 2009 pandemic M segment in supporting efficient transmission, and may be a highly important means by which influenza viruses restore HA/NA balance following reassortment or transfer to new host environments.

ACKNOWLEDGEMENTS

We are grateful to Ron Fouchier for the A/Netherlands/602/2009 (H1N1) virus and reverse genetics system pHW NL602. We also appreciate the work of Hong Yi and Jeannette Taylor of the Robert P. Apkarian Integrated Electron Microscopy Core for TEM and SEM sample processing. We thank the Georgia Research Alliance for support to JS and AL through equipment grants.

This work was funded by the Centers for Excellence in Influenza Research and Surveillance (CEIRS) contract number HHSN266200700006C.

REFERENCES

1. **Dacso CC, Couch RB, Six HR, Young JF, Quarles JM, Kasel JA.** 1984. Sporadic occurrence of zoonotic swine influenza virus infections. *J Clin Microbiol* **20**:833-835.
2. **de Jong JC, de Ronde-Verloop JM, Bangma PJ, van Kregten E, Kerckhaert J, Paccaud MF, Wicki F, Wunderli W.** 1986. Isolation of swine-influenza-like A(H1N1) viruses from man in Europe, 1986. *Lancet* **2**:1329-1330.
3. **Gregory V, Bennett M, Thomas Y, Kaiser L, Wunderli W, Matter H, Hay A, Lin YP.** 2003. Human infection by a swine influenza A (H1N1) virus in Switzerland. *Arch Virol* **148**:793-802.
4. **Rota PA, Rocha EP, Harmon MW, Hinshaw VS, Sheerar MG, Kawaoka Y, Cox NJ, Smith TF.** 1989. Laboratory characterization of a swine influenza

- virus isolated from a fatal case of human influenza. *J Clin Microbiol* **27**:1413-1416.
5. **Wells DL, Hopfensperger DJ, Arden NH, Harmon MW, Davis JP, Tipple MA, Schonberger LB.** 1991. Swine influenza virus infections. Transmission from ill pigs to humans at a Wisconsin agricultural fair and subsequent probable person-to-person transmission. *JAMA* **265**:478-481.
 6. **Myers KP, Olsen CW, Gray GC.** 2007. Cases of swine influenza in humans: a review of the literature. *Clin Infect Dis* **44**:1084-1088.
 7. **Garten RJ, Davis CT, Russell CA, Shu B, Lindstrom S, Balish A, Sessions WM, Xu X, Skepner E, Deyde V, Okomo-Adhiambo M, Gubareva L, Barnes J, Smith CB, Emery SL, Hillman MJ, Rivailler P, Smagala J, de Graaf M, Burke DF, Fouchier RA, Pappas C, Alpuche-Aranda CM, Lopez-Gatell H, Olivera H, Lopez I, Myers CA, Faix D, Blair PJ, Yu C, Keene KM, Dotson PD, Jr., Boxrud D, Sambol AR, Abid SH, St George K, Bannerman T, Moore AL, Stringer DJ, Blevins P, Demmler-Harrison GJ, Ginsberg M, Kriner P, Waterman S, Smole S, Guevara HF, Belongia EA, Clark PA, Beatrice ST, Donis R, Katz J, Finelli L, Bridges CB, Shaw M, Jernigan DB, Uyeki TM, Smith DJ, Klimov AI, Cox NJ.** 2009. Antigenic and genetic characteristics of swine-origin 2009 A(H1N1) influenza viruses circulating in humans. *Science* **325**:197-201.
 8. **Smith GJ, Vijaykrishna D, Bahl J, Lycett SJ, Worobey M, Pybus OG, Ma SK, Cheung CL, Raghwani J, Bhatt S, Peiris JS, Guan Y, Rambaut A.** 2009.

- Origins and evolutionary genomics of the 2009 swine-origin H1N1 influenza A epidemic. *Nature* **459**:1122-1125.
9. **Chou YY, Albrecht RA, Pica N, Lowen AC, Richt JA, Garcia-Sastre A, Palese P, Hai R.** 2011. The M segment of the 2009 new pandemic H1N1 influenza virus is critical for its high transmission efficiency in the guinea pig model. *J Virol* **85**:11235-11241.
 10. **Yen HL, Liang CH, Wu CY, Forrest HL, Ferguson A, Choy KT, Jones J, Wong DD, Cheung PP, Hsu CH, Li OT, Yuen KM, Chan RW, Poon LL, Chan MC, Nicholls JM, Krauss S, Wong CH, Guan Y, Webster RG, Webby RJ, Peiris M.** 2011. Hemagglutinin-neuraminidase balance confers respiratory-droplet transmissibility of the pandemic H1N1 influenza virus in ferrets. *Proc Natl Acad Sci U S A* **108**:14264-14269.
 11. **Lakdawala SS, Lamirande EW, Suguitan AL, Jr., Wang W, Santos CP, Vogel L, Matsuoka Y, Lindsley WG, Jin H, Subbarao K.** 2011. Eurasian-origin gene segments contribute to the transmissibility, aerosol release, and morphology of the 2009 pandemic H1N1 influenza virus. *PLoS Pathog* **7**:e1002443.
 12. **Ma W, Liu Q, Bawa B, Qiao C, Qi W, Shen H, Chen Y, Ma J, Li X, Webby RJ, Garcia-Sastre A, Richt JA.** 2012. The neuraminidase and matrix genes of the 2009 pandemic influenza H1N1 virus cooperate functionally to facilitate efficient replication and transmissibility in pigs. *J Gen Virol* **93**:1261-1268.

13. **Sorrell EM, Wan H, Araya Y, Song H, Perez DR.** 2009. Minimal molecular constraints for respiratory droplet transmission of an avian-human H9N2 influenza A virus. *Proc Natl Acad Sci U S A* **106**:7565-7570.
14. **Tumpey TM, Maines TR, Van Hoeven N, Glaser L, Solorzano A, Pappas C, Cox NJ, Swayne DE, Palese P, Katz JM, Garcia-Sastre A.** 2007. A two-amino acid change in the hemagglutinin of the 1918 influenza virus abolishes transmission. *Science* **315**:655-659.
15. **Herfst S, Schrauwen EJ, Linster M, Chutinimitkul S, de Wit E, Munster VJ, Sorrell EM, Bestebroer TM, Burke DF, Smith DJ, Rimmelzwaan GF, Osterhaus AD, Fouchier RA.** 2012. Airborne transmission of influenza A/H5N1 virus between ferrets. *Science* **336**:1534-1541.
16. **Imai M, Watanabe T, Hatta M, Das SC, Ozawa M, Shinya K, Zhong G, Hanson A, Katsura H, Watanabe S, Li C, Kawakami E, Yamada S, Kiso M, Suzuki Y, Maher EA, Neumann G, Kawaoka Y.** 2012. Experimental adaptation of an influenza H5 HA confers respiratory droplet transmission to a reassortant H5 HA/H1N1 virus in ferrets. *Nature* **486**:420-428.
17. **Van Hoeven N, Pappas C, Belser JA, Maines TR, Zeng H, Garcia-Sastre A, Sasisekharan R, Katz JM, Tumpey TM.** 2009. Human HA and polymerase subunit PB2 proteins confer transmission of an avian influenza virus through the air. *Proc Natl Acad Sci U S A* **106**:3366-3371.
18. **Steel J, Lowen AC, Mubareka S, Palese P.** 2009. Transmission of influenza virus in a mammalian host is increased by PB2 amino acids 627K or 627E/701N. *PLoS Pathog* **5**:e1000252.

19. **Maines TR, Chen LM, Matsuoka Y, Chen H, Rowe T, Ortin J, Falcon A, Nguyen TH, Mai le Q, Sedyaningsih ER, Harun S, Tumpey TM, Donis RO, Cox NJ, Subbarao K, Katz JM.** 2006. Lack of transmission of H5N1 avian-human reassortant influenza viruses in a ferret model. *Proc Natl Acad Sci U S A* **103**:12121-12126.
20. **Noton SL, Medcalf E, Fisher D, Mullin AE, Elton D, Digard P.** 2007. Identification of the domains of the influenza A virus M1 matrix protein required for NP binding, oligomerization and incorporation into virions. *J Gen Virol* **88**:2280-2290.
21. **Rossman JS, Lamb RA.** 2011. Influenza virus assembly and budding. *Virology* **411**:229-236.
22. **Bui M, Whittaker G, Helenius A.** 1996. Effect of M1 protein and low pH on nuclear transport of influenza virus ribonucleoproteins. *J Virol* **70**:8391-8401.
23. **Rossman JS, Jing X, Leser GP, Lamb RA.** 2010. Influenza virus M2 protein mediates ESCRT-independent membrane scission. *Cell* **142**:902-913.
24. **Ciampor F, Thompson CA, Grambas S, Hay AJ.** 1992. Regulation of pH by the M2 protein of influenza A viruses. *Virus Res* **22**:247-258.
25. **Grambas S, Hay AJ.** 1992. Maturation of influenza A virus hemagglutinin-- estimates of the pH encountered during transport and its regulation by the M2 protein. *Virology* **190**:11-18.
26. **Shimbo K, Brassard DL, Lamb RA, Pinto LH.** 1996. Ion selectivity and activation of the M2 ion channel of influenza virus. *Biophys J* **70**:1335-1346.

27. **Takeuchi K, Lamb RA.** 1994. Influenza virus M2 protein ion channel activity stabilizes the native form of fowl plague virus hemagglutinin during intracellular transport. *J Virol* **68**:911-919.
28. **Bourmakina SV, Garcia-Sastre A.** 2003. Reverse genetics studies on the filamentous morphology of influenza A virus. *J Gen Virol* **84**:517-527.
29. **Elleman CJ, Barclay WS.** 2004. The M1 matrix protein controls the filamentous phenotype of influenza A virus. *Virology* **321**:144-153.
30. **Burleigh LM, Calder LJ, Skehel JJ, Steinhauer DA.** 2005. Influenza A viruses with mutations in the m1 helix six domain display a wide variety of morphological phenotypes. *J Virol* **79**:1262-1270.
31. **Bialas KM, Desmet EA, Takimoto T.** 2012. Specific residues in the 2009 H1N1 swine-origin influenza matrix protein influence virion morphology and efficiency of viral spread in vitro. *PLoS ONE* **7**:e50595.
32. **Roberts PC, Lamb RA, Compans RW.** 1998. The M1 and M2 proteins of influenza A virus are important determinants in filamentous particle formation. *Virology* **240**:127-137.
33. **Rossman JS, Jing X, Leser GP, Balannik V, Pinto LH, Lamb RA.** 2010. Influenza virus m2 ion channel protein is necessary for filamentous virion formation. *J Virol* **84**:5078-5088.
34. **Seladi-Schulman J, Steel J, Lowen AC.** 2013. Spherical influenza viruses have a fitness advantage in embryonated eggs, while filament-producing strains are selected in vivo. *Journal of Virology* **Accepted**.

35. **Palese P, Shaw ML.** 2006. Orthomyxoviridae: The Viruses and Their Replication, p. 1648-1689. *In* Knipe DM, Howley PM (ed.), *Fields Virology*, 5th ed, vol. II. Lippencott Williams and Wilkins, Philadelphia.
36. **Matrosovich MN, Matrosovich TY, Gray T, Roberts NA, Klenk HD.** 2004. Neuraminidase is important for the initiation of influenza virus infection in human airway epithelium. *J Virol* **78**:12665-12667.
37. **Wagner R, Matrosovich M, Klenk HD.** 2002. Functional balance between haemagglutinin and neuraminidase in influenza virus infections. *Rev Med Virol* **12**:159-166.
38. **Shtyrya Y, Mochalova L, Voznova G, Rudneva I, Shilov A, Kaverin N, Bovin N.** 2009. Adjustment of receptor-binding and neuraminidase substrate specificities in avian-human reassortant influenza viruses. *Glycoconj J* **26**:99-109.
39. **Lu B, Zhou H, Ye D, Kemble G, Jin H.** 2005. Improvement of influenza A/Fujian/411/02 (H3N2) virus growth in embryonated chicken eggs by balancing the hemagglutinin and neuraminidase activities, using reverse genetics. *J Virol* **79**:6763-6771.
40. **Das SR, Hensley SE, David A, Schmidt L, Gibbs JS, Puigbo P, Ince WL, Bennink JR, Yewdell JW.** 2011. Fitness costs limit influenza A virus hemagglutinin glycosylation as an immune evasion strategy. *Proc Natl Acad Sci U S A* **108**:E1417-1422.
41. **Das SR, Hensley SE, Ince WL, Brooke CB, Subba A, Delboy MG, Russ G, Gibbs JS, Bennink JR, Yewdell JW.** 2013. Defining influenza A virus

- hemagglutinin antigenic drift by sequential monoclonal antibody selection. *Cell Host Microbe* **13**:314-323.
42. **Hensley SE, Das SR, Bailey AL, Schmidt LM, Hickman HD, Jayaraman A, Viswanathan K, Raman R, Sasisekharan R, Bennink JR, Yewdell JW.** 2009. Hemagglutinin receptor binding avidity drives influenza A virus antigenic drift. *Science* **326**:734-736.
43. **Aoki FY, Boivin G, Roberts N.** 2007. Influenza virus susceptibility and resistance to oseltamivir. *Antivir Ther* **12**:603-616.
44. **Xu R, Zhu X, McBride R, Nycholat CM, Yu W, Paulson JC, Wilson IA.** 2012. Functional balance of the hemagglutinin and neuraminidase activities accompanies the emergence of the 2009 H1N1 influenza pandemic. *J Virol* **86**:9221-9232.
45. **Lowen AC, Mubareka S, Tumpey TM, Garcia-Sastre A, Palese P.** 2006. The guinea pig as a transmission model for human influenza viruses. *Proc Natl Acad Sci U S A* **103**:9988-9992.
46. **Fodor E, Devenish L, Engelhardt OG, Palese P, Brownlee GG, Garcia-Sastre A.** 1999. Rescue of influenza A virus from recombinant DNA. *J Virol* **73**:9679-9682.
47. **Chutinimitkul S, Herfst S, Steel J, Lowen AC, Ye J, van Riel D, Schrauwen EJ, Bestebroer TM, Koel B, Burke DF, Sutherland-Cash KH, Whittleston CS, Russell CA, Wales DJ, Smith DJ, Jonges M, Meijer A, Koopmans M, Rimmelzwaan GF, Kuiken T, Osterhaus AD, Garcia-Sastre A, Perez DR, Fouchier RA.** 2010. Virulence-associated substitution D222G in the

- hemagglutinin of 2009 pandemic influenza A(H1N1) virus affects receptor binding. *J Virol* **84**:11802-11813.
48. **Munster VJ, de Wit E, van den Brand JM, Herfst S, Schrauwen EJ, Bestebroer TM, van de Vijver D, Boucher CA, Koopmans M, Rimmelzwaan GF, Kuiken T, Osterhaus AD, Fouchier RA.** 2009. Pathogenesis and transmission of swine-origin 2009 A(H1N1) influenza virus in ferrets. *Science* **325**:481-483.
49. **Gao Q, Brydon EW, Palese P.** 2008. A seven-segmented influenza A virus expressing the influenza C virus glycoprotein HEF. *J Virol* **82**:6419-6426.
50. **Lowen AC, Mubareka S, Tumpey TM, García-Sastre A, Palese P.** 2006. The guinea pig as a transmission model for human influenza viruses. *PNAS* **103**:9988-9992.
51. **Steel J, Staeheli P, Mubareka S, Garcia-Sastre A, Palese P, Lowen AC.** 2010. Transmission of pandemic H1N1 influenza virus and impact of prior exposure to seasonal strains or interferon treatment. *J Virol* **84**:21-26.
52. **Steel J, Palese P, Lowen AC.** 2011. Transmission of a 2009 pandemic influenza virus shows a sensitivity to temperature and humidity similar to that of an H3N2 seasonal strain. *J Virol* **85**:1400-1402.
53. **Kaminski MM, Ohnemus A, Staeheli P, Rubbenstroth D.** 2013. Pandemic 2009 H1N1 influenza A virus carrying a Q136K mutation in the neuraminidase gene is resistant to zanamivir but exhibits reduced fitness in the guinea pig transmission model. *J Virol* **87**:1912-1915.

54. **Bouvier NM, Lowen AC, Palese P.** 2008. Oseltamivir-resistant influenza A viruses are transmitted efficiently among guinea pigs by direct contact but not by aerosol. *Journal of virology* **82**:10052-10058.
55. **Shangguan T, Siegel DP, Lear JD, Axelsen PH, Alford D, Bentz J.** 1998. Morphological changes and fusogenic activity of influenza virus hemagglutinin. *Biophys J* **74**:54-62.
56. **Itoh Y, Shinya K, Kiso M, Watanabe T, Sakoda Y, Hatta M, Muramoto Y, Tamura D, Sakai-Tagawa Y, Noda T, Sakabe S, Imai M, Hatta Y, Watanabe S, Li C, Yamada S, Fujii K, Murakami S, Imai H, Kakugawa S, Ito M, Takano R, Iwatsuki-Horimoto K, Shimojima M, Horimoto T, Goto H, Takahashi K, Makino A, Ishigaki H, Nakayama M, Okamatsu M, Warshauer D, Shult PA, Saito R, Suzuki H, Furuta Y, Yamashita M, Mitamura K, Nakano K, Nakamura M, Brockman-Schneider R, Mitamura H, Yamazaki M, Sugaya N, Suresh M, Ozawa M, Neumann G, Gern J, Kida H, Ogasawara K, Kawaoka Y.** 2009. In vitro and in vivo characterization of new swine-origin H1N1 influenza viruses. *Nature* **460**:1021-1025.
57. **Govorkova EA.** 2013. Consequences of resistance: in vitro fitness, in vivo infectivity, and transmissibility of oseltamivir-resistant influenza A viruses. *Influenza Other Respir Viruses* **7 Suppl 1**:50-57.
58. **Yen HL, Herlocher LM, Hoffmann E, Matrosovich MN, Monto AS, Webster RG, Govorkova EA.** 2005. Neuraminidase inhibitor-resistant influenza viruses may differ substantially in fitness and transmissibility. *Antimicrob Agents Chemother* **49**:4075-4084.

59. **Herlocher ML, Truscon R, Elias S, Yen HL, Roberts NA, Ohmit SE, Monto AS.** 2004. Influenza viruses resistant to the antiviral drug oseltamivir: transmission studies in ferrets. *J Infect Dis* **190**:1627-1630.
60. **Bloom JD, Gong LI, Baltimore D.** 2010. Permissive secondary mutations enable the evolution of influenza oseltamivir resistance. *Science* **328**:1272-1275.
61. **Ali A, Avalos RT, Ponimaskin E, Nayak DP.** 2000. Influenza virus assembly: effect of influenza virus glycoproteins on the membrane association of M1 protein. *J Virol* **74**:8709-8719.
62. **Barman S, Ali A, Hui EK, Adhikary L, Nayak DP.** 2001. Transport of viral proteins to the apical membranes and interaction of matrix protein with glycoproteins in the assembly of influenza viruses. *Virus Res* **77**:61-69.
63. **Mitnaul LJ, Castrucci MR, Murti KG, Kawaoka Y.** 1996. The cytoplasmic tail of influenza A virus neuraminidase (NA) affects NA incorporation into virions, virion morphology, and virulence in mice but is not essential for virus replication. *J Virol* **70**:873-879.

CHAPTER 2

Residue 41 of the Eurasian avian-like swine influenza A virus matrix protein modulates virion filament length and efficiency of contact transmission

Patricia J. Campbell, Constantinos S. Kyriakis, Nicolle Marshall, Suganthi Suppiah, Jill Seladi-Schulman, Shamika Danzy, Anice C. Lowen and
John Steel

This work was published in 2014 in the Journal of Virology.

Article Citation:

Campbell PJ, Suppiah S, Marshall N, Kyriakis CS, Seladi-Schulman J, Danzy S, Lowen AC, Steel J. 2014. Residue 41 of the Eurasian avian-like swine influenza A virus matrix protein modulates virion filament length and efficiency of contact transmission. J Virol 88(13):7569.

ABSTRACT

Position 41 of the influenza A virus matrix protein encodes a highly conserved alanine in human and avian lineages. Nonetheless, strains of the Eurasian avian-like swine (Easw) lineage demonstrate change at this position, and A/swine/Spain/53207/04 (H1N1) (SPN04) encodes a proline. To assess the impact of this naturally occurring polymorphism on viral fitness, we utilized reverse genetics to produce recombinant viruses encoding wild-type M1 41P (rSPN04-P) and consensus 41A (rSPN04-A) residues. Relative to rSPN04-A, rSPN04-P virus displayed reduced growth *in vitro*. In the guinea pig model, rSPN04-P transmitted to fewer contact animals than rSPN04-A and failed to infect guinea pigs from low dose inoculum. Moreover, the P41A change altered virion morphology, reducing the number and length of filamentous virions, as well as reducing the neuraminidase activity of virions. The lab-adapted human isolate, A/PR/8/34 (H1N1) (PR8), is non-transmissible in the guinea pig model, making it a useful background in which to identify certain viral factors that enhance transmissibility. We assessed transmission in the context of single, double and triple reassortant viruses between PR8 and SPN04: PR8/SPN04 M, PR8/SPN04 M+NA, and PR8/SPN04 M+NA+HA, encoding either matrix 41 A or P were generated. In each case, the virus possessing 41P transmitted less well than the corresponding 41A-encoding virus. In summary, we have identified a naturally occurring mutation in the influenza A virus matrix protein that impacts transmission efficiency and can alter virion morphology and neuraminidase activity.

IMPORTANCE

We have developed a practical model for examining the genetics underlying transmissibility of the Eurasian avian-like swine lineage viruses, which contributed M and NA segments to the 2009 pandemic strain. Herein we use our system to investigate the impact on viral fitness of a naturally occurring polymorphism at matrix (M1) position 41 in an Easw isolate. Position 41 has been implicated previously in adaptation to laboratory substrates and to mice. Here we show that the polymorphism at M1 41 has limited effect on growth in vitro, but changes the morphology of the virus and impacts growth and transmission in the guinea pig model.

INTRODUCTION

In 1979, an avian influenza A virus of the H1N1 subtype entered swine populations in Belgium and Germany and established a stable lineage that has since spread across Europe and Asia (1-3). The resultant Eurasian avian-like swine virus (Easw) lineage continues to circulate in Eurasia today (4). Zoonoses of Easw lineage influenza A viruses to humans are typically self-limiting and clinically mild events (5) which do not lead to sustained human-to-human transmission (6-10). Nevertheless, the M and NA segments derived from the Easw lineage (11) are important for the highly transmissible phenotype of the 2009 pandemic H1N1 virus (12-14). Thus, viruses of the Easw lineage are important for animal health, can cause human disease, and have a demonstrated potential to contribute to the emergence of pandemic strains. Still, very little is known about the genetic and

molecular factors that influence the transmission and replication of Eurasian avian-like swine viruses (15).

The influenza A virus matrix (M1) protein is encoded in the bicistronic M gene segment. The protein functions in both virus assembly and budding (16-19): it recruits the viral ribonucleoprotein (vRNP) complex to the cell surface during virion assembly (17, 20, 21) and lines the inner surface of the viral membrane.

Additionally, M1 provides structural integrity to the influenza virion through interaction with HA and NA glycoproteins (17, 21, 22). The M1 protein is a major determinant of influenza virion morphology (23-27).

Clinical isolates of influenza A virus typically include filamentous virions, whereas lab adaptation often produces strains that exhibit an exclusively spherical morphology (24, 28, 29). The biological relevance of filamentous influenza virions is currently unclear. Mutations arising in the M1 gene can convert an exclusively spherical influenza virus to one that produces a pleomorphic mixture of spheres and filaments, and vice versa (23-28). Elleman and colleagues (24) reported that the morphology of the lab adapted strains A/PR/8/34 and A/WSN/33 differ from that of the human isolate, A/Victoria/3/75, and mapped the phenotypic difference to matrix protein residues 41, 95, and 218. Roberts and colleagues also demonstrated that residue 41 of the matrix protein affects virion morphology (27). In both of these studies, replacement of the alanine at position 41 with valine led to a loss in filamentous morphology.

Interestingly, an alanine-to-valine polymorphism at residue 41 of the matrix has been identified upon adaptation to mice in multiple influenza A strains (30-32).

The mutation has been linked to increases in replication and virulence in the mouse model (31, 32).

The SPN04 virus possesses a highly unusual polymorphism at position 41 of the matrix protein, encoding a proline. A minority of Easw viruses encode a valine at position 41 and the predominant residue is alanine.

We hypothesized that the proline at position 41 of the SPN04 matrix protein would alter virion morphology and, although naturally occurring may attenuate the growth and transmission of the SPN04 virus. By testing this hypothesis we aimed to shed light on the biological significance of filamentous influenza virions. Our results show that substitution of the widely conserved alanine for proline at position 41 of the matrix protein reduces transmission between guinea pigs, both in the context of the Eurasian avian-like swine virus, A/swine/Spain/53207/04, and in the PR8-based reassortant viruses tested. The A41P mutation concomitantly increased the filament length of each of the viruses.

MATERIALS AND METHODS

Ethics statement

This study was performed in accordance with the recommendations in the *Guide for the Care and Use of Laboratory Animals* of the National Institutes of Health (32b). Animal husbandry and experimental procedures were approved by the Emory University Institutional Animal Care and Use Committee (IACUC protocol 2001001 071214GA).

Cells

Human tracheo-bronchial epithelial (HTBE) cells, purchased from Lonza, were cultured on Transwell filters at an air-liquid interface, and maintained in basal epithelial growth medium (BEGM) supplied to the basolateral chamber as directed by the manufacturer. Madin-Darby Canine Kidney (MDCK) cells were maintained in minimal essential medium (MEM) supplemented with 10% fetal bovine serum (FBS) and penicillin-streptomycin. 293T cells were maintained in Dulbecco's MEM supplemented with 10% FBS.

Guinea pigs

Female Hartley strain guinea pigs weighing 300 to 350 g were obtained from Charles River Laboratories. Inoculation and nasal lavage were performed as described previously (33). Prior to all procedures, guinea pigs were sedated with a mixture of ketamine and xylazine (30 mg/kg of body weight and 2 mg/kg, respectively).

Reverse genetics system

Recombinant virus was generated as previously described (34). Briefly, viral RNA, extracted from A/swine/Spain/53207/04 (H1N1) influenza virus, was reverse transcribed and amplified using influenza segment-specific primers (35), resulting in 8 specific cDNA products, corresponding to each of the viral gene segments. Six cDNAs (NS, M, NA, NP, HA and PA) were flanked by LguI restriction enzyme sites. PB1 and PB2 segments were flanked by sequences allowing cloning into pPol1

plasmid by recombination (36). cDNAs were digested with LglI as appropriate and subsequently cloned by ligation or recombination into the pPol1 plasmid.

Viruses

A/NL/602/09 (H1N1) (a kind gift of Ron Fouchier) virus is an early 2009 pandemic H1N1 strain that was isolated from a patient in The Netherlands. A/Puerto Rico/8/1934 (H1N1) [PR8]-based and A/swine/Spain/53207/2004 (H1N1) [SPN04]-based viruses were recovered by reverse genetics following previously described procedures (34, 37). Briefly, 8- or 12- plasmid rescue systems, based on pDZ (38) for PR8 (8 plasmids) and pPol1 for SPN04 (12 plasmids, including pCAGGS WSN PA, PB1, PB2 and NP support plasmids), were used to transfect 293T cells. Reassortant viruses were recovered by using the relevant plasmids from both systems (see **Fig. 1** for depiction of virus gene constellations). One day after transfection, 293T cells and associated medium were collected and injected into 11-day-old embryonated chicken eggs. Stock titers were determined by plaque assay on MDCK cells. A mutation was introduced into the pPol1 SPN04 M segment plasmid, which altered residue 41 from a proline to an alanine, generating the pPol1 SPN04 M 41A plasmid. Viruses containing this mutation were rescued in the same manner as described above.

Immunostaining and enumeration of plaques

Characterization of plaque phenotypes on MDCK cells was performed as described previously (39). For immunostaining, polyclonal guinea pig anti-PR8

serum, or anti-SPN04 serum (raised in-house) were used as the primary antibodies; horseradish peroxidase-linked anti-guinea pig IgG (Invitrogen) was used as the secondary antibody and TruBlue (KPL) peroxidase substrate was used for staining. A total of 125 plaques formed by each virus were measured, using ImageJ software, and statistical analyses were performed on the results using Prism software.

Multicycle growth experiments

MDCK cells were inoculated at a multiplicity of infection (MOI) of 0.002 PFU/cell. Following a 45-min incubation at 37°C, inoculum was removed and monolayers were washed with PBS. Dishes were then incubated at 37°C and samples of growth medium collected at 1, 12, 24, 48 and 72 hours postinfection (hpi). Titers were determined by plaque assay on MDCK cells.

HTBE cells were washed with PBS to remove mucus and then inoculated at an MOI of 0.001 PFU/cell by adding virus in a 100- μ l volume of PBS to the apical surface and incubating at 37°C for 45-min. The inoculum was then removed, and the cells washed with PBS. At 1, 12, 24, 48 and 72 hpi, virus was collected from the apical surface of the cells by adding 200 μ l PBS, incubating at 37°C for 30 min and then collecting the 200 μ l of supernatant. Titers were determined by plaque assay on MDCK cells.

Neuraminidase activity

To compare the neuraminidase activity associated with the viruses, 5×10^5 PFU of each variant was incubated in the presence of the fluorogenic sialoside, 2-(4-

methylumbelliferyl)-D-N-acetylneuraminic acid (MUNANA; Sigma), at final concentration of 150 μ M in a total volume of 100 μ l. Fluorescence, which is emitted upon cleavage of the MUNANA substrate by the influenza virus neuraminidase enzyme, was detected using a BioTek Synergy H1 plate reader, and recorded every minute for 45 min. The slopes of the resultant fluorescence curves of each pair of viruses were compared. Each experiment included triplicate samples for each virus, and experiments were performed at least three times.

Transmission experiments

In order to assess transmission, four guinea pigs were inoculated by the intranasal route with 10³ or, in some cases, 10² PFU of virus in 300 μ l PBS. At 24 h postinoculation, infected animals were each placed in a cage with a naïve guinea pig. The four cages were subsequently placed within an environmental chamber (Caron 6040) set to 20% relative humidity and 10°C. Nasal washes were collected from all 8 animals on days 2, 4, 6, and 8 post-infection, as previously described (40).

Electron microscopy

(i) Transmission electron microscopy. For imaging of virions, MDCK cells were inoculated at MOI of 5. At 18 hours postinfection, cells were fixed with 2.5% glutaraldehyde, post-fixed with 1% OsO₄ and 1.5% potassium ferrocyanide, rinsed with distilled water, and dehydrated through a series of ethanol washes. For transmission electron microscopy (TEM), monolayers were embedded in Eponate 12 resin, and stained with 5% uranyl acetate and 2% lead citrate at the Emory

Robert P. Apkarian Integrated Electron Microscopy Core. After sample preparation, grids were imaged using a Hitachi H-7500 transmission electron microscope and attached charged-couple device (CCD).

(ii) *Scanning electron microscopy.* For scanning electron microscopy (SEM), the chips underwent critical point drying in a Polaron E-3000 unit, were fixed to aluminum stubs, coated with 20nm of chromium, and imaged using a Topcon DS130F scanning electron microscope.

RESULTS

In vitro characterization of recombinant viruses

Using reverse genetics, a set of eight recombinant viruses was generated. The set comprised the recombinant (r) wild-type (WT) SPN04 (rSPN04-P) and SPN04 M41A (rSPN04-A) viruses, which differed in the identity of residue 41 of the matrix protein (proline or alanine), and six reassortants between A/PR/8/34 (PR8) and SPN04: PR8/SPN04 M; PR8/SPN04 M41A; PR8/SPN04 M+NA; PR8/SPN04 M41A+NA; PR8/SPN04 M+NA+HA; and PR8/SPN04 M41A+NA+HA (**Fig. 1**). rPR8 virus was rescued as previously described (28). The SPN04 virus rescue system was generated for this study. The cloned SPN04 cDNAs were confirmed to be of the correct size by restriction enzyme digest with XbaI and each plasmid was fully sequenced to confirm agreement with Genbank accession sequences (CY010584; CY010581; CY010582; CY010583; CY010580; CY010585; CY010586; CY010587).

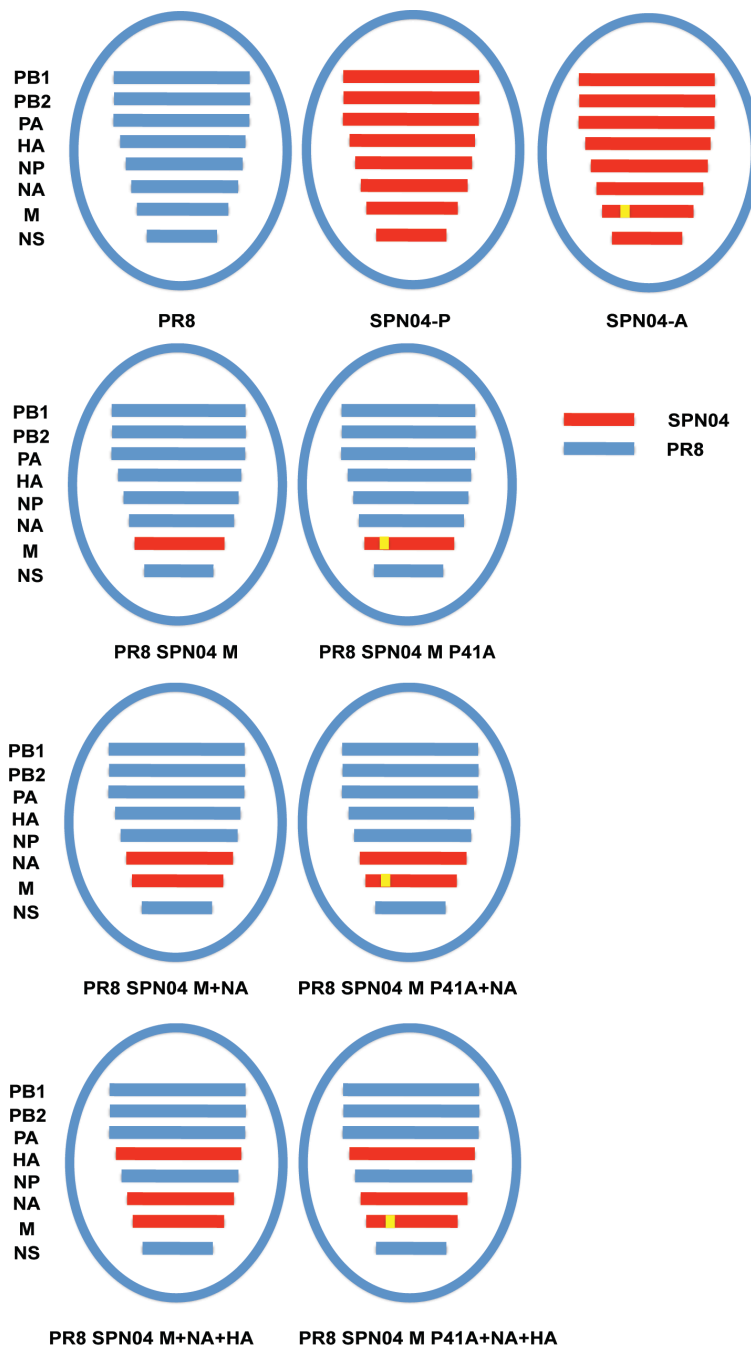


Figure 1. Schematic diagram of recombinant viruses. Genotypes of each recombinant virus used in the study are depicted. Blue and red bars represent genes from A/PR/8/34 (H1N1) (PR8) and A/swine/Spain/53207/04 (H1N1) (SPN04) viruses, respectively. The yellow bar indicates the presence of a point mutation encoding a proline to alanine change at position 41 of the matrix protein.

(i) SPN04-based viruses

Initial characterization of the viruses was performed *in vitro*. In MDCK cells, the biologic and the recombinant wild-type SPN04 viruses grew with comparable kinetics and to similar peak titers of approximately 1×10^8 PFU/ml after 48 h. No significant difference was found between the areas under the curve (AUC) for each virus (\log_{10} 9.70 for WT versus \log_{10} 9.65 for recombinant virus; $P=0.13$ by unpaired *t*-test), confirming that the recombinant virus was not attenuated due to unwanted mutations in the genome (**Fig. 2A**). Next, the growth of wild-type rSPN04-P and the point mutant rSPN04-A viruses were assayed on fully differentiated HTBE cells cultured at air-liquid interface and on MDCK cells. In HTBE cells, the average AUC for the rSPN04-A virus was significantly higher than that for the rSPN04-P virus (\log_{10} 9.51 versus \log_{10} 9.27; $P=0.012$ by unpaired *t*-test) (**Fig. 2B**). Similarly, in MDCK cells the rSPN04-A virus had a significantly higher average AUC than that for the rSPN04-P virus (\log_{10} 10.15 versus \log_{10} 9.81; $P=0.001$ by unpaired *t*-test) (**Fig. 2C**). Finally, during growth in MDCK cells, a reduction in plaque size attributable to the alanine-to-proline mutation was shown to be statistically significant ($P<0.05$; one-way analysis of variance) (**Fig. 2E**). In summary, the alanine-to-proline substitution in the matrix protein resulted in reduced growth phenotypes of the SPN04 virus in multiple *in vitro* assays.

(ii) PR8-based reassortant viruses

Since the lab-adapted PR8 virus does not transmit among guinea pigs, reassortant viruses with a PR8 backbone can be a sensitive platform on which to identify

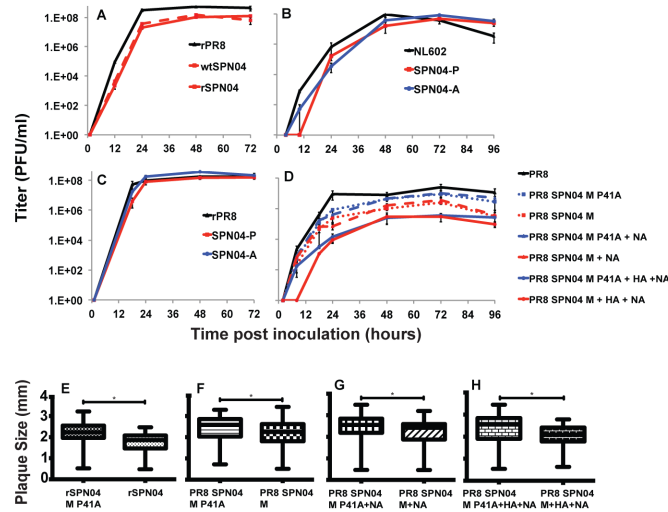


Figure 2. Characterization of recombinant viruses in HTBE and MDCK cells.

A. MDCK cells were infected at a low MOI (0.002) with recombinant PR8, rSPN04 or WT SPN04 viruses. Released virus was collected from the supernatant and enumerated by plaque assay at indicated time-points. **B.** HTBE cells were infected at a low MOI (0.001) with recombinant NL602, SPN04-P or SPN04-A viruses, and incubated at 37°C in 5% CO₂ for 96 hours. Released virus was collected from the apical surface of differentiated cells and enumerated by plaque assay. **C.** MDCK cells were infected at a low MOI (0.002) with recombinant PR8, SPN04-P or SPN04-A viruses. Released virus was collected and enumerated as described in **(A)**. **D.** MDCK cells were infected at a low MOI (0.002) with recombinant PR8, PR8/SPN04 M41P, PR8/SPN04 M41A, PR8/SPN04 M41P+NA, PR8/SPN04 M41A+NA, PR8/SPN04 M41P+NA+HA, or PR8/SPN04 M41A+NA+HA viruses. Each virus possessing a proline at position 41 had marginally delayed kinetics of growth relative to the viruses possessing an alanine at that position. Moreover, PR8/SPN04 M41P and PR8/SPN04 M41P+NA viruses grew to slightly lower peak titers than the isogenic virus possessing alanine at position 41. Released virus was collected from the supernatant and enumerated as described in **A**. Plaque size of each recombinant virus was measured at 48h postinfection following immunostaining of infected MDCK cells. Values for the diameter of at least 125 plaques were plotted for each pair of recombinant viruses as indicated **(E-H)**. Statistically significant differences between plaque sizes are denoted by an asterisk ($P < 0.05$).

polymorphisms that affect transmission (12, 28). We applied this approach to the SPN04 virus and, because the influenza matrix protein is known to interact with the cytoplasmic tails of the influenza glycoproteins (19), we evaluated multiple reassortant viruses possessing the HA, NA and M segments of SPN04, comparing three pairs of viruses possessing the alanine to proline substitution in the matrix protein of SPN04, as follows: PR8/SPN04 M and PR8/SPN04 M41A; PR8/SPN04 M+NA and PR8/SPN04 M41A+NA; PR8/SPN04 M+NA+HA and PR8/SPN04 M41A+NA+HA.

Low-multiplicity growth curves performed in MDCK cells demonstrated that viruses possessing the HA, NA and M segments from SPN04 grew more poorly than other PR8-based viruses, regardless of the nature of the polymorphism at position 41 of the matrix (**Fig. 2D**), and that there was no significant difference between the AUCs for the pair of 5:3 reassortant viruses ($\log_{10}7.15$ for PR8/SPN04 M+NA+HA versus $\log_{10}7.25$ for PR8/SPN04 M41A+NA+HA; $P=0.56$ by unpaired *t*-test). Those reassortants carrying the PR8 HA were more fit in MDCK cells than those carrying the SPN04 HA. Given that the WT rSPN04 virus grew to high titers in MDCK cells, the data collectively suggest an incompatibility between the SPN04 HA and gene product(s) of the PR8 virus internal genes. Significant differences were observed between the growth phenotypes of the PR8/SPN04 M and PR8/SPN04 M41A, as well as the PR8/SPN04 M+NA and PR8/SPN04 M41A+NA virus pairs in MDCK cells (**Fig. 2D**). PR8/SPN04 M41A virus had a significantly higher average AUC compared to the PR8/SPN04 M41P virus ($\log_{10}8.55$ versus $\log_{10}7.95$; $P=0.0003$ by unpaired *t*-test). Similarly, PR8/SPN04 M41A+NA virus had a significantly higher average AUC

than PR8/SPN04 M41P+NA virus ($\log_{10}8.62$ versus $\log_{10}8.11$; $P=0.001$ by unpaired t -test).

The plaque size of each of the PR8/SPN04 reassortant viruses was assessed. A total of 125 plaques formed by each virus on MDCK cells were measured. For each virus pair, a statistically significant reduction in plaque size was observed with the PR8/SPN04 virus encoding proline, relative to that encoding alanine at matrix position 41 ($P<0.05$; one-way analysis of variance), (**Fig. 2F to H**). In summary, the alanine-to-proline substitution in the matrix protein had an attenuating effect on growth phenotypes of the PR8/SPN04-reassortant viruses *in vitro*, while PR8-based viruses possessing the SPN04 HA grew more poorly than viruses possessing the PR8 HA in MDCK cells.

Morphology of 41P- versus 41A-encoding viruses

As previous studies have demonstrated that an alanine-to-valine polymorphism at position 41 of the matrix protein affects the morphology of multiple influenza A strains (23, 24, 27), we wished to examine the effect of the proline to alanine change at this position on virion morphology. Using electron microscopy, we studied MDCK cells infected with viruses encoding each amino acid. rSPN04-P exhibits a highly filamentous phenotype in MDCK cells, as observed by either scanning or transmission electron microscopy (**Fig. 3A and B**). Examples of filaments greater than 10 μm in length were visible by SEM. The mutation of P41 in the rSPN04 virus matrix to A41 alters the morphology of the virion, reducing the length of the filaments from larger than 10 μm to a typical length of approximately 1

µm or less (**Fig. 3C and D**) (**Table 1**). rSPN04-P virus yielded 36% of virions greater than 300 nm in length, as measured by TEM, compared to 26% for rSPN04-A virus. Moreover, only the proline-encoding virus displayed filaments greater than 1 µm in length as assayed by TEM. The same trend was observed with two pairs of the PR8/SPN04 reassortant viruses: PR8/SPN04 M41P and PR8/SPN04 M41P+NA possessed 24% and 71% of virions greater than 300 nm in length (**Fig. 3A, B, E, and F**), as measured by TEM, compared to 4% and 56% for the respective alanine-encoding viruses (**Fig. 3C, D, G, and H**). Again, only the proline containing viruses possessed filaments greater than 1 µm in length (**Table 1**). Surprisingly, for the PR8/SPN04 M 41P+NA+HA and PR8/SPN04 M 41A+NA+HA viruses, the same trends in virion morphology were not observed. Similarly to the PR8/SPN04 M41P and PR8/SPN04 M41P+NA viruses, the proline containing 5:3 reassortant virus possessed virions measured at greater than 1 µm in length, while the PR8/SPN04 M41A+HA+NA virus did not. Nonetheless, the alanine-containing virus possessed a greater proportion of filamentous virions between 300 nm and 1 µm than the proline-containing variant.

Neuraminidase activity of 41P- versus 41A-encoding viruses

As we have previously observed a correlation between neuraminidase activity of influenza virions and extent of filamentous morphology (41), we tested whether the NA activity of the matrix 41P-encoding viruses differed from those of the 41A-encoding strains. For this purpose, we used an *in vitro* assay based on the fluorescent substrate MUNANA. Three of the four pairs of viruses (SPN04,

PR8/SPN04 M, and PR8/SPN04 M+NA), showed higher neuraminidase activity in the proline-encoding variants (**Fig. 4A, B, and C**), and this activity correlated with presence of higher proportions of virions greater than 300 nm in length (**Table 1**). Conversely, in the alanine-containing variant of the PR8/SPN04 M+HA+NA virus, the neuraminidase activity was higher than that of the proline-containing variant (**Fig. 4D**). Notably, in this pair of viruses, it is the 41A variant that has a higher proportion of particles >300nm in length. Thus, in each case, the neuraminidase activity of the virions correlated with increased filament length.

Growth and contact transmission in the guinea pig model

We employed a guinea pig contact model, as previously described (33, 42), in order to assess the effect of the alanine-to-proline mutation on the infectivity, replication and transmission of the rSPN04 virus. As shown in **Fig. 5A**, at an inoculum dose of 1,000 PFU, the inclusion of a proline at position 41 resulted in productive infection with rSPN04-P in three of four guinea pigs, and transmission occurred from one of these animals to a cage mate. By comparison, four out of four animals were infected with rSPN04-A virus at this inoculum dose, and two transmission events occurred (**Fig. 5B**). Due to the small numbers of animals involved in this experiment, the observed differences had no statistical significance, either in terms of the replication levels or transmission efficiency achieved.

At an inoculum dose of 100 PFU, no guinea pigs were infected with the rSPN04-P virus (**Fig. 5C**), whereas two out of four guinea pigs were infected with the rSPN04-A virus, and one accompanying transmission event occurred (**Fig. 5D**);

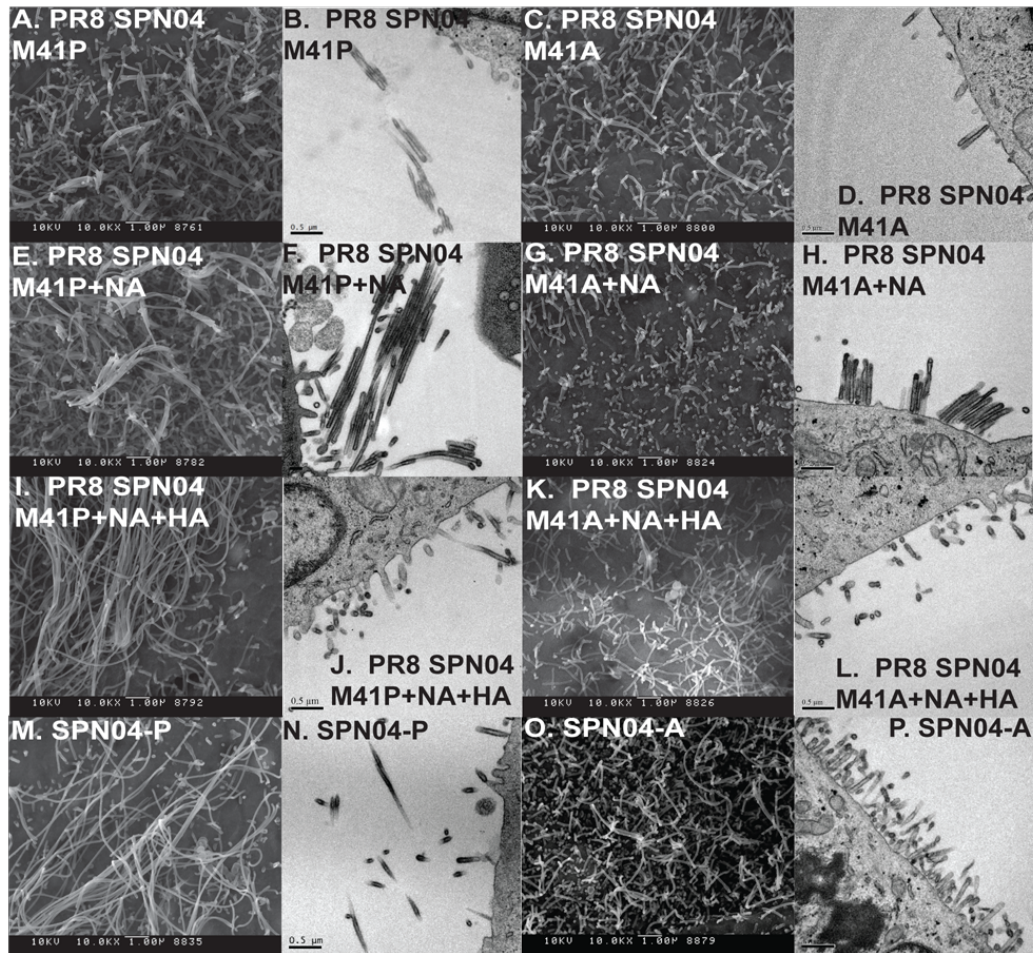


Figure 3. A proline at residue 41 of matrix protein increases filament length of recombinant viruses. Virion morphologies are shown in representative SEM (A, C, E, G, I, K, M, and O) or TEM (B, D, F, H, J, L, N, and P) images. Adherent MDCK cells were infected at an MOI of 5.0, or mock infected, and incubated for 18 h before fixing and staining. Reassortant viruses possessing a proline at position 41 of the matrix protein (as indicated) exhibited formation of long filamentous virions (A, B, E, F, I, and J). Those viruses possessing alanine at position 41 displayed virions consisting of considerably shorter filaments (C, D, G, H, K, and L). SPN04-P virus displays pleiomorphic virions, including highly filamentous examples (M and N), whereas SPN04-A produced virions with a markedly reduced length of approximately 1 μm or less (O and P). Magnification, X10,000 (A, C, E, G, I, K, M, and O) or X40,000 (B, D, F, H, J, L, N, and P). Bars, 1.00 μm (A, C, E, G, I, K, M, and O), 0.2 μm (F), or 0.5 μm (B, D, H, J, L, N, and P).

TABLE 1 Reassortant viruses, measured using TEM, differ in the prevalence of filamentous virions
% of particles of indicated length^a

Morphology	Particle length (nm)	SPN04		rPRA/SPN04 M		rPRA/SPN04 M+NA		rPRR/SPN04 M+HA+NA	
		M1 41P	M1 41A	M1 41P	M1 41A	M1 41P	M1 41A	M1 41P	M1 41A
Spherical	<100	36	19	45	49	5	17	43	32
	100-200	26	31	21	37	18	21	38	38
	200-300	2	12	9	10	6	6	8	7
	Total	64	74	76	96	29	44	89	77
Filamentous	300-500	10	8.3	6	2	20	15	3	10
	500-1,000	20	18	2	2	22	41	4	12
	>1,000	6	0	8	0	29	0	4	1
	Total	36	26	24	4*	71	56	11**	23.3
Total particles		50	84	86	51	82	78	73	73

^a Among infected, sectioned MDCK cells. *, the percentage of filamentous virions (>300 nm in length) in preline-containing virus was significantly higher ($P > 0.05$) than in alumine-containing isogenic virions based on a difference of proportions test; **, the percentage of filamentous virions (>300 nm in length) in preline-containing virions was significantly lower ($P > 0.05$) than in alumine-containing isogenic virions based on a difference of proportions test.

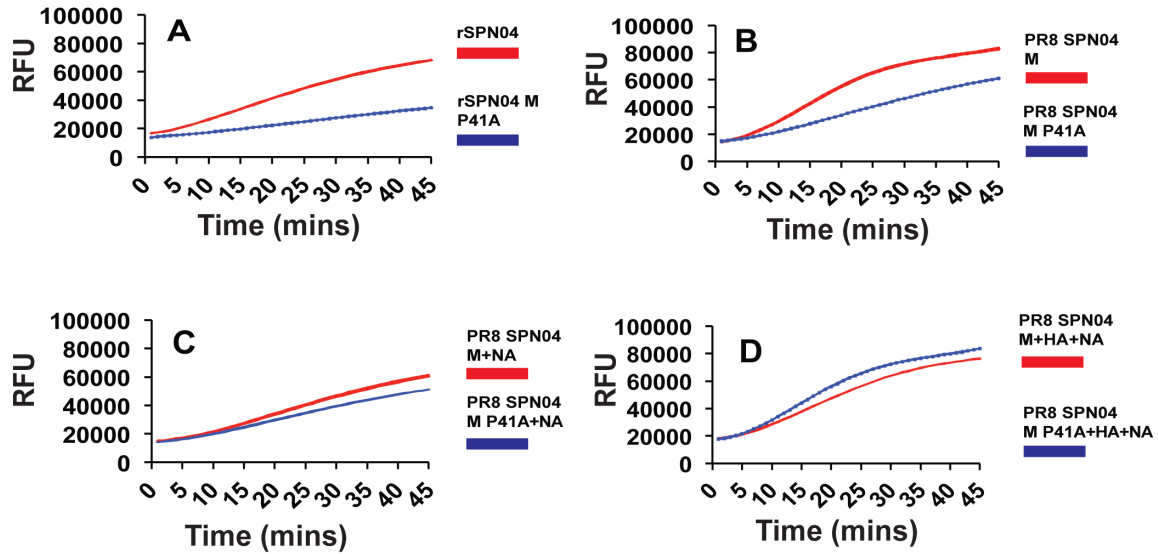


Figure 4. A proline at residue 41 of matrix protein increases neuraminidase activity of select recombinant viruses *in vitro*. The neuraminidase activity of each virus (as indicated) was measured through the cleavage of the fluorogenic substrate 2-(4-methylumbelliferyl)-D-N-acetylneuraminic acid (MUNANA). Virus was incubated in the presence of MUNANA at 37°C for 45 min, and the relative fluorescence was measured at 1-min intervals. Plots displaying (tightly overlapping) triplicate samples of each virus are shown. Each graph is representative of at least three replicate experiments.

however, statistically significant differences in replication or transmission were not demonstrated.

Next we conducted contact transmission experiments involving the PR8-based reassortant viruses. Overall, viruses possessing the SPN04 matrix protein encoding a proline at position 41 transmitted poorly compared to the viruses possessing alanine at this position, broadly reproducing the phenotype observed in the SPN04 genetic background.

The PR8/SPN04 M41P virus did not transmit to any of eight guinea pigs by contact, and replicated to approximately 10^4 to 10^5 PFU by day 2 postinoculation, as measured in nasal washes (**Fig. 5E**). In contrast, PR8/SPN04 M41A virus transmitted to four of eight naïve cage mates, and replicated to peak titers of approximately 10^6 PFU by day 2 postinfection (**Fig. 5F**). The PR8/SPN04 M41A virus replicated to significantly higher average titers on day 2 post-inoculation ($P=0.0027$; unpaired *t*-test), as well as having a significantly higher average AUC throughout the period of the infection ($P=0.0189$; unpaired *t*-test) than the PR8/SPN04 M41P virus. The cumulative number of transmission events was also significantly different ($P=0.019$; unpaired *t*-test). Similarly, the PR8/SPN04 M41P+NA virus did not transmit and replicated to approximately 10^4 to 10^5 PFU by day 2 postinfection (**Fig. 3G**). In contrast, PR8/SPN04 M41A+NA virus transmitted to four of eight naïve cage mates, and replicated to peak titers of approximately 10^6 PFU by day 2 postinfection (**Fig. 3H**). The PR8/SPN04 M41A+NA virus replicated to significantly higher average titers on day 2 postinoculation than the proline-encoding virus ($P<0.0001$; unpaired *t*-test),

although the average AUC throughout the period of the infection was not significantly different between the two groups of animals ($P=0.78$; unpaired t -test). The cumulative number of transmission events was, however, significantly different ($P=0.019$; unpaired t -test).

Consistent with the *in vitro* data obtained on virus growth, both PR8-based viruses possessing the SPN04 HA replicated to lower levels than the viruses possessing the PR8 HA. Nonetheless, the PR8/SPN04 M41P+NA+HA virus transmitted to only one of eight cage mates (**Fig. 5I**), while the PR8/SPN04 M41A+NA+HA virus transmitted to five out of eight animals (**Fig. 5J**). The cumulative number of transmission events showed a slight statistical significance ($P=0.04$; unpaired t -test); however neither the day 2 nasal wash titers, or the average AUC were significantly different between the two groups of animals. Thus, in each background tested, a lower transmission efficiency was observed for viruses encoding proline at position 41 of the matrix protein than for those encoding alanine.

DISCUSSION

Overall, our results suggest that, dependent upon the specific gene constellation of the virus, the proline residue at position 41 can increase the filamentous nature of the influenza A virion and that this phenotype correlates with a decrease in transmission efficiency, a decrease in replicative capacity, and an increase in neuraminidase activity over an isogenic virus possessing an alanine at

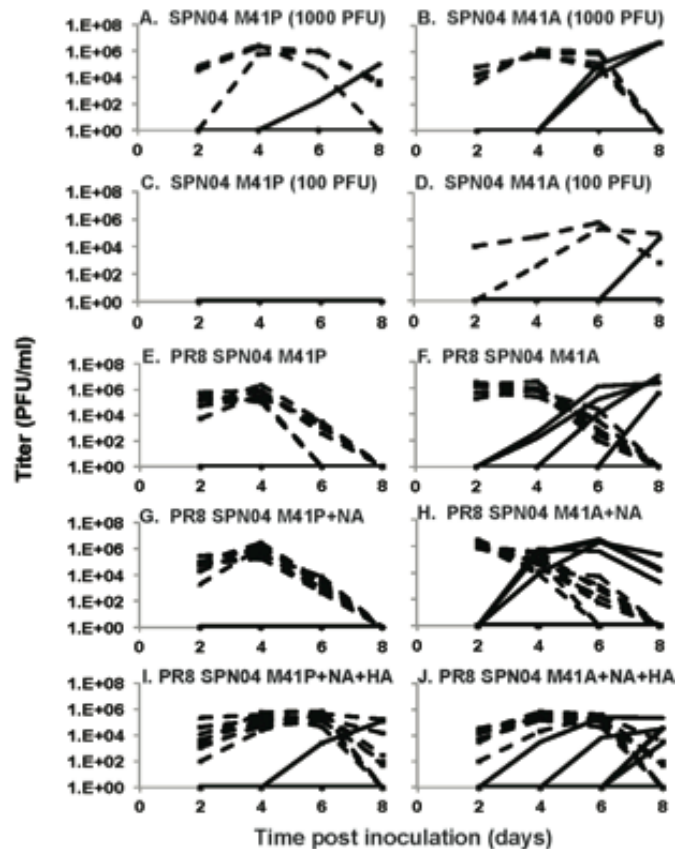


Figure 5. A proline at residue 41 of matrix protein attenuates growth and transmission of recombinant viruses in guinea pigs. **A.** Three out of four guinea pigs inoculated with 1,000 PFU of SPN04-P virus were productively infected and one transmission to a cage mate occurred on day 6 postinfection. **B.** No guinea pigs were productively infected following inoculation with 100 PFU of SPN04-P virus. **C.** All guinea pigs inoculated with 1,000 PFU of SPN04-A virus were infected, and two transmission events occurred on day 6 postinfection. **D.** Two out of four guinea pigs inoculated with 100 PFU of SPN04-A became infected and one transmission to a cage mate occurred on day 8 postinfection (**E** to **H**). Eight guinea pigs infected with either PR8/SPN04 M41P (**E**) or PR8/SPN04 M41P +NA (**G**) virus did not transmit the virus to cage mates. In contrast, guinea pigs infected with PR8/SPN04 M41A (**F**) or PR8/SPN04 M41A+NA (**H**) virus displayed an earlier peak of replication and were permissive for 4/8 transmission events. (**I**) Guinea pigs infected with PR8/SPN04 M41P+NA+HA showed 1/ 8 transmission events. (**J**) Animals infected with PR8/SPN04 M41A+NA+HA virus were subject to 5/8 transmission events, although replication kinetics were similar between the two strains (compare graphs in panels **I** and **J**). Virus titers were determined by plaque assay from nasal washes collected every 2 days after infection from inoculated (1,000 PFU; dashed lines) and contact-exposed (solid lines) guinea pigs. Virus titers were determined by plaque assay of nasal washes collected every 2 days after infection from inoculated (100 or 1,000 PFU; dashed lines) and contact exposed (solid lines) guinea pigs. SPN04-A contains the consensus M segment of Eurasian avian-like swine virus lineage.

matrix position 41.

Among the influenza A virus sequences deposited in GenBank, the proline at position 41 of the matrix protein is unique, encoded only by the SPN04 isolate. However, a few other Eurasian avian-like swine influenza strains encode a valine at this position, suggesting that the lineage tolerates polymorphism at this locus to some extent. We have not tested the effect of valine on the morphology of the SPN04 influenza virion.

The structure of the amino terminal portion (amino acids 2 to 158) of the matrix protein has been solved using X-ray crystallography (43). The crystallized structure consists of nine α -helices and eight loop regions. Position 41 lies within α -helix 3, consisting of amino acids 39 to 48, and is likely solvent exposed. Based on this positioning, the nature of the residue at position 41 could affect oligomerization of the matrix protein, or interaction with other viral or cellular factors. Of note, the cyclic nature of the proline side chain is incompatible with the formation of an α -helix, introducing a kink or a break in the structure; thus, α -helix 3 is most likely disrupted in the SPN04 matrix protein.

Several previous studies have examined the effect of mutations in the matrix protein on the morphology of the influenza A virus. Lamb and colleagues examined the morphology of influenza A virions using the A/Udorn/301/72 (H3N2) [A/Udorn] strain (27). A/Udorn possesses an alanine at position 41 of the matrix, in common with the majority of human H3N2 isolates, and is noted for its filamentous nature, with approximately 15% of virions being long-filamentous in nature (27). Interestingly, an A41V change in the A/Udorn matrix protein results in a complete

loss of filamentous virions, as assayed in gradient-purified virion preparations (27). Similarly, Elleman and colleagues noted that the filamentous human influenza isolate A/Victoria/3/75 (H3N2) (A/Victoria) could be altered to a spherical morphology by introduction of a valine at position 41 of matrix protein (24). In addition, the commonly used laboratory adapted strains of influenza PR8 and A/WSN/33 also possess a valine at position 41 of the matrix protein and are spherical in nature (24, 28). It should be noted, however, that PR8 and A/WSN/33 also possess several other amino acid changes relative to the seasonal H1N1 human influenza A virus consensus sequence, and morphology may be affected by several of these differences. Nonetheless, overall these data suggest the importance of position 41 in determining the morphology of numerous unrelated influenza A viruses.

The alanine-to-valine change in the matrix has been reported in several strains of influenza A virus that are virulent to mice: A/Port Chalmers/1/73 (44), A/FPV/34 (45), A/PR/8/34 (31) and A/WSN/33 (30). Indeed, the mutation was observed to arise during mouse adaptation in the A/Port Chalmers/1/73, background (44). Thus, effects of M1 position 41 on virulence have been demonstrated. We note, however, that in these studies, polymorphism at M1 position 41 arose under circumstances where the selective pressure to transmit had been removed. Thus, here we tested the impact of M1 position 41 on transmission. Replacement of the alanine at position 41 of the Eurasian avian-like swine virus matrix protein with proline reduces viral transmission in a contact model. Interestingly, the reliance of efficient transmission on an alanine at M1 position 41

was evident whether its replacement with proline resulted in an observable loss in replicative fitness or not. These findings are consistent with the idea that an alanine at position 41 is optimal for efficient transmission of influenza A virus.

Evidence that molecular determinants of transmissibility reside within the M segment of influenza virus arose following the 2009 swine-origin pandemic, whereupon an influenza strain derived from two parental swine virus lineages that do not possess efficient human transmissibility crossed the species barrier, and proceeded to infect over 1 billion people worldwide (46). The unusual genotype of the pandemic strain, encompassing 6 gene segments from the North American TRIG lineage, and the M and NA segments from the Eurasian avian-like swine lineage prompted investigators to study the contribution of the M segment to transmissibility of the pandemic strain. Chou and colleagues demonstrated that the M segment of the pandemic strain A/California/4/2009 restored transmissibility in the guinea pig model to the non-transmissible A/Puerto Rico/8/1934 (H1N1) virus (12). Interestingly, A/Puerto Rico/8/1934 encodes valine at position 41 of the matrix protein, whereas A/California/4/2009 encodes an alanine, among several other changes between the two matrix proteins. Further evidence for the importance of the Eurasian origin M segment to transmission of the 2009 pandemic lineage was obtained in ferret (13) and pig (47) models.

Due to the role of the M segment in determining transmission efficiency, we predicted that filamentous influenza virions may be maintained in nature because they are important for transmission. However, our present findings show that viruses carrying M1 41P transmit with lower efficiency than the corresponding, less

filamentous variants carrying M1 41A. Nevertheless, we hesitate to conclude that filaments disfavor transmission or that morphology does not affect transmission. A more plausible explanation is that morphology and transmission are linked, but the relationship between particle length and transmissibility is affected (perhaps even mediated by) other viral factors, such as NA activity and HA avidity (41).

Based on our present results, and those presented in reference 41, we hypothesize that the pleomorphic nature of avian influenza virus is necessary to support optimal fitness. Thus, spherical and filamentous virions may play complementary and distinct roles within the respiratory tract of the host to promote spread and transmission. Such a mechanism could exploit putative differences in, for example, attachment and release properties of the virions. We furthermore suggest that the proportion, or length, of filaments that supports optimal replication may vary, depending on strain-specific properties of HA and NA.

ACKNOWLEDGEMENTS

We thank Peter Palese for the pCAGGS expression plasmid, and pPol1 reverse genetics plasmid, and Adolfo García-Sastre for the pDZ PR8 rescue system. We are grateful to Gustavo Real-Soldevilla for the A/swine/Spain/53207/04 (H1N1) virus. We also appreciate the work of Hong Yi and Jeannette Taylor of the Robert P. Apkarian Integrated Electron Microscopy Core for TEM and SEM sample processing. We thank the Georgia Research Alliance for support to JS and ACL through equipment grants. This work was funded by the Centers for Excellence in Influenza Research and Surveillance (CEIRS) contract number HHSN266200700006C.

REFERENCES

1. **Pensaert M, Ottis K, Vandeputte J, Kaplan MM, Bachmann PA.** 1981. Evidence for the natural transmission of influenza A virus from wild ducks to swine and its potential importance for man. *Bull World Health Organ* **59**:75-78.
2. **Scholtissek C, Burger H, Bachmann PA, Hannoun C.** 1983. Genetic relatedness of hemagglutinins of the H1 subtype of influenza A viruses isolated from swine and birds. *Virology* **129**:521-523.
3. **Chen Y, Zhang J, Qiao C, Yang H, Zhang Y, Xin X, Chen H.** 2013. Co-circulation of pandemic 2009 H1N1, classical swine H1N1 and avian-like swine H1N1 influenza viruses in pigs in China. *Infect Genet Evol* **13**:331-338.
4. **Kyriakis CS, Brown IH, Foni E, Kuntz-Simon G, Maldonado J, Madec F, Essen SC, Chiapponi C, Van Reeth K.** 2011. Virological surveillance and preliminary antigenic characterization of influenza viruses in pigs in five European countries from 2006 to 2008. *Zoonoses Public Health* **58**:93-101.
5. **Zell R, Scholtissek C, Ludwig S.** 2013. Genetics, evolution, and the zoonotic capacity of European Swine influenza viruses. *Curr Top Microbiol Immunol* **370**:29-55.
6. **Dacso CC, Couch RB, Six HR, Young JF, Quarles JM, Kasel JA.** 1984. Sporadic occurrence of zoonotic swine influenza virus infections. *J Clin Microbiol* **20**:833-835.

7. **de Jong JC, de Ronde-Verloop JM, Bangma PJ, van Kregten E, Kerckhaert J, Paccaud MF, Wicki F, Wunderli W.** 1986. Isolation of swine-influenza-like A(H1N1) viruses from man in Europe, 1986. *Lancet* **2**:1329-1330.
8. **Gregory V, Bennett M, Thomas Y, Kaiser L, Wunderli W, Matter H, Hay A, Lin YP.** 2003. Human infection by a swine influenza A (H1N1) virus in Switzerland. *Arch Virol* **148**:793-802.
9. **Rota PA, Rocha EP, Harmon MW, Hinshaw VS, Sheerar MG, Kawaoka Y, Cox NJ, Smith TF.** 1989. Laboratory characterization of a swine influenza virus isolated from a fatal case of human influenza. *J Clin Microbiol* **27**:1413-1416.
10. **Myers KP, Olsen CW, Gray GC.** 2007. Cases of swine influenza in humans: a review of the literature. *Clin Infect Dis* **44**:1084-1088.
11. **Smith GJ, Vijaykrishna D, Bahl J, Lycett SJ, Worobey M, Pybus OG, Ma SK, Cheung CL, Raghwani J, Bhatt S, Peiris JS, Guan Y, Rambaut A.** 2009. Origins and evolutionary genomics of the 2009 swine-origin H1N1 influenza A epidemic. *Nature* **459**:1122-1125.
12. **Chou YY, Albrecht RA, Pica N, Lowen AC, Richt JA, Garcia-Sastre A, Palese P, Hai R.** 2011. The M segment of the 2009 new pandemic H1N1 influenza virus is critical for its high transmission efficiency in the guinea pig model. *J Virol* **85**:11235-11241.
13. **Lakdawala SS, Lamirande EW, Suguitan AL, Jr., Wang W, Santos CP, Vogel L, Matsuoka Y, Lindsley WG, Jin H, Subbarao K.** 2011. Eurasian-origin gene segments contribute to the transmissibility, aerosol release, and

- morphology of the 2009 pandemic H1N1 influenza virus. *PLoS Pathog* **7**:e1002443.
14. **Yen HL, Liang CH, Wu CY, Forrest HL, Ferguson A, Choy KT, Jones J, Wong DD, Cheung PP, Hsu CH, Li OT, Yuen KM, Chan RW, Poon LL, Chan MC, Nicholls JM, Krauss S, Wong CH, Guan Y, Webster RG, Webby RJ, Peiris M.** 2011. Hemagglutinin-neuraminidase balance confers respiratory-droplet transmissibility of the pandemic H1N1 influenza virus in ferrets. *Proc Natl Acad Sci U S A* **108**:14264-14269.
 15. **Kuntz-Simon G, Madec F.** 2009. Genetic and antigenic evolution of swine influenza viruses in Europe and evaluation of their zoonotic potential. *Zoonoses Public Health* **56**:310-325.
 16. **Wu CY, Jeng KS, Lai MM.** 2011. The SUMOylation of matrix protein M1 modulates the assembly and morphogenesis of influenza A virus. *J Virol* **85**:6618-6628.
 17. **Rossman JS, Lamb RA.** 2011. Influenza virus assembly and budding. *Virology* **411**:229-236.
 18. **Calder LJ, Wasilewski S, Berriman JA, Rosenthal PB.** 2010. Structural organization of a filamentous influenza A virus. *Proc Natl Acad Sci U S A* **107**:10685-10690.
 19. **Nayak DP, Balogun RA, Yamada H, Zhou ZH, Barman S.** 2009. Influenza virus morphogenesis and budding. *Virus Res* **143**:147-161.

20. **Bui M, Whittaker G, Helenius A.** 1996. Effect of M1 protein and low pH on nuclear transport of influenza virus ribonucleoproteins. *J Virol* **70**:8391-8401.
21. **Noton SL, Medcalf E, Fisher D, Mullin AE, Elton D, Digard P.** 2007. Identification of the domains of the influenza A virus M1 matrix protein required for NP binding, oligomerization and incorporation into virions. *J Gen Virol* **88**:2280-2290.
22. **Barman S, Ali A, Hui EK, Adhikary L, Nayak DP.** 2001. Transport of viral proteins to the apical membranes and interaction of matrix protein with glycoproteins in the assembly of influenza viruses. *Virus Res* **77**:61-69.
23. **Bourmakina SV, Garcia-Sastre A.** 2003. Reverse genetics studies on the filamentous morphology of influenza A virus. *J Gen Virol* **84**:517-527.
24. **Elleman CJ, Barclay WS.** 2004. The M1 matrix protein controls the filamentous phenotype of influenza A virus. *Virology* **321**:144-153.
25. **Burleigh LM, Calder LJ, Skehel JJ, Steinhauer DA.** 2005. Influenza A viruses with mutations in the m1 helix six domain display a wide variety of morphological phenotypes. *J Virol* **79**:1262-1270.
26. **Bialas KM, Desmet EA, Takimoto T.** 2012. Specific residues in the 2009 H1N1 swine-origin influenza matrix protein influence virion morphology and efficiency of viral spread in vitro. *PLoS ONE* **7**:e50595.
27. **Roberts PC, Lamb RA, Compans RW.** 1998. The M1 and M2 proteins of influenza A virus are important determinants in filamentous particle formation. *Virology* **240**:127-137.

28. **Seladi-Schulman J, Steel J, Lowen AC.** 2013. Spherical Influenza Viruses Have a Fitness Advantage in Embryonated Eggs, while Filament-Producing Strains Are Selected In Vivo. *J Virol* **87**:13343-13353.
29. **Choppin PW, Murphy JS, Tamm I.** 1960. Studies of two kinds of virus particles which comprise influenza A2 virus strains. III. Morphological characteristics: independence to morphological and functional traits. *J Exp Med* **112**:945-952.
30. **Ward AC.** 1995. Specific changes in the M1 protein during adaptation of influenza virus to mouse. *Arch Virol* **140**:383-389.
31. **Ward AC.** 1997. Virulence of influenza A virus for mouse lung. *Virus Genes* **14**:187-194.
32. **Smeenk CA, Brown EG.** 1994. The influenza virus variant A/FM/1/47-MA possesses single amino acid replacements in the hemagglutinin, controlling virulence, and in the matrix protein, controlling virulence as well as growth. *J Virol* **68**:530-534.
- 32b. National Research Council. 2011. Guide for the care and use of laboratory animals, 8th ed. National Academies Press. Washington, DC.
33. **Lowen AC, Mubareka S, Tumpey TM, Garcia-Sastre A, Palese P.** 2006. The guinea pig as a transmission model for human influenza viruses. *Proc Natl Acad Sci U S A* **103**:9988-9992.
34. **Fodor E, Devenish L, Engelhardt OG, Palese P, Brownlee GG, Garcia-Sastre A.** 1999. Rescue of influenza A virus from recombinant DNA. *J Virol* **73**:9679-9682.

35. **Hoffmann E, Stech J, Guan Y, Webster RG, Perez DR.** 2001. Universal primer set for the full-length amplification of all influenza A viruses. *Arch Virol* **146**:2275-2289.
36. **Liu Q, Wang S, Ma G, Pu J, Forbes NE, Brown EG, Liu JH.** 2009. Improved and simplified recombineering approach for influenza virus reverse genetics. *J Mol Genet Med* **3**:225-231.
37. **Steel J, Lowen AC, Mubareka S, Palese P.** 2009. Transmission of influenza virus in a mammalian host is increased by PB2 amino acids 627K or 627E/701N. *PLoS Pathog* **5**:e1000252.
38. **Quinlivan M, Zamarin D, Garcia-Sastre A, Cullinane A, Chambers T, Palese P.** 2005. Attenuation of equine influenza viruses through truncations of the NS1 protein. *J Virol* **79**:8431-8439.
39. **Gao Q, Brydon EW, Palese P.** 2008. A seven-segmented influenza A virus expressing the influenza C virus glycoprotein HEF. *J Virol* **82**:6419-6426.
40. **Lowen AC, Mubareka S, Tumpey TM, García-Sastre A, Palese P.** 2006. The guinea pig as a transmission model for human influenza viruses. *PNAS* **103**:9988-9992.
41. **Campbell PJ, Danzy S, Kyriakis CS, Deymier MJ, Lowen AC, Steel J.** 2014. The M segment of the 2009 pandemic influenza virus confers increased neuraminidase activity, filamentous morphology, and efficient contact transmissibility to a/puerto rico/8/1934-based reassortant viruses. *J Virol* **88**:3802-3814.

42. **Lowen AC, Steel J, Mubareka S, Palese P.** 2008. High temperature (30 degrees C) blocks aerosol but not contact transmission of influenza virus. *J Virol* **82**:5650-5652.
43. **Sha B, Luo M.** 1997. Structure of a bifunctional membrane-RNA binding protein, influenza virus matrix protein M1. *Nat Struct Biol* **4**:239-244.
44. **Zebedee SL, Lamb RA.** 1989. Nucleotide sequences of influenza A virus RNA segment 7: a comparison of five isolates. *Nucleic Acids Res* **17**:2870.
45. **Scholtissek C, Vallbracht A, Flehmig B, Rott R.** 1979. Correlation of pathogenicity and gene constellation of influenza A viruses. II. Highly neurovirulent recombinants derived from non-neurovirulent or weakly neurovirulent parent virus strains. *Virology* **95**:492-500.
46. **Van Kerkhove MD, Hirve S, Koukounari A, Mounts AW.** 2013. Estimating age-specific cumulative incidence for the 2009 influenza pandemic: a meta-analysis of A(H1N1)pdm09 serological studies from 19 countries. *Influenza Other Respir Viruses* **7**:872-886.
47. **Ma W, Liu Q, Bawa B, Qiao C, Qi W, Shen H, Chen Y, Ma J, Li X, Webby RJ, Garcia-Sastre A, Richt JA.** 2012. The neuraminidase and matrix genes of the 2009 pandemic influenza H1N1 virus cooperate functionally to facilitate efficient replication and transmissibility in pigs. *J Gen Virol* **93**:1261-1268.

CHAPTER 3

Reassortant viruses harboring the 2009 pandemic influenza virus matrix protein have replication and transmission advantages over those containing a matrix protein from the pandemic precursor Eurasian avian-like swine lineage

Patricia J. Campbell, Shamika Danzy, Anice C. Lowen and John Steel

The work of this chapter is in preparation for publication.

ABSTRACT

The novel 2009 pandemic H1N1 influenza virus [pH1N1] was highly transmissible, having infected approximately 24% of the population by 2010. Previous investigations found that the pH1N1 M segment, which originated from the Eurasian avian-like swine [EAsw] lineage, conferred filamentous morphology, increased NA activity, and efficient transmission efficiency to A/Puerto Rico/8/34 (H1N1) [PR8]. However, since the M segment encodes both the M1 matrix protein and the M2 proton channel, the protein product(s) responsible for the observed phenotypes remained unknown. To investigate the contribution of the pH1N1 M1 protein to virus replication, morphology, NA activity, and transmission efficiency, we individually and collectively introduced three M1 amino acids (and one concurrent M2 residue) that differentiate the EAsw lineage M1 from the pH1N1 lineage into the pH1N1 isolate, A/Netherlands/602/2009 (H1N1) [NL602]. We then utilized reverse genetics to introduce the M segments into the PR8 background. The PR8/EAsw M and PR8/EAsw M1+NL602 M2 (M2 C19Y) viruses displayed significantly reduced transmission efficiencies compared to the PR8/NL602 M virus in the guinea pig model, despite a relative increase in NA activity for the PR8/EAsw M virus. The decrease in transmissibility mapped to the M1 N207S mutation, which did not affect virus morphology, but decreased *in vivo* replication and neuraminidase activity of the PR8/NL602 M virus. Additionally, while the NL602 M1 S30G and M248I (M2 C19Y) mutations reduced PR8/NL602 M filament number, the reduction did not result in decreased NA activity or transmissibility. Overall, these data demonstrate that the pH1N1 M1 protein, and M1 207N in particular,

contribute to the transmissibility of recombinant PR8 viruses independent of virus morphology and NA activity.

INTRODUCTION

Influenza A virus [IAV] pandemics cause significant global morbidity and mortality. Pandemic IAVs are antigenically divergent from circulating human strains and are capable of causing sustained human-to-human transmission. The most recent 2009 pandemic H1N1 influenza virus (pH1N1) was highly transmissible, having infected approximately 24% of the population by 2010 (1). pH1N1 resulted from reassortment between the Eurasian-avian like swine [EAsw] (M and NA segments) and North American triple reassortant swine (remaining segments) lineages (2). Importantly, although swine H1N1 viruses have circulated in the porcine reservoir for years and sporadic zoonoses have been reported, human infections have typically been self-limiting (3-5). The fact that neither swine pH1N1 parental lineage has become independently transmissible between humans suggests that viral factors encoded by the unique pH1N1 gene constellation are responsible for its high transmission efficiency.

The ability of IAVs to transmit between hosts has been linked to many viral factors. Although changes in receptor specificity (6) and acid stability (7, 8) of the hemagglutinin [HA] protein, and replicative capacity of the polymerase complex (9, 10), have been associated with cross-species transmission of IAV from birds to humans, the swine-origin pH1N1 HA and polymerase subunits were already

adapted to (mammalian) swine (11, 12). Instead, recent studies utilized reverse genetics to demonstrate that the pH1N1 M segment was important for efficient transmission of recombinant viruses harboring North American triple reassortant swine gene segments (13-15). However, the protein products and molecular mechanisms behind the contribution of the M segment to IAV transmission remained unknown.

The IAV M segment encodes both the matrix protein [M1] and the proton channel [M2]. The M1 protein serves as the structural component of the virion by oligomerizing into a helically arranged capsular structure beneath the viral membrane (16-18), aids in trafficking of the viral ribonucleoprotein complexes to the membrane for virus assembly (19, 20), and directly interacts with the cytoplasmic tails of the M2, neuraminidase [NA], and HA proteins (18, 21-23). In addition, recent studies used electron microscopy to evaluate the morphology of recombinant viruses that contained genetically variable M1 and M2 proteins and demonstrated that M1 is a major determinant of virion shape (24, 25). While all IAV populations are pleomorphic, clinical and low-passage-number isolates typically contain a higher number of filamentous, rather than spherical, virions and these may be lost upon passage in laboratory substrates (26). Although the selective advantage for filaments within the viral lifecycle remains unknown, a correlation between the prevalence of filaments and virus NA activity has been found for viruses differing only in their M1 protein sequences, suggesting that modulation of virion morphology by the matrix protein may optimize NA functionality *in vivo* (27, 28).

We recently reported that reassortant viruses containing the M segment from the pH1N1 patient isolate, A/NL/602/2009/ (H1N1) [NL602], transmitted efficiently between guinea pigs and that transmission correlated with virion morphology and neuraminidase activity (30). Since viruses of the EAsw lineage remain highly inefficient in transmission between humans, and the M1 protein can affect both *in vitro* phenotypes, we hypothesized that specific pH1N1 matrix protein residues, not present in the EAsw lineage, would contribute to the transmission phenotype conferred by the pH1N1 M segment through alterations of virus morphology and / or NA activity. We tested this hypothesis by evaluating the replication and transmission efficiency of PR8-based reassortant viruses harboring either wild-type or M1 / M2 chimeric EAsw and NL602 M segments in the guinea pig model. We found that reversion of the NL602 M1 sequence back to that of the EAsw lineage decreased transmission efficiency of the PR8/ NL602 M virus. The increased transmissibility of the PR8/ NL602 M virus mapped, in part, to an asparagine residue at M1 position 207. In agreement with previous reports, we found that specific amino acid changes within the matrix protein could differentially alter both virus morphology and NA activity; however, the changes did not correlate fully with transmission efficiency. In summary, our results demonstrate that functions encoded by the matrix protein can affect influenza virus transmission independent of virus morphology and NA activity.

MATERIALS AND METHODS

Ethics statement

This study was performed in accordance with the recommendations in the Guide for the Care and Use of Laboratory Animals of the National Institutes of Health. Animal husbandry and experimental procedures were approved by the Emory University Institutional Animal Care and Use Committee (IACUC protocol 2001001 071214GA).

Cells

Madin-Darby Canine Kidney (MDCK) cells were maintained in minimum essential medium (MEM) supplemented with 10% FBS and penicillin-streptomycin. 293T cells were maintained in Dulbecco's MEM supplemented with 10% FBS. Human alveolar adenocarcinoma (A549) cells were maintained in Kaign's modification of Ham's F12 medium (F12-K) supplemented with 10% FBS and penicillin-streptomycin.

Guinea Pigs

Female Hartley strain guinea pigs weighing 300 to 350 g were obtained from Charles River Laboratories. Prior to intranasal inoculation, nasal lavage, or CO₂ euthanasia, guinea pigs were sedated with a mixture of ketamine and xylazine (30 mg/kg of body weight and 2 mg/kg, respectively). Intranasal inoculation and nasal lavage were performed using PBS as a diluent as described previously (31).

Viruses

Recombinant viruses containing seven gene segments from the lab-adapted strain A/Puerto Rico/8/34 (H1N1) [PR8], and the M segment from the pH1N1 isolate A/Netherlands/602/2009 (H1N1) [NL602], or the EAsw strain A/swine/Spain/53207/2004 (H1N1) [SPN04], were recovered by plasmid-based reverse genetics following previously described procedures (10, 16, 29, 32). Since the EAsw SPN04 M segment contains a unique proline residue at M1 position 41, the previously described pPolI-SPN04 M1 P41A plasmid, encoding the consensus EAsw M1 sequence, was utilized to rescue the PR8/ EAsw M virus (29, 31). Sequence comparison of the pH1N1 and EAsw M segments revealed 15 amino acid differences, including three within the matrix protein. The NL602 matrix protein encodes serine, asparagine, and methionine residues at positions 30, 207, and 248, while the EAsw matrix protein includes glycine, serine, and isoleucine residues at these same positions (**Fig. 1A**). Moreover, since M1 codon 248 is located within the region of coding overlap between the M1 and M2 proteins, an amino acid change at this position introduces a concurrent change at M2 codon 19 (**Fig. 1A**).

To determine the contribution of amino acid changes between the pH1N1 and EAsw lineage M segments to virus replication and transmission, we used point mutagenesis to revert the position 30S, position 207N, and 248M residues in the pHW-NL602 M plasmid to the consensus EAsw amino acids. These plasmids were utilized to rescue the single mutant PR8/ NL M1 S30G, PR8/ NL M1 N207S, and PR8/ NL M1 M248I (M2 C19Y) viruses (**Fig. 1B**). In addition, all three substitutions were introduced collectively into the pHW-NL602 M plasmid to facilitate rescue

of the M1/M2 chimeric PR8/ EAsw M1+NL602 M2 (M2 C19Y) virus (**Fig. 1B**).

Virus Replication Kinetics

MDCK and A549 cells were infected at MOI 0.02 PFU/ cell. After a 45-minute incubation period at 37°C, cell surfaces were washed three times with 1X PBS and incubated at 37°C. Supernatants were collected at 2, 12, 24, 48, and 72 hours post infection. Supernatant virus titers were determined by plaque assay on MDCK cells.

Electron Microscopy

(i) Transmission Electron Microscopy. To image virions budding from the cell surface, 6-well dishes of MDCK cells were infected with influenza virus at MOI 5.0. After a 45-minute incubation period at 37°C, inocula were removed, cells were washed 3 times with 1X PBS, and incubated at 37°C for 17-24 hours. After being washed with 1X PBS, cells were fixed with 2.5% glutaraldehyde, post-fixed with 1% OsO₄ and 1.5% potassium ferrocyanide, rinsed with distilled water, and dehydrated by solution washing with increasing concentrations of ethanol. MDCK cell monolayers were then embedded in Eponate 12 resin, stained with 5% uranyl acetate and 2% lead citrate, and thin-sectioned at the Emory P. Apkarian Integrated Electron Microscopy Core. Thin sections were imaged on copper grids using a Hitachi H-7500 microscope and attached CCD camera.

To image purified virions, embryonated hen's eggs (Hy-Line) were inoculated with 1000 PFU of virus, incubated at 37°C for 48 hours, and chilled at 4°C overnight. Allantoic fluids were then harvested and clarified through centrifugation

at 5,000 rpm for 10 minutes at 4°C, and subsequent ultracentrifugation using a SW32 rotor at 10,000 rpm for 30 minutes at 4°C. The clarified supernatants were layered onto 30% sucrose cushions and purified through ultracentrifugation with a SW32 rotor at 25,000 rpm for 2 hours at 4°C. Virus pellets were resuspended in 100ul of PBS. Purified virus suspensions were then added to glow-discharged carbon coated copper grids for 2 minutes and briefly rinsed three times with distilled water. Grids were then negatively stained with 1% aqueous methylamine tungstate for 20 seconds and imaged using a Hitachi H-7500 microscope and attached CCD camera.

(iii) Particle to PFU Ratio Determination. In order to count individual virions, partially purified influenza virus was obtained through sucrose-cushion purification of infected allantoic fluid, essentially as described above, although virus pellets were resuspended in 1X TBS instead of 1X PBS. Purified viruses were then dialyzed against 1600 ml of 1X TBS supplemented with 2 mM CaCl₂ using 0.1 – 0.5 ml Slide-A-Lyzer dialysis cassettes (ThermoScientific). To determine the particle number for each purified virus, 1.3 x 10¹¹ of sonicated polystyrene latex spheres (0.3 nm; Ladd Research) in 3 µl were mixed with an equal volume of 0.125% 1X PBS-Tween20 solution. The sphere solution was then mixed 1:1 with an equal volume of purified virus and incubated on glow-discharged carbon coated copper grids for 2 minutes, rinsed three times with distilled water, and negatively stained for 20 seconds with 1% aqueous methylamine tungstate. Five fields of view at pre-determined grid locations were collected using a Hitachi H-7500 transmission electron microscope

and attached CCD. A minimum of 625 virions and 60 spheres were counted from virus images using ImageJ64 software, sphere and particle averages were determined, and particle per ml concentrations were calculated. Purified virus titers were determined by plaque assays on MDCK cells. The particle per ml concentration was divided by the PFU per ml concentration for each virus to determine the particle to PFU ratio (**Table 2**).

Neuraminidase Activity

To compare the neuraminidase activities of viruses differing only in the genetic composition of their M segments, enzyme kinetic data were obtained for each virus using the fluorogenic sialoside, 2-(4-methylumbelliferyl)-D-N-acetylneuraminic acid [MUNANA] (Sigma). Virus input concentrations were normalized to particle number, as determined by transmission electron microscopy. For each virus, 1×10^8 particles were incubated with 1 to 150 μ M MUNANA using 32.5 mM MES buffer (Sigma) as a diluent. Relative fluorescence units (RFU) were recorded every minute for 45 minutes at 37°C using a BioTek Synergy H1 plate reader. The linear slopes of the resultant RFU curves were calculated at each MUNANA concentration and used as initial velocity (V_0) values in the Michaelis-Menten non-linear regression algorithm for enzyme kinetics modeling using GraphPad Prism software. To verify that differences in virus NA activity were not due to mutations in the NA protein, the NA segment from each virus was sequenced using universal NA segment primers (10, 16, 29, 32, 33).

Virus Transmission

Four female Hartley strain guinea pigs were inoculated intranasally with 10 PFU of the relevant virus in 300ul of 1X PBS. Twenty-four hours post-inoculation, each guinea pig was placed in a cage with an uninfected guinea pig. All four cages were then housed in an environmental chamber (Caron 6040) to maintain 20% humidity at 10°C. Nasal washes were collected from all guinea pigs at days 2, 4, 6, and 8 post-inoculation, as previously described (31). Nasal wash virus titers were determined by plaque assay on MDCK cells.

RESULTS

***In vitro* characterization of recombinant viruses.** The lab-adapted influenza virus, A/Puerto Rico/8/34 (H1N1) [PR8], grows to high titers in laboratory substrates and is non-transmissible in the guinea pig model (13, 16, 27), making it an ideal genetic background for the efficient propagation of recombinant strains *in vitro* and the assessment of reassortant virus transmission. To compare the replication and transmission of influenza viruses differing only in the genetic composition of their M segments, we utilized reverse genetics to rescue recombinant PR8 viruses. Three of the resultant viruses contained wild-type M segments: the wild-type PR8, PR8/ EAsw M, and PR8/ NL602 M viruses (**Fig. 1B**). Sequence alignment of the EAsw and NL602 M1 proteins revealed three amino acid differences at positions 30, 207, and 248. To obtain reassortant PR8 viruses containing M segments that were sequence-intermediate between the pH1N1

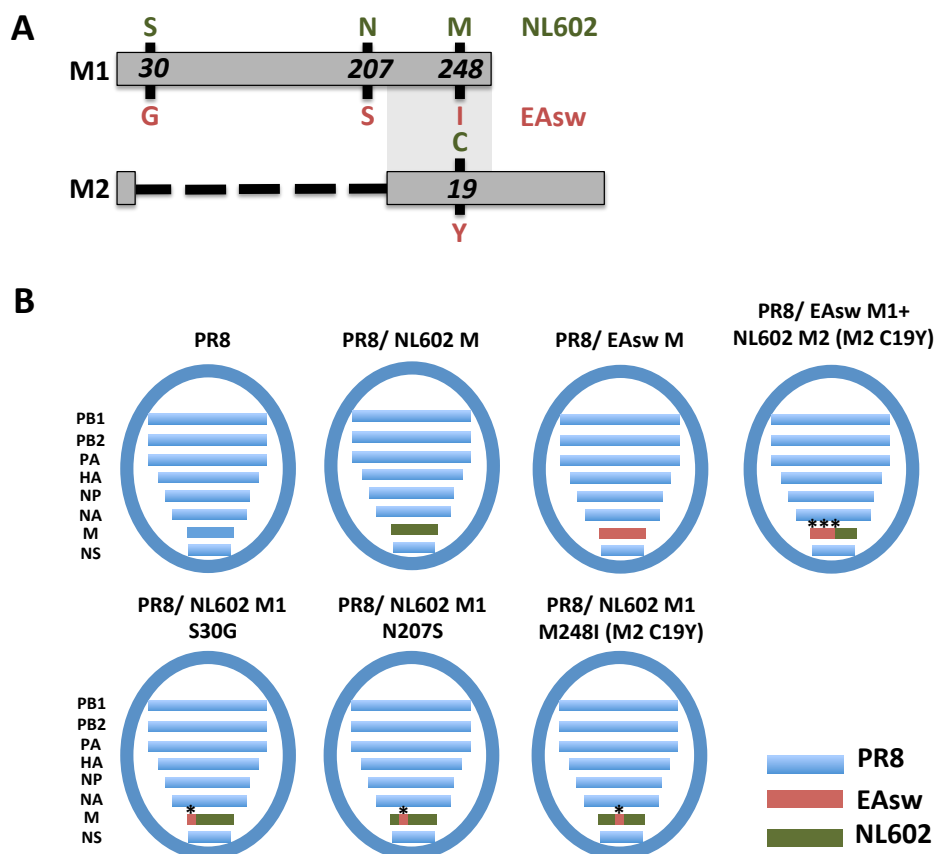


Figure 1. Wild-type, M1/M2 chimeric, and mutant M segments were used in a plasmid-based reverse genetics system to generate a panel of recombinant PR8 viruses. (A) Schematic of the M segment, showing both the M1 and M2 protein products (grey boxes). Amino acids distinguishing the Eurasian avian-like swine (SPN04 M1 P41A; red letters and pH1N1 (NL602; green letters) matrix proteins at residues 30, 207, and 248 are highlighted. Due to its placement in the region of M1/M2 coding overlap (shaded region), the M1 M248I mutation makes a concurrent M2 C19Y change, as indicated. Other amino acid differences in M2 between the strains are not shown. (B) Reassortant viruses containing gene segments from the PR8 (A/Puerto Rico/8/34 (H1N1)) (blue bars), Eurasian avian-like swine (A/swine/Spain/53207/2004 (H1N1) M1 P41A) (red bars), and 2009 pandemic H1N1 NL602 (A/Netherlands/602/2009 (H1N1)) isolate (green bars) are represented. Amino acid changes (S30G, N207S, M248I (M2 C19Y)) introduced in combination (EA sw M1+NL602 M2 (M2 C19Y) or singly (S30G, N207S, M248I (M2 C19Y)) into the M segment of the PR8/ NL602 M virus are indicated with asterisks.

and EAsw lineages, we utilized point mutagenesis to singly or collectively revert the three divergent amino acids in the NL602 M segment to the EAsw residues (S30G, N207S, and M248I). Additionally, since the M1 codon 248 falls within the region of M1/M2 coding overlap, the M248I mutation introduced a concurrent M2 C19Y change (**Fig. 1A**) into the ORF of the proton channel protein. Mutagenesis of the NL602 M segment therefore generated the PR8/ NL602 M1 S30G, PR8/ NL602 M1 N207S, PR8/ NL602 M1 M248I (M2 C19Y), and PR8/ EAsw M1+NL602 M2 (M2 C19Y) viruses (**Fig. 1B**).

To compare the growth of the recombinant viruses *in vitro*, low multiplicity growth curve experiments were carried out with MDCK and human airway A549 cell lines. All recombinant viruses replicated efficiently in both substrates (**Fig. 2**). There was no significant difference in growth between the PR8, PR8/ EAsw M, PR8/ NL602 M, and PR8/ EAsw M1+NL602 M2 (M2 C19Y) viruses from 24 to 72 hours in MDCK cells (**Fig. 2A**). However, surprisingly, the wild-type PR8 virus grew to substantially higher titers than the reassortant viruses in human airway A549 cells (**Fig. 2B**). The observed reduction in reassortant virus growth may be due to functional incompatibility between the introduced M segments and remaining PR8 segments and / or protein products.

In addition, when we evaluated the *in vitro* growth of the point mutant viruses, we found that the M1 S30G mutation did not significantly affect replication of the PR8/ NL602 M virus ($P > 0.05$ by one-way ANOVA with Dunnet's post test) from 12 to 72 hours in either substrate (**Fig. 2C and D**). Conversely, introduction of the N207S and M248I (M2 C19Y) mutations resulted in a significant decrease in

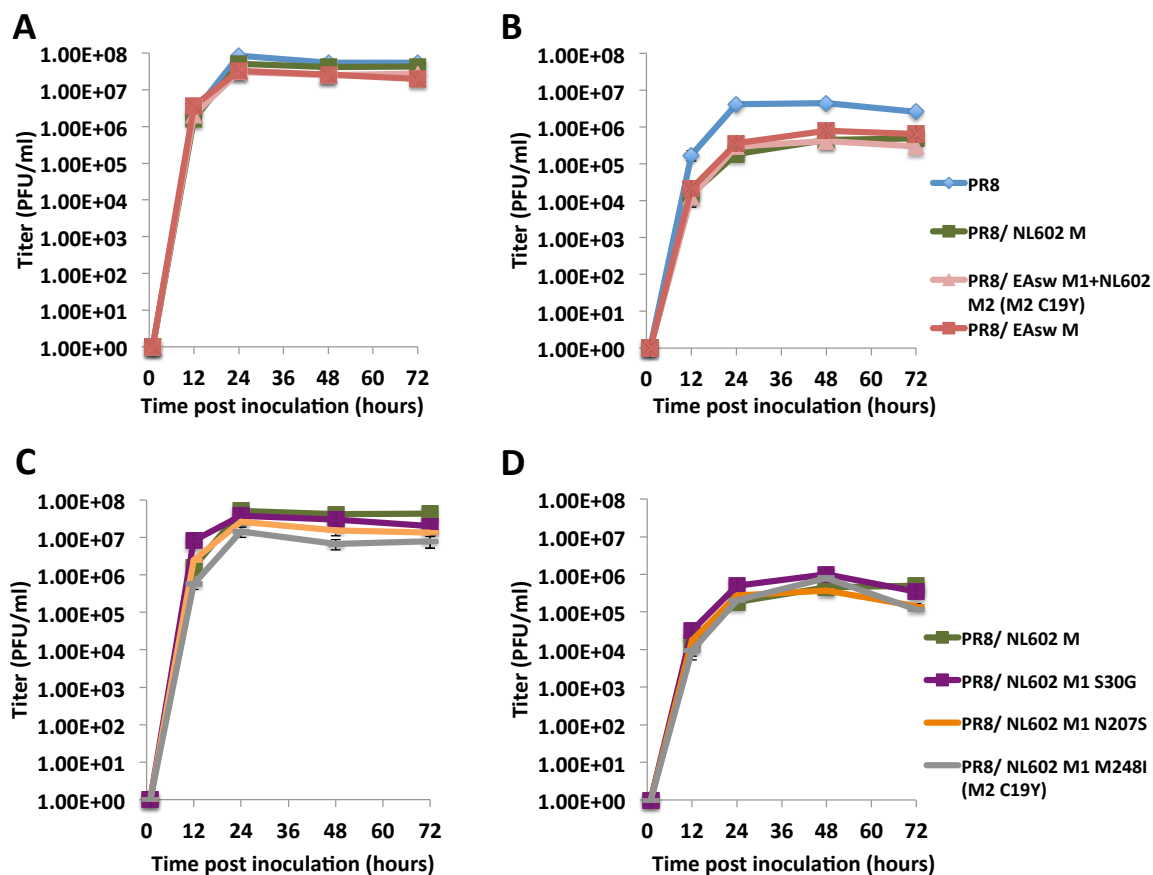


Figure 2. PR8 viruses harboring NL602 and EAsw M segments replicated similarly *in vitro*, while the single M248I (M2 C19Y) mutation reduced growth of the PR8/ NL602 M virus in MDCK cells. (A, C) MDCK cells and (B, D) A549 cells were infected in triplicate at MOI 0.02 with either recombinant PR8, PR8/ NL602 M, PR8/ EAsw M, and PR8/ EAsw M1+NL602 M2 (M2 C19Y) viruses (A, B) or PR8/ NL602 M, PR8/ NL602 M1 S30G, PR8/ NL602 M1 N207S, and PR8/ NL602 M1 M248I (M2 C19Y) viruses (C, D). Supernatants were collected from infected cells every 12 h for 72 h and enumerated by plaque assay. Data are presented from one of three independent experiments.

PR8/ NL602 M growth from 24 to 72 and 12 to 72 hours, respectively, in MDCK cells ($P < 0.05$ by one-way ANOVA with Dunnet's post test), but only had significantly reduced growth in the A549 cell line at 72 hours ($P < 0.05$ by one-way ANOVA with Dunnet's post test) (**Fig. 2C and D**). In summary, we found that (i) inclusion of heterologous M segments in the PR8 background reduced the fitness of reassortant viruses relative to the PR8 virus in A549 cells, (ii) there is no difference in replicative capacity between reassortant PR8 viruses harboring wild-type pH1N1 or EAsw matrix proteins, and (iii) the NL602 M1 N207S and M248I (M2 19-Y) mutations may result in modestly reduced virus growth of PR8/ NL602 M *in vitro*.

Morphology of recombinant viruses. Since previous studies by us and others observed a correlation between filamentous morphology and increased transmission efficiency of recombinant viruses harboring the pH1N1 M segment (14, 16), and the M1 matrix protein is a determinant of virion shape (25, 26), we assessed the morphology of our recombinant viruses by transmission electron microscopy. To quantify differences in morphology between virus populations, the long axes of negatively stained purified virions [NS] or virions budding from infected MDCK cells imaged by transmission electron microscopy [TEM] were measured (**Table 1**). Virions were determined to be filamentous if their long axis measured greater than 500nm in length. Consistent with previous studies (26, 27), we found that our wild-type PR8 virus was almost entirely spherical (0.2% by NS and 0% by TEM) while our PR8/ NL602 M virus was significantly more filamentous

Table 1 PR8/ NL602 M1 residues differentially alter virus morphology.

Morphology and particle length (nm)	Virus Prevalence ^a (%)													
	PR8		PR8/ NL602 M		PR8/ EAsw M		PR8/ EAsw M1+ NL602 M2 (M2 C19Y)		PR8/ NL602 M1 S30G		PR8/ NL602 M1 N2075		PR8/ NL602 M1 M248I (M2 C19Y)	
	NS	TEM	NS	TEM	NS	TEM	NS	TEM	NS	TEM	NS	TEM	NS	TEM
Spherical														
< 100	6.5	75.5	2.7	42.4	3.9	49.0	1.6	26.5	4.6	56.4	5.5	40.0	4.8	63.4
100 - 200	80.6	24.5	75.2	43.0	84.2	37.3	88.6	54.3	80.0	31.4	75.3	34.9	84.0	30.3
200 - 300	9.5	0.0	14.0	4.1	7.1	9.8	7.0	13.0	11.8	4.1	11.5	10.9	6.0	3.4
300 - 500	3.2	0.0	5.3	2.3	3.4	2.0	2.5	4.9	3.2	7.0	5.5	6.3	3.4	1.4
All spheres	99.8	100.0	97.2	91.8	98.6	98.1	99.6	98.8	99.7	98.8	97.9	92.0	98.2	98.6
Filamentous														
500 - 1000	0.2	0.0	2.3	4.7	1.2	2.0	0.3	1.2	0.2	1.2	1.9	4.6	1.2	0.7
> 1000	0.0	0.0	0.5	3.5	0.2	0.0	0.1	0.0	0.1	0.0	0.3	3.4	0.6	0.7
All filaments	0.2^b	0.0	2.8	8.2	1.4	1.9	0.4^b	1.2^b	0.3^b	1.2^b	2.1	8.0	1.8	1.4^b
Total no. of particles	845	53	786	172	589	51	690	162	990	172	746	175	499	145

^a NS, negative-stain TEM of released virus; TEM, TEM of infected, sectioned MDCK cells.

^b Percentage of filamentous virions (<500 nm in length) is significantly different ($P < 0.05$) from that of PR8/NL602 M by difference of proportions test.

(2.8% by NS and 8.2% by TEM) ($P < 0.05$ by difference in proportions test) (16) (**Fig. 3** and **Table 1**). The PR8/ EAsw M virus did not produce as many filaments as the PR8/ NL602 M virus, yielding 1.4% and 1.9% of virions greater than 500 nm in length by NS and TEM, respectively (**Fig. 3** and **Table 1**). In addition, PR8/ EAsw M1+NL602 M2 (M2 C19Y) also had significantly fewer filaments (0.4% by NS and 1.2% by TEM) than PR8/ NL602 M ($P < 0.05$ by difference of proportions test) (**Fig. 3** and **Table 1**). Interestingly, we found that inclusion of the M1 S30G mutation alone significantly reduced the prevalence of TEM filaments in the PR8/ NL602 M population from 8.2% to the 1.2% associated with the PR8/ EAsw M1+NL602 M2 (M2 C19Y) virus ($P < 0.05$ by difference of proportions test). These results suggest that the EAsw glycine residue at matrix protein position 30 could impact the observed decrease in filament number associated with the EAsw M1 (**Fig. 4** and **Table 1**). Additionally, the PR8/ NL602 M1 M248I virus also showed significantly fewer filaments budding from MDCK cells (1.4% by TEM; $P < 0.05$ by difference of proportions test), although the observed reduction was not as great in the purified virus preparation (2.8% to 1.8% by NS) (**Fig. 4** and **Table 1**). However, since fewer

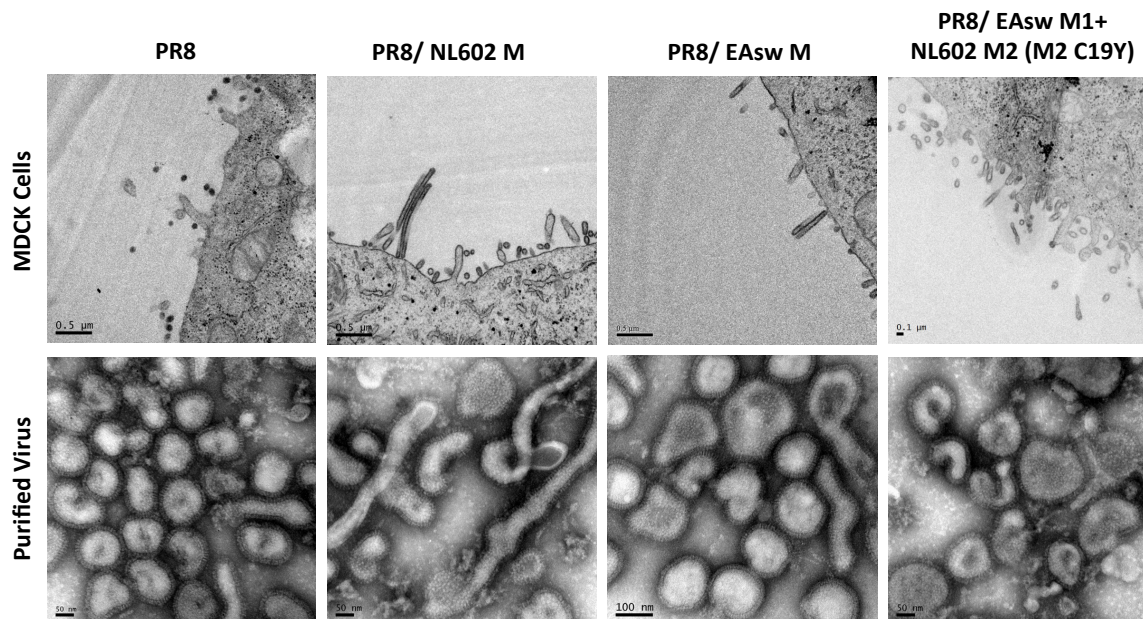


Figure 3. Introduction of the EAsw matrix protein reduced the filamentous morphology of the PR8/ NL602 M virus. Transmission electron micrographs show the morphology of PR8, PR8/ NL602 M, PR8/ EAsw M, and PR8/ EAsw M1+NL602 M2 (M2 C19Y) viruses, as indicated. Micrographs in the top row display cross-sections of MDCK cells infected with the indicated viruses at MOI 5.0 for 24 h before fixation, sectioning, and staining (40,000X magnification). The bottom row of micrographs are of sucrose cushion-purified and negatively stained virus (200,000X magnification). Bars, 0.5 μm and 0.1 μm (top row) and 50nm or 100nm (bottom row), as marked.

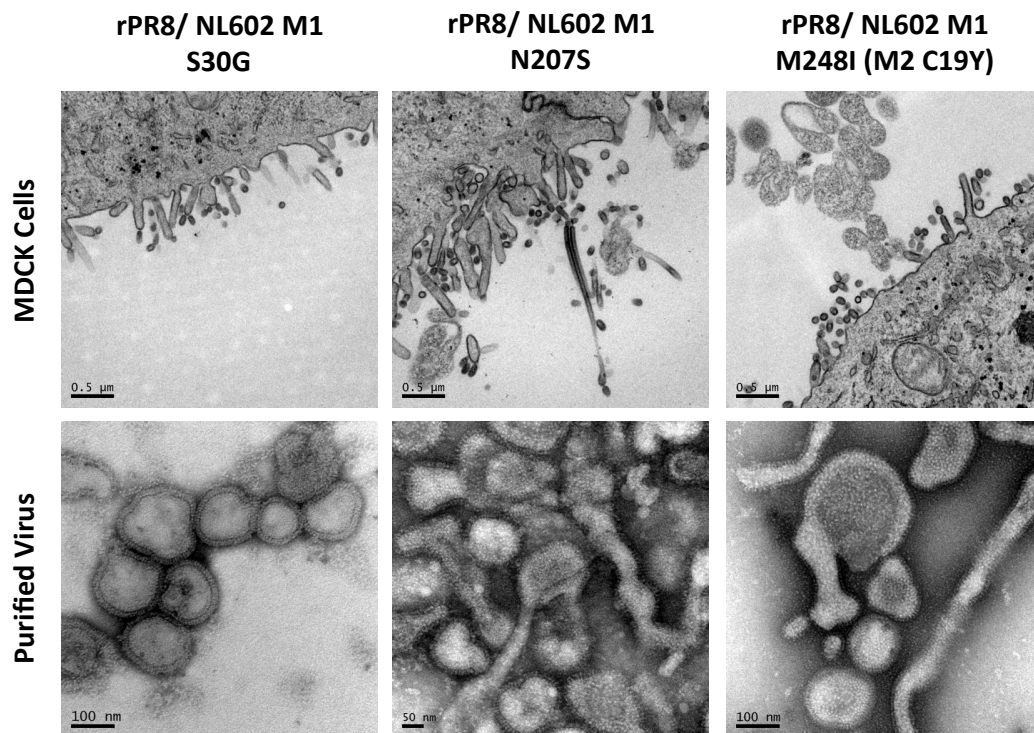


Figure 4. EAsw matrix protein 30G, 207S, and 248I (M2 19Y) residues differentially impacted PR8/ NL602 M virus morphology. Transmission electron micrographs show the morphology of PR8/ NL602 M1 S30G, PR8/ NL602 M1 N207S, and PR8/ NL602 M1 M248I (M2 C19Y) viruses, as indicated. Micrographs in the top row display cross-sections of MDCK cells infected with the indicated viruses at MOI 5.0 for 24 h before fixation, sectioning, and staining (40,000X magnification). The bottom row of micrographs are of sucrose-purified and negatively stained virus (200,000X magnification). Bars, 0.5 μ m (top row) and 50nm or 100nm (bottom row), as marked.

PR8/ NL602 M1 M248I (M2 C19Y) virions were measured by TEM, the filament number may be underrepresented compared to the NS methodology (**Table 1**). Lastly, replacement of the asparagine at position 207 in the NL602 matrix protein with a serine did not affect virus morphology by either methodology, suggesting that the asparagine residue does not contribute dominantly to the filamentous morphology conferred by the NL602 M1 protein (**Fig. 4** and **Table 1**). In fact, the PR8/ NL602 M1 N207S virus was the only reassortant that retained virions greater than 1 μm in length at the same prevalence as the PR8/ NL602 wild type virus (3.4% and 3.5% by TEM, respectively) (**Table 1**). In summary, the PR8/ NL602 M virus was more filamentous than viruses containing the EAsw M1 protein, and the observed increase in filament prevalence of the NL602 M virus could be mapped to either the M1 30S or M1 248M (M2 19C) residues.

Neuraminidase activity of recombinant viruses. Since previous studies by us and others have found that an increase in filamentous virus morphology correlated with an increase in neuraminidase activity (14, 16, 28, 29), we assessed the neuraminidase activities of the recombinant viruses against the fluorogenic sialoside, MUNANA. In our previous studies, we normalized virus concentration by plaque forming units (28, 29). However, since influenza virus populations are known to contain non-infectious particles that would not be detected by plaque assay but might still incorporate functional NA protein, and we had observed differences in particle to PFU ration between the viruses used in the present study,

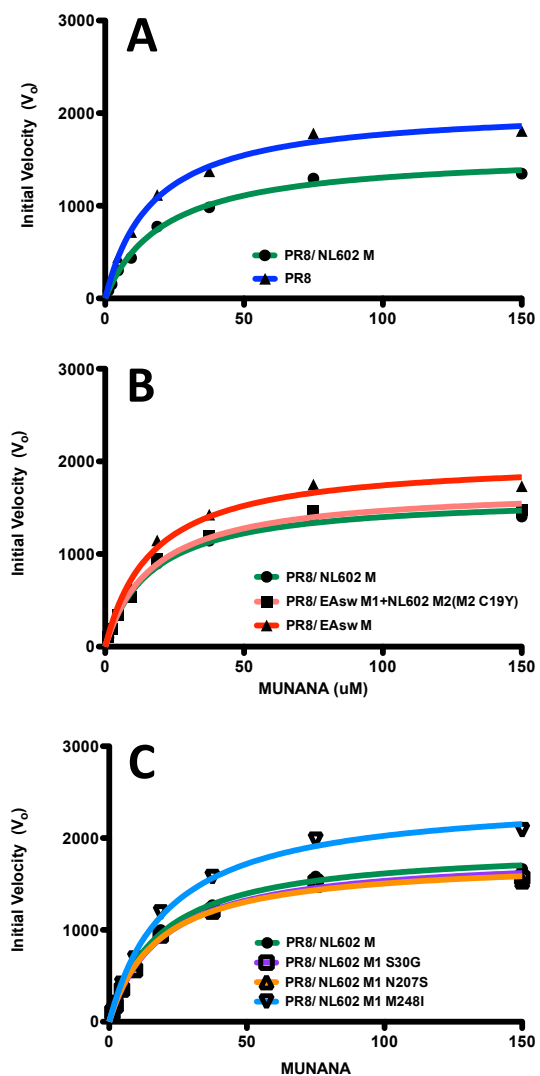


Figure 5. PR8 virions harboring PR8 and EAsw M segments have higher V_{max} , but not K_m , against MUNANA than those with NL602 and EAsw M1+NL602 M2 (M2 C19Y) M segments. Neuraminidase enzyme kinetics shown as Michaelis-Menten plots. Equal particle numbers were input for each purified virus (1×10^8 particles) with 1 – 150 μM of the fluorogenic siauloside, MUNANA and the resultant fluorescence curves were used to calculate the initial velocity (V_o) values using for non-linear regression modeling. NA activity curves are shown for (A) PR8 and PR8/NL602 M, (B) PR8/NL602 M, PR8/EAsw M, PR8/EAsw M1+NL602 M2 (M2 C19Y), and (C) PR8/NL602 M, PR8/NL602 M1 S30G, PR8/NL602 M1 N207S, and PR8/NL602 M1 M248I (M2 C19Y) viruses. Data is from one of two independent experiments with two technical replicates per experiment.

Table 2 PR8 viruses with PR8, EAsw M, and NL602 M1 M248I (M2 C19Y) M segments have higher V_{max} , but not K_m , against MUNANA compared to the PR8/ NL602 M virus.

Group No. ^a	Virus	Purified Virus		Neuraminidase Activity ^b	
		Particle: PFU Ratio ^c	Input (particles)	V_{max} ^d (SE; 95% CI)	K_m (SE; 95% CI)
1	PR8	33.3	1×10^8	2072 (1967 - 2176)	17.1 (14.3 - 19.8)
	PR8/ NL602 M	221.3		1579 (1495 - 1664)	21.2 (17.8 - 24.7)
2	PR8/ EAsw M	145.8	1×10^8	2036 (1910 - 2161)	16.9 (13.6 - 20.3)
	PR8/ EAsw M1+NL602 M2 (M2 C19Y)	208.3		1724 (1634 - 1813)	17.5 (14.6 - 20.4)
	PR8/ NL602 M	221.3		1634 (1554 - 1713)	16.8 (14.1 - 19.4)
3	PR8/ NL602 M1 M248I (M2 C19Y)	475.4	1×10^8	2462 (2365 - 2558)	21.6 (19.0 - 24.1)
	PR8/ NL602 M	255.2		1915 (1857 - 1974)	18.6 (16.9 - 20.4)
	PR8/ NL602 M1 S30G	146.4		1825 (1756 - 1894)	19.0 (16.7 - 21.2)
	PR8/ NL602 M1 N207S	733.1		1772 (1699 - 1845)	17.7 (15.4 - 20.1)

^a Each group of viruses was assayed separately. For each virus, presented data represent two technical replicates from one of two independent experiments.

^b NA activity was determined by incubating virus with 1 - 150 μ M of the fluorogenic sialoside, MUNANA, and using the generated relative fluorescence units to calculate initial velocities (V_0) for their application to the non-linear Michaelis-Menten algorithm.

^c Purified virus particle concentrations were calculated through enumeration of negatively stained purified virions alongside polystyrene latex spheres of a known concentration and PFU concentrations were determined by plaque assays on MDCK cells.

^d Enzyme kinetics data were fit to the Michaelis-Menten equation by nonlinear regression to determine the Michaelis constant (K_m) and maximum velocity (V_{max}) of substrate conversion. CI, confidence interval. SE, standard errors.

we herein normalized input of our PR8-based viruses by particle number, as determined by electron microscopy.

Although previous studies demonstrated a correlation between increased NA activity and filamentous morphology (16, 28, 29), we did not observe this association. In fact, the less filamentous PR8/ NL602 M1 M248I (M2 C19Y), PR8/ EAsw M, and PR8 viruses had the highest levels of NA activity, while the filamentous PR8/ NL602 M and spherical PR8/ NL M1 S30G viruses had comparably reduced V_{max} values, and the filamentous PR8/ NL602 M1 N207S virus displayed the lowest level of activity (**Table 1**, **Table 2** and **Fig. 5A, B**, and **C**). Importantly, despite the differences in V_{max} , all viruses maintained K_m values with overlapping confidence intervals, demonstrating that the results were not produced by changes in the affinity of the PR8 NA protein for the MUNANA substrate.

These data likely differ from previous reports because they were collected

from a total number of virions (particles), as opposed to only those virions that are infectious (PFU). Indeed, we determined that our reassortant viruses had different particle to PFU ratios, however, defective particle number did not correlate with NA activity (**Table 2**). Taken together, these results suggest that NA activity can be independent of virus morphology and production of defective particles. affinity of the PR8 NA protein for the MUNANA substrate.

These data likely differ from previous reports because they were collected from a total number of virions (particles), as opposed to only those virions that are infectious (PFU). Indeed, we determined that our reassortant viruses had different particle to PFU ratios, however, defective particle number did not correlate with NA activity (**Table 2**). Taken together, these results suggest that NA activity can be independent of virus morphology and production of defective particles.

Replication and transmission efficiency of recombinant viruses in the guinea pig model. Studies using the guinea pig model have demonstrated that the PR8 virus is non-transmissible with an inoculum dose of either 100 or 1000 PFU, while the wild-type NL602 and PR8/ NL602 M viruses transmit to 100% and 75% of contact animals at both doses, respectively (13, 16, 27). In order to assess differences in infectivity, replication, and transmission of the reassortant PR8 viruses, guinea pigs were inoculated intranasally with a dose of 10 PFU of virus. At this low dose, there were no significant differences in infectivity between the reassortant viruses, with each virus infecting eight to ten of the 12 inoculated animals, as indicated in Figure 6. Even with an inoculum of 10 PFU, the PR8/ NL602

M virus transmitted to 78% of the exposed animals and replicated to approximately 10^5 PFU by day two post-inoculation (**Fig. 6A**). In contrast, the PR8/ EAsw M virus transmitted to only one contact animal (12.5% efficiency) ($P = 0.0093$; unpaired t -test) and replicated to significantly lower titers ($\sim 10^4$) by day two post-inoculation in the infected animals ($P = 0.0002$; unpaired t -test) (**Fig. 6B**). In addition, the PR8/ EAsw M1+NL602 M2 (M2 C19Y) virus also transmitted to significantly fewer guinea pigs (20%) ($P = 0.0120$; unpaired t -test) although replication was not statistically different from the PR8/ NL602 M virus (10^5 PFU / mL at day two) in the infected animals (**Fig. 6C**). Strikingly, the single mutant PR8/ NL602 M1 N207S virus also transmitted with a significantly reduced efficiency (17%) ($P = 0.0300$; unpaired t -test) and replicated to significantly lower titers at day 2 ($\sim 10^4$ PFU / mL) in the infected animals ($P = 0.041$; unpaired t -test) (**Fig. 6E**). Additionally, both the PR8/ NL602 M1 S30G and PR8/ NL602 M1 M248I (M2 C19Y) viruses transmitted less efficiently than the wild-type PR8/ NL602 M virus, although neither difference was significant, and only the PR8/ NL602 M1 M248I (M2 C19Y) virus had significantly reduced titers ($\sim 10^4$ PFU / mL) in the infected guinea pigs at day two postinoculation ($P = 0.014$; unpaired t -test) (**Fig. 6D and F**). In summary, significantly reduced transmission efficiencies were observed for viruses containing the EAsw matrix protein, or the single NL602 M1 N207S point mutation, compared with the PR8/ NL602 M virus.

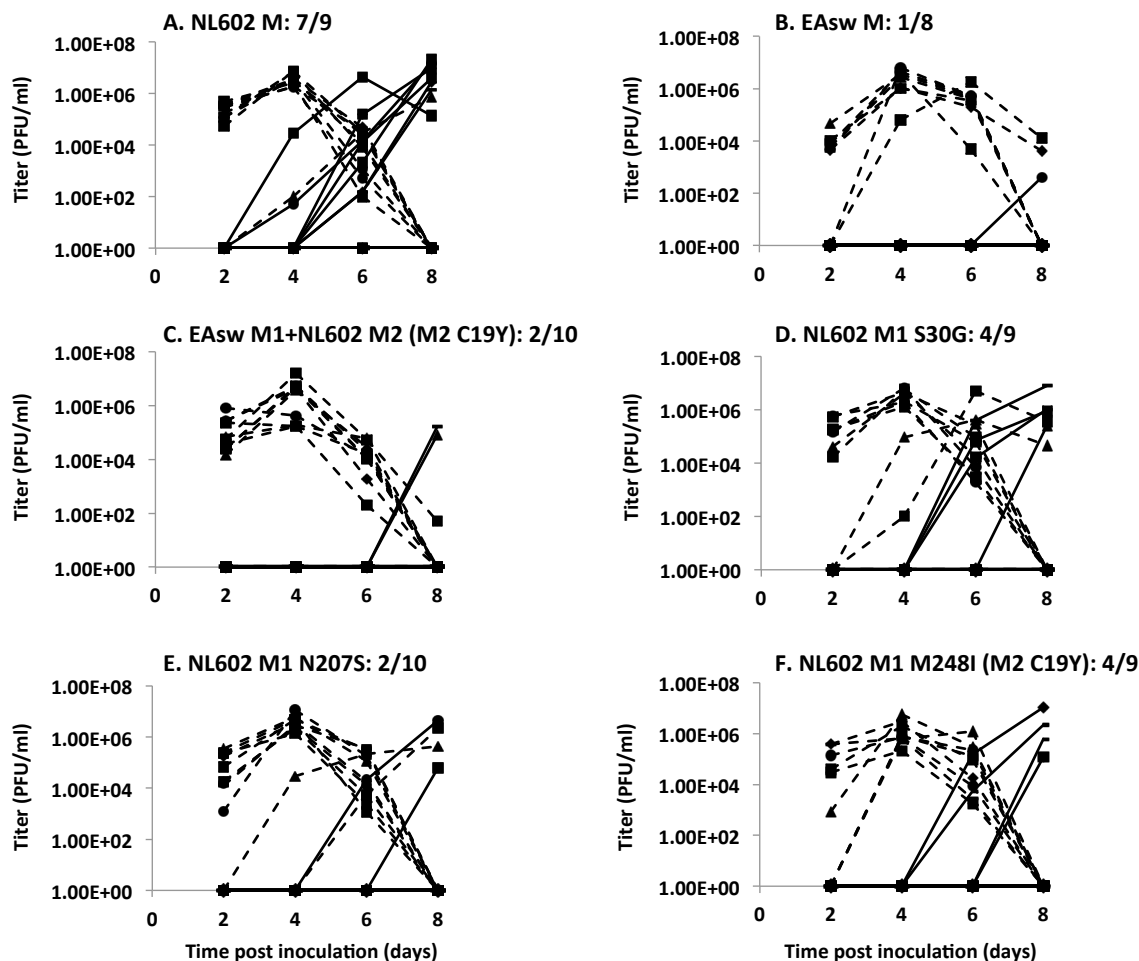


Figure 6. PR8 viruses harboring the EAsw M1 protein, or the single NL602 M1 N207S mutation, have reduced transmission efficiency compared to the PR8/ NL602 M virus in the guinea pig model. Guinea pigs were inoculated intranasally with 10 PFU of (A) PR8/ NL602 M, (B) PR8/ EAsw M, (C) PR8/ EAsw M1+NL602 M2 (M2 C19Y), (D) PR8/ NL602 M1 S30G, (E) PR8/ NL602 M1 N207S, or (F) PR8/ NL602 M1 M248I (M2 C19Y), placed with a naïve co-caged animal 24 h post inoculation, and housed in environmental chambers controlled for temperature (10°C) and humidity (20%). Nasal washes were collected from inoculated (dashed lines) and contact-exposed (solid lines) guinea pigs every two days for eight days and virus titers were determined by plaque assay on MDCK cells.

DISCUSSION

We have demonstrated that recombinant PR8 viruses containing EAsw, the EAsw M1+NL602 M2 (M2 C19Y), and mutant NL602 M1 N207S M segments transmit with significantly reduced efficiency between guinea pigs compared to the PR8/ NL602 M virus. Prior investigations utilized reassortant viruses containing the pH1N1 M, M and NA, or M, NA, and HA segments to demonstrate a critical role for the pH1N1 M segment in virus transmissibility (1-4). Herein, we demonstrated that the PR8/ NL602 M virus maintains transmissibility between guinea pigs when the inoculum dose is reduced from 100 to 10 PFU (2). The low dose of the inoculum underscores the robust ability of this virus to replicate in and transmit between animals and may increase the sensitivity of the assay in detecting differences in virus transmission efficiencies. Our data indicate a reduction in PR8/ NL602 M virus transmissibility that maps to the EAsw M1 protein and, more specifically, to the EAsw serine residue at M1 position 207. Additionally, although reduced compared to PR8/ NL602 M, the transmission efficiencies of the PR8/ EAsw M1+NL602 M2 (M2 C19Y) and PR8/ NL602 M1 N207S viruses were higher than that of PR8/ EAsw M, suggesting potential additional contributions of the NL602 M1 and /or M2 protein to virus transmissibility.

Available structural data (5, 6) have shown that M1 is composed, in part, of nine alpha helices that are joined by eight loop regions. In addition, Calder and colleagues (7) utilized electron cryotomography to demonstrate that M1 oligomerizes into a helix beneath the cell-derived viral membrane and that the pitch

of the helix differs for viruses exhibiting spherical and filamentous virions. The NL602 and EAsw lineage matrix proteins share 98.8% sequence identity, differing only at codons 30, 207, and 248. M1 position 30 falls within the second α -helix. Amino acid substitution within α -helix 2 could affect M1 oligomerization and/ or the helical arrangement, or M1 interaction with other proteins, resulting in the observed change in virion morphology. Since the structure has only been solved for M1 amino acids 2 – 158, the residues at positions 207 and 248 have unknown structural and functional relationships.

The matrix protein 30S, 207N, and 248M residues are present in 98.2%, 99.9%, and 99.9% of all pH1N1 isolate sequences in the Influenza Research Database, respectively. In contrast, human H3N2 isolates overwhelmingly contain M1 30D (99.9%) and 207S (99.6%) residues, suggesting that the ability of the N207S mutation to affect virus transmissibility may be specific to the H1N1 subtype. In addition, the European and Asian swine H1N1 isolates encode M1 30G (36%), N207S (97.1%), and M248I (56.3%) residues among greater sequence variability. The genetic diversity between the swine H1N1 matrix proteins, compared to those of the human lineages, suggests that the M1 from this reservoir may be more permissive to novel mutations that could impact viral fitness and transmissibility.

In addition to its other roles in the viral life cycle, the matrix protein has recently been shown to be a major determinant of influenza morphology (8, 9). Numerous M1 amino acids have been associated with changes in virion shape, including residues 30, 41, 87, 95, 102, 169, 198, 204, 207, and 209 (8-14). Of these, the T169I and Q198K mutations were found to independently confer an almost

entirely spherical morphology to the otherwise filamentous NL602 virus, while reducing its early replication and time-to-transmission, but not transmission efficiency, in the guinea pig model. In addition, Bialas and colleagues recently introduced S30D, N207S, and T209A mutations into the matrix protein of the early pH1N1 isolate, A/California/04/2009 (H1N1) [Cal04]. Our results confirm their finding that substitution of the pH1N1 M1 207N residue with a serine results in a filamentous virus population.

Filamentous virions are selected for *in vivo* (11), while repeated passage of a filamentous virus in laboratory substrates often selects for a more spherical morphology (11, 15, 16). We previously observed a correlation between filamentous virus morphology and transmission efficiency between recombinant PR8 viruses containing different combinations of NL602 M, NA, and HA segments (2). These combined findings led us to propose that there was a positive correlation between virus morphology and transmissibility; however, our current results do not support this hypothesis. Although the S30G and M248I (M2 C19Y) mutations both decrease the filament number associated with the PR8/ NL602 M virus, they did not significantly affect transmission. Additionally, while the N207S mutation did not decrease the number of filaments produced by PR8/ NL602 M, nor did it decrease the percentage of filaments greater than 1 μm in length, it significantly reduced virus replication and transmission. Although these results are contrary to previous reports (2, 4) that observed a correlation between increased filament number and transmission efficiency, they are in agreement with other studies (11, 12) that did not observe the association. Altogether, these data suggest that although filaments

are selected for *in vivo*, their affect, if any, on transmission, may be strain-specific or partly dependent upon other viral or host factors. Therefore, the basis for the selection of filaments within a host remains unknown.

Based on a previously observed correlation between a more filamentous morphology and increased NA activity, we proposed a model (2) in which more filamentous virions produce greater levels of NA activity and subsequently transmit more efficiently between hosts. However, we did not observe an association between morphology and enzyme activity for our recombinant PR8 viruses. In contrast, the less filamentous PR8/ NL602 M1 M248I (M2 C19Y), PR8/ EAsw M, and PR8 viruses displayed higher V_{\max} values than the filamentous PR8/ NL602 M virus, while the filamentous PR8/ NL602 M1 N207S virus had the lowest V_{\max} . The apparent discrepancy between our current and previous observations may be explained by previously unappreciated differences in the total number of evaluated virions, as well as other unknown factors, such as virion stability or M1-protein interactions. Herein, we discovered up to 100-fold differences between the particle / PFU ratios for our recombinant viruses that were independent of virus morphology. These data confirmed previous studies (12, 17), which reported that neuraminidase activity is dependent upon the matrix protein. However, the mechanism by which the M1 protein can modulate NA activity remains unknown.

In addition to a correlation between virus morphology and NA activity, previous studies (2, 18) found that neuraminidase activity correlated with virus transmissibility. In contrast to these reports, transmissibility of our recombinant PR8 viruses was independent of their enzyme activity. Although the S30G mutant

had the highest V_{max} , followed by the PR8, EAsw M, NL602 M, EAsw M1+NL602 M2 (M2 C19Y), and N207S viruses, their transmission efficiencies were 44%, 0%, 12.5%, 78%, 20%, and 17%, respectively. These data may indicate that the link between neuraminidase activity and virus transmissibility is strain-specific or that a concurrent functional change, such as optimized NA/ HA balance, must occur for the phenotype to be observed.

Since our transmission data do not correlate with changes in virion morphology or NA activity, the mechanism by which the M1 protein is affecting virus transmissibility remains unknown. M1 plays many roles in the virus life cycle, including vRNP trafficking to the plasma membrane, virus assembly, direct protein-protein interaction, and virus budding. Recently, Bialas and colleagues (19) investigated the potential affect of pH1N1 M1 amino acid changes on levels of VLP production and showed that the S30D and N207S/T209A mutations reduced VLP release, but not association of M1 with the plasma membrane, *in vitro*. S30G and N207S single mutants were not included in the assay. Although we did not quantify VLP production for our recombinant viruses, it is unlikely that a reduction in virion release is responsible for the low transmissibility of the N207S mutant, as it was reduced for the S30 mutant, which did not affect transmission of our recombinant PR8/ NL602 M virus in the guinea pig model.

In conclusion, our data demonstrate a role for the influenza matrix protein in H1N1 virus replication and transmission. More specifically, we show that loss of the conserved asparagine residue at position 207 in the NL602 M1 protein results in reduced replication and transmissibility in the guinea pig model. These data suggest

that functions encoded by the influenza matrix protein can affect virus transmissibility and that the effect can be independent of virus morphology and NA activity.

REFERENCES

1. **Van Kerkhove MD, Hirve S, Koukounari A, Mounts AW, for the H1N1pdm serology working group.** 2013. Estimating age-specific cumulative incidence for the 2009 influenza pandemic: a meta-analysis of A(H1N1)pdm09 serological studies from 19 countries. *Influenza and Other Respiratory Viruses* **7**:872–886.
2. 2009. Emergence of a Novel Swine-Origin Influenza A (H1N1) Virus in Humans. *N Engl J Med* **360**:2605–2615.
3. **Komadina N, Roque V, Thawatsupha P, Rimando-Magalong J, Waicharoen S, Bomasang E, Sawanpanyalert P, Rivera M, Iannello P, Hurt AC, Barr IG.** 2007. Genetic analysis of two influenza A (H1) swine viruses isolated from humans in Thailand and the Philippines. *Virus Genes* **35**:161–165.
4. **Myers KP, Olsen CW, Gray GC.** 2007. Cases of swine influenza in humans: a review of the literature. *Clinical Infectious Diseases* **44**:1084–1088.
5. **Shinde V, Bridges CB, Uyeki TM, Shu B, Balish A, Xu X, Lindstrom S, Gubareva LV, Deyde V, Garten RJ, Harris M, Gerber S, Vagasky S, Smith F, Pascoe N, Martin K, Dufficy D, Ritger K, Conover C, Quinlisk P, Klimov A,**

- Bresee JS, Finelli L.** 2009. Triple-Reassortant Swine Influenza A (H1) in Humans in the United States, 2005–2009. *N Engl J Med* **360**:2616–2625.
6. **Tumpey TM, Maines TR, Van Hoeven N, Glaser L, Solorzano A, Pappas C, Cox NJ, Swayne DE, Palese P, Katz JM, Garcia-Sastre A.** 2007. A Two-Amino Acid Change in the Hemagglutinin of the 1918 Influenza Virus Abolishes Transmission. *Science* **315**:655–659.
7. **Imai M, Watanabe T, Hatta M, Das SC, Ozawa M, Shinya K, Zhong G, Hanson A, Katsura H, Watanabe S, Li C, Kawakami E, Yamada S, Kiso M, Suzuki Y, Maher EA, Neumann G, Kawaoka Y.** 2012. Experimental adaptation of an influenza H5 HA confers respiratory droplet transmission to a reassortant H5 HA/H1N1 virus in ferrets. *Nature* 1–11.
8. **Herfst S, Schrauwen EJA, Linster M, Chutinimitkul S, de Wit E, Munster VJ, Sorrell EM, Bestebroer TM, Burke DF, Smith DJ, Rimmelzwaan GF, Osterhaus ADME, Fouchier RAM.** 2012. Airborne Transmission of Influenza A/H5N1 Virus Between Ferrets. *Science* **336**:1534–1541.
9. **Van Hoeven N, Belser JA, Szretter KJ, Zeng H, Staeheli P, Swayne DE, Katz JM, Tumpey TM.** 2009. Pathogenesis of 1918 Pandemic and H5N1 Influenza Virus Infections in a Guinea Pig Model: Antiviral Potential of Exogenous Alpha Interferon To Reduce Virus Shedding. *Journal of Virology* **83**:2851–2861.
10. **Steel J, Lowen AC, Mubareka S, Palese P.** 2009. Transmission of influenza virus in a mammalian host is increased by PB2 amino acids 627K or 627E/701N. *PLoS Pathog* **5**:e1000252.
11. **Bradley KC, Jones CA, Tompkins SM, Tripp RA, Russell RJ, Gramer MR,**

- Heimburg-Molinaro J, Smith DF, Cummings RD, Steinhauer DA.** 2011. Comparison of the receptor binding properties of contemporary swine isolates and early human pandemic H1N1 isolates (Novel 2009 H1N1). *Virology* **413**:169–182.
12. **Herfst S, Chutinimitkul S, Ye J, de Wit E, Munster VJ, Schrauwen EJA, Bestebroer TM, Jonges M, Meijer A, Koopmans M, Rimmelzwaan GF, Osterhaus ADME, Perez DR, Fouchier RAM.** 2010. Introduction of Virulence Markers in PB2 of Pandemic Swine-Origin Influenza Virus Does Not Result in Enhanced Virulence or Transmission. *Journal of Virology* **84**:3752–3758.
13. **Chou YY, Albrecht RA, Pica N, Lowen AC, Richt JA, Garcia-Sastre A, Palese P, Hai R.** 2011. The M Segment of the 2009 New Pandemic H1N1 Influenza Virus Is Critical for Its High Transmission Efficiency in the Guinea Pig Model. *Journal of Virology* **85**:11235–11241.
14. **Lakdawala SS, Lamirande EW, Suguitan AL, Wang W, Santos CP, Vogel L, Matsuoka Y, Lindsley WG, Jin H, Subbarao K.** 2011. Eurasian-Origin Gene Segments Contribute to the Transmissibility, Aerosol Release, and Morphology of the 2009 Pandemic H1N1 Influenza Virus. *PLoS Pathog* **7**:e1002443.
15. **Ma W, Liu Q, Bawa B, Qiao C, Qi W, Shen H, Chen Y, Ma J, Li X, Webby RJ, Garcia-Sastre A, Richt JA.** 2012. The neuraminidase and matrix genes of the 2009 pandemic influenza H1N1 virus cooperate functionally to facilitate efficient replication and transmissibility in pigs. *Journal of General Virology* **93**:1261–1268.

16. **Shtykova EV, Baratova LA, Fedorova NV, Radyukhin VA, Ksenofontov AL, Volkov VV, Shishkov AV, Dolgov AA, Shilova LA, Batishchev OV, Jeffries CM, Svergun DI.** 2013. Structural Analysis of Influenza A Virus Matrix Protein M1 and Its Self-Assemblies at Low pH. *PLoS ONE* **8**:e82431.
17. **Calder LJ, Wasilewski JA, Berrimen JA, Rosenthal PB.** 2010. Structural organization of a filamentous influenza A virus. *Proceedings of the National Academy of Sciences* **107**:10685–10690.
18. **Ruigrok RWH, Barge A, Durrer P, Brunner J, Ma K, Whittaker GR.** 2000. Membrane Interaction of Influenza Virus M1 Protein. *Virology* **267**:289–298.
19. **Bui M, Whittaker G, Helenius A.** 1996. Effect of M1 protein and low pH on nuclear transport of influenza virus ribonucleoproteins. *Journal of Virology* **70**:8391–8401.
20. **Rossmann JS, Lamb RA.** 2011. Influenza virus assembly and budding. *Virology* **411**:229–236.
21. **Chen BJ, Leser GP, Jackson D, Lamb RA.** 2008. The Influenza Virus M2 Protein Cytoplasmic Tail Interacts with the M1 Protein and Influences Virus Assembly at the Site of Virus Budding. *Journal of Virology* **82**:10059–10070.
22. **Enami M, Enami K.** 1996. Influenza virus hemagglutinin and neuraminidase glycoproteins stimulate the membrane association of the matrix protein. *Journal of Virology* **70**:6653–6657.
23. **McCown MF, Pekosz A.** 2006. Distinct Domains of the Influenza A Virus M2 Protein Cytoplasmic Tail Mediate Binding to the M1 Protein and Facilitate Infectious Virus Production. *Journal of Virology* **80**:8178–8189.

24. **Bourmakina SV.** 2003. Reverse genetics studies on the filamentous morphology of influenza A virus. *Journal of General Virology* **84**:517–527.
25. **Elleman CJ, Barclay WS.** 2004. The M1 matrix protein controls the filamentous phenotype of influenza A virus. *Virology* **321**:144–153.
26. **Seladi-Schulman J, Steel J, Lowen AC.** 2013. Spherical influenza viruses have a fitness advantage in embryonated eggs, while filament-producing strains are selected in vivo. *Journal of Virology* **87**:13343–13353.
27. **Seladi-Schulman J, Campbell PJ, Suppiah S, Steel J, Lowen AC.** 2014. Filament-Producing Mutants of Influenza A/Puerto Rico/8/1934 (H1N1) Virus Have Higher Neuraminidase Activities than the Spherical Wild-Type. *PLoS ONE* **9**:e112462.
28. **Campbell PJ, Kyriakis CS, Marshall N, Suppiah S, Seladi-Schulman J, Danzy S, Lowen AC, Steel J.** 2014. Residue 41 of the Eurasian avian-like swine influenza A virus matrix protein modulates virion filament length and efficiency of contact transmission. *Journal of Virology* **88**:7569–7577.
29. **Campbell PJ, Danzy S, Kyriakis CS, Deymier MJ, Lowen AC, Steel J.** 2014. The m segment of the 2009 pandemic influenza virus confers increased neuraminidase activity, filamentous morphology, and efficient contact transmissibility to a/puerto rico/8/1934-based reassortant viruses. *Journal of Virology* **88**:3802–3814.
30. **Lowen AC, Mubareka S, Tumpey TM, Garcia-Sastre A, Palese P.** 2006. The guinea pig as a transmission model for human influenza viruses. *Proceedings of the National Academy of Sciences* **103**:9988–9992.

31. **Fodor E, Devenish L, Engelhardt OG, Palese P, Brownlee GG, Garcia-Sastre A.** 1999. Rescue of influenza A virus from recombinant DNA. *Journal of Virology* **73**:9679–9682.
32. **Hoffmann E, Stech J, Guan Y, Webster RG, Perez DR.** 2001. Universal primer set for the full-length amplification of all influenza A viruses. *Archives of Virology* **146**:2275–2289.

CHAPTER 4

CONCLUSION

Influenza pandemics cause significant global morbidity and mortality and pose considerable challenges to global public health systems. The pandemics occur when an antigenically novel influenza A virus [IAV] emerges from the animal reservoir and is introduced into the human population *in toto* or through reassortment with a circulating human strain. Because the virus is antigenically divergent from contemporary circulating strains, there is no pre-existing immunity in the population, which allows for a greater rate of virus spread. The most recent 2009 pandemic H1N1 virus (pH1N1) was rapidly transmitted around the globe, having infected approximately 24% of the population within one year of its emergence from the swine reservoir (258). The novel genotype of the pH1N1 lineage resulted from a reassortment event that replaced the M and NA segments of a North American triple reassortant swine virus [NAtr] with those of a virus from the Eurasian avian-like swine [EAsw] lineage (118). Several recent studies have focused on identifying the genetic changes that contributed to pH1N1 transmissibility, on the basis that the pandemic virus emerged from two parental lineages that transmitted very poorly between humans. By utilizing reverse genetics, a number of investigators, including ourselves, found that the pH1N1 M segment, with or without the NA segment, was critical for its transmissibility in ferrets, guinea pigs, and swine (222-224). This finding was significant, as the M segment had not previously been implicated in IAV transmission. However, the

mechanism(s) by which the pH1N1 M segment affects virus transmissibility remain unknown. Identification of the genetic factors and underlying mechanisms involved in IAV transmission between humans is essential to inform novel treatment strategies and surveillance efforts toward the identification of strains with pandemic potential. Therefore, in this work, we aimed to identify the protein product(s) and molecular mechanism(s) responsible for the contribution of the M segment to IAV transmission.

Collective introduction of pH1N1 M, NA, and HA segments into an otherwise non-transmissible virus reproduces the 100% transmission efficiency of wild-type pH1N1 in the guinea pig model

In Chapter 1 of this study, we demonstrate that inclusion of the M segment from the pH1N1 isolate, A/Netherlands/602/2009 (H1N1) [NL602], along with its cognate NA and HA segments in the recombinant A/Puerto Rico/8/34 (H1N1) [PR8] background, results in virus transmission between guinea pigs with the same efficiency (100%) as the wild type NL602 virus. In addition, inclusion of the NL602 M segment alone could independently confer transmissibility to an otherwise non-transmissible (PR8) virus, as previously reported (259). Importantly, the NL602 NA and HA segments, without the M segment, were insufficient for virus transmission at low dose, demonstrating that all three segments were required for the virus to achieve optimal transmission efficiency. Since the influenza HA and NA glycoproteins share sialic acid as a substrate, a balance between HA binding for cell entry and NA cleavage for nascent virion release must be achieved for productive

viral replication (220, 221). As NA/ HA balance was recently suggested to be critical factor for pH1N1 transmissibility (220), and the NA and HA segments together are insufficient for contact transmission of a recombinant PR8 virus at a low dose, we suggest that independent functions encoded within the M segment, and / or functional interactions between the M, NA, and HA proteins are required to achieve the optimal transmission efficiency of the pH1N1 virus, potentially working through a mechanism which involves modulation of glycoprotein incorporation onto the surface of the virions.

Our M-glycoprotein interaction model, described in Chapter 1, is supported by enzyme kinetic data showing that introduction of the NL602 M segment into the PR8 and PR8/ NL602 NA+HA viruses significantly alters the levels of NA activity. To our knowledge, this data provided the first evidence that NA enzyme activity can be modulated by the virus M segment. Interestingly, viruses that contained the NL602 M segment, and cleaved sialic acid at higher rates, also produced a greater number of filamentous virions with the potential to incorporate higher levels of glycoprotein. However, in the absence of NA protein incorporation data, the association between virus morphology and NA activity remains correlative. Therefore, the mechanism by which the M segment modulates NA activity remains unknown. It is possible that functions encoded by either the M1 or M2 protein alter NA protein incorporation, distribution, or presentation on the surface of the virion. This previously unappreciated relationship between NA activity and the viral M segment is significant, as (i) previously reported differences in enzyme kinetics between different strains of influenza can no longer be assumed to be solely reflective of their

respective NA proteins; (ii) genetic variability within the M segment could alter levels of activity between otherwise isogenic viruses *in vivo* leading to increased levels of virion release from infected cells; and (iii) the swapping of M segments between viruses through reassortment could produce viruses with improved NA/HA balance.

A single amino acid change within the IAV matrix protein can simultaneously alter virus morphology, NA activity, and transmission efficiency in the guinea pig model

Sequence analysis of the EAsw strain, A/swine/Spain/53207/2004 (H1N1) [SPN04], led to the identification of a unique proline residue at position 41 of the matrix protein. By reverting the proline back to an alanine residue, which is highly conserved at this position in swine, human, and avian lineages, we demonstrated that inclusion of the proline, in the context of the SPN04 M segment decreases transmission efficiency of recombinant SPN04 and PR8-based viruses in the guinea pig model, while concurrently increasing virus NA activity and filamentous morphology (Chapter 2). Although previous studies demonstrated that genetic polymorphism at M1 41 could alter virus morphology (181, 183, 184) and lead to laboratory substrate and mouse adaptation (260, 261), this represents the first report of its impact on virus transmissibility. Since M1 position 41 is located within an alpha helix of the matrix protein, inclusion of a proline residue likely results in disruption of the M1 secondary structure, which could alter protein oligomerization or affect M1-protein interactions *in vivo*. Indeed, since changes in virus morphology

have been shown to be associated with modifications to the curvature of the M1 helix beneath the plasma membrane (79), it is possible that the M1 P41A mutation alters M1-M1 interactions to affect virion structure. Whether the observed dependency of virus NA activity on M1 position 41 is indicative of a direct M1-NA interaction or indirectly due to changes in M1 oligomerization has yet to be determined. However, this data not only support the observed correlation in Chapter 1, whereby viruses with a more highly filamentous population have greater levels of NA activity in an M segment-dependent manner, but suggest that the matrix protein may be responsible for this dependence. The fact that morphology and enzyme activity did not correlate with virus transmission for the M1 41A- and P-encoding viruses may be indicative of other, more dominant, effects of the M1 41 proline residue within a host, that attenuate virus fitness. However, it is possible that filament selection *in vivo*, and the corresponding increase in NA enzymatic activity, is either independent of virus transmissibility or is secondary to other viral factors, such as an optimal NA/ HA balance.

These data expand on the work of Chapter 1, by demonstrating that, in addition to the M segment, a single amino acid change within the encoded M1 protein, can impact IAV transmission. Consistent with other negative sense RNA viruses, IAVs possess a high mutation rate due to their error prone RNA-dependent RNA polymerase. Although human and avian lineages maintain a highly conserved alanine residue at M1 position 41 over time, according to the Influenza Research Database, the Eurasian and Asian swine H1N1 subtype viruses encode both M1 41 valine and alanine residues. The ability of Eurasian swine H1N1 viruses to tolerate,

to some extent, polymorphisms within a segment involved in the transmissibility of the human pandemic virus is of notable public health significance and underscores the importance of continued surveillance efforts within this reservoir.

The pH1N1 M segment confers transmissibility to an otherwise non-transmissible recombinant virus through functions encoded by its matrix protein

Given that changes in virus morphology and NA activity correlated with transmissibility of viruses harboring the pH1N1 M segment, as described in Chapter 1, and a single amino acid change within the matrix protein resulted in changes in morphology as well as transmission efficiency of PR8-based viruses, as reported in Chapter 2, we hypothesized that amino acid changes in the M1 protein of the pH1N1 M segment, relative to the precursor Eurasian swine matrix protein, would confer an increase in the transmissibility of a virus encoding such changes. Since the pH1N1 M segment originated from the EAsw lineage (118), we compared the replication and transmission efficiencies of PR8-based viruses containing wild-type, M1/M2 chimeric, or M1 single mutant NL602 M segments. Using a low-dose inoculum in the guinea pig model, we found that the PR8/ NL602 M virus had a transmission advantage over the PR8/ EAsw M virus, which was partially dependent upon the NL602 matrix protein, and mapped to an asparagine residue at M1 position 207. However, importantly, we cannot rule out a role for the pH1N1 M2 proton channel in the transmission phenotype of the pH1N1 M segment, as the transmission efficiencies of the PR8/ EAsw M1+NL602 M2 (M2 C19Y) and PR8/

NL602 M1 N207S mutants (20%) were not as low as that of the virus possessing the wild-type EAsw M segment (12.5%; although the difference between the three was insignificant).

Unfortunately, the M1 structure has only been solved for the first 158 amino acids (74, 78), and therefore structure-functional relationships relevant to position 207 remain unknown. Recently, a study demonstrated that *in vitro* VLP production was reduced for a pH1N1 matrix protein harboring a N207S/T209A double mutation (99), however; the effect was not unique to this motif, as it was also observed for a mutant with a S30D mutation. Since the introduction of a S30G mutation into the NL602 M segment in our study did not significantly reduce virus transmissibility, and the independent contribution of the N207S mutation to VLP production was not assessed in the study performed by the Takimoto laboratory, the dependence of reduced particle production on the 207N residue and its potential relationship to virus transmission remain unclear. Therefore, the mechanism by which the asparagine at position 207 in the NL602 matrix protein is exerting its effect on virus transmission remains unknown, although it is possible that it affects M1-protein interactions. Certainly, the N207S substitution resulted in an increased particle/ PFU ratio and decreased NA activity, suggesting that a reduction in virion stability could have reduced NA protein (or glycoprotein) incorporation. A reduction in the number of active NA proteins on the surface of the virions could impact rates of virion release or NA/ HA balance, thereby impacting the number of virions capable of productive infection and available for transmission to a new host. However, since defective particle number and neuraminidase activity

did not correlate between all reassortant viruses or with transmission efficiency of our recombinant viruses in the guinea pig model, it is likely that there is more than one requirement for transmissibility, such as a combination of virion stability and optimal NA/ HA balance, among other possible mechanisms.

Novel swine H3N2v viruses contain the pH1N1 M segment, transmit more readily to humans than other swine-origin IAVs, and can cause limited human-to-human transmission

In 2009, pH1N1 emerged from the swine reservoir, spread globally among humans, was reintroduced to swine in multiple countries, and began to reassort with co-circulating endemic H1N1, H1N2, and H3N2 swine viruses (262-267). To date, at least 10 genotypes of novel reassortant H3N2 swine viruses, all containing the pH1N1 M segment, have been detected within the US swine population (268-270). Zoonoses with an H3N2 variant virus [H3N2v] containing seven H3N2 segments and the pH1N1 M segment were first detected in 2011 (271, 272). By October 2014, there were 343 H3N2v infections reported across 13 states, including 18 hospitalizations and one death (144, 148). However, due to the limited laboratory confirmation and subtyping of clinical isolates of IAV, actual case numbers may be higher.

The majority of detected H3N2v infections have been linked to direct exposure with swine at agricultural fairs and were self-limiting, however, there have been reports of limited transmission between children (269, 271, 272). Recent investigations into the transmissibility of the novel viruses have demonstrated that

more than one H3N2v genotype can transmit efficiently by direct contact between pigs (273) and ferrets (274) and by respiratory droplet between ferrets (274). Although currently untested, it is possible that the pH1N1 M segment is contributing to H3N2v transmissibility, given that it was shown to be important for efficient transmission of pH1N1-based viruses (222-224), and swine-origin H3N2 viruses have not previously been transmissible between humans. Of note, the 14 human H3N2v matrix protein sequences available within the Influenza Research Database share 99% sequence identity with the pH1N1 M1 consensus sequence and all isolates contained the asparagine residue at position 207. It may be that replication and transmission of the novel reassortant H3N2v viruses in a human host is improved by functions encoded by the pH1N1-origin M segment, or M1 protein, but that other viral factors encoded in the swine lineage genome are currently preventing the viruses from achieving optimal transmissibility among humans. Further research will be needed in order to test the contribution of the pH1N1-origin M segment, and/ or M1 protein, to the cross-species transmissibility of the novel H3N2v viruses.

Overall Conclusions

In conclusion, we have demonstrated that functions encoded by the M segment can impact IAV morphology, NA activity, and transmissibility. Specific amino acids within the M segment-encoded matrix protein can contribute to these *in vitro* and *in vivo* phenotypes. Our data demonstrate that although a filamentous morphology may be selected for *in vivo*, it does not always correlate with virus

transmissibility, suggesting that transmissibility is most likely a polygenic phenotype. In addition, we found that virus NA activity is dependent upon the M1 matrix protein. Although M1 residues appear to modulate enzyme activity, levels of neuraminidase activity alone are not predictive of transmission efficiency. We therefore suggest that functions encoded by the matrix protein impact virus particle/ PFU ratio, morphology, and NA activity, which may independently or cooperatively impact virus transmissibility. Collectively, these studies provide insights into the protein products and mechanisms underlying the contribution of the M segment to IAV transmission. Identification and investigation of the viral factors that promote IAV transmission will ultimately aid in the development of novel therapeutic strategies and enhance surveillance efforts for the identification of IAV strains with pandemic potential.

REFERENCES

1. **Hause BM, Collin EA, Liu R, Huang B, Sheng Z, Lu W, Wang D, Nelson EA, Li F.** 2014. Characterization of a Novel Influenza Virus in Cattle and Swine: Proposal for a New Genus in the Orthomyxoviridae Family. *mBio* **5**:e00031–14–e00031–14.
2. **Palese P, Shaw ML.** 2007. Orthomyxoviridae: the viruses and their replication, pp. 1647–1690. *In* Knipe, DM, Howley, PM (eds.), *Fields Virology*, 5 ed. Lippincott Williams & Wilkins, Philadelphia.
3. **Yoon S-W, Webby RJ, Webster RG.** 2014. Evolution and Ecology of Influenza A Viruses, pp. 359–375. *In* *Current Topics in Microbiology and Immunology*. Springer International Publishing, Cham.
4. **Bodewes R, Morick D, de Mutsert G, Osinga N, Bestebroer T, van der Vliet S, Smits SL, Kuiken T, Rimmelzwaan GF, Fouchier RAM, Osterhaus ADME.** 2013. Recurring Influenza B Virus Infections in Seals. *Emerg. Infect. Dis.* **19**:511–512.
5. **Tong S, Li Y, Rivaller P, Conrardy C, Castillo DAA, Chen L-M, Recuenco S, Ellison JA, Davis CT, York IA, Turmelle AS, Moran D, Rogers S, Shi M, Tao Y, Weil MR, Tang K, Rowe LA, Sammons S, Xu X, Frace M, Lindblade KA, Cox NJ, Anderson LJ, Rupprecht CE, Donis RO.** 2012. A distinct lineage of influenza A virus from bats. *PNAS* **109**:4269–4274.
6. **Tong S, Zhu X, Li Y, Shi M, Zhang J, Bourgeois M, Yang H, Chen X, Recuenco S, Gomez J.** 2013. New world bats harbor diverse influenza A

- viruses. PLoS Pathog **9**:e1003657.
7. **Lowen AC, Mubareka S, Tumpey TM, Garcia-Sastre A, Palese P.** 2006. The guinea pig as a transmission model for human influenza viruses. Proceedings of the National Academy of Sciences **103**:9988–9992.
 8. **Shope RE.** 1935. THE INFECTION OF MICE WITH SWINE INFLUENZA VIRUS. J. Exp. Med. **62**:561–572.
 9. **Smith W, Andrewes CH, Laidlaw PP.** 1933. A virus obtained from influenza patients. The Lancet **222**:66–68.
 10. **Geraci JR, St Aubin DJ, Barker IK, Webster RG, Hinshaw VS, Bean WJ, Ruhnke HL, Prescott JH, Early G, Baker AS, Madoff S, Schooley RT.** 1982. Mass mortality of harbor seals: pneumonia associated with influenza A virus. Science **215**:1129–1131.
 11. **Keawcharoen J, Oraveerakul K, Kuiken T, Fouchier RAM, Amonsin A, Payungporn S, Noppornpanth S, Wattanodorn S, Theambooniers A, Tantilertcharoen R, Pattanarangsarn R, Arya N, Ratanakorn P, Osterhaus DME, Poovorawan Y.** 2004. Avian influenza H5N1 in tigers and leopards. Emerg. Infect. Dis. **10**:2189–2191.
 12. **Klingeborn B, Englund L, Rott R, Juntti N, Rockborn G.** 1985. An avian influenza A virus killing a mammalian species--the mink. Brief report. Archives of Virology **86**:347–351.
 13. **Hinshaw VS, Bean WJ, Geraci J, Fiorelli P, Early G, Webster RG.** 1986. Characterization of two influenza A viruses from a pilot whale. Journal of Virology **58**:655–656.

14. **O S, B T, F P, J N.** 1958. Isolation of a virus causing respiratory disease in horses. *Acta Virol* **2**:52–61.
15. **Crawford PC, Dubovi EJ, Castleman WL, Stephenson I, Gibbs E, Chen L, Smith C, Hill RC, Ferro P, Pompey J.** 2005. Transmission of equine influenza virus to dogs. *Science* **310**:482–485.
16. **Paniker CK, Nair CM.** 1970. Infection with A2 Hong Kong influenza virus in domestic cats. *Bull. World Health Organ.* **43**:859–862.
17. **Centers for Disease Control and Prevention (CDC).** 1997. Isolation of avian influenza A (H5N1) viruses from humans--Hong Kong, May-December 1997. *MMWR Morb. Mortal. Wkly. Rep.* **46**:1204.
18. **Myers KP, Setterquist SF, Capuano AW, Gray GC.** 2007. Infection Due to 3 Avian Influenza Subtypes in United States Veterinarians. *Clinical Infectious Diseases* **45**:4–9.
19. **Blair PJ, Putnam SD, Krueger WS, Chum C, Wierzba TF, Heil GL, Yasuda CY, Williams M, Kasper MR, Friary JA, Capuano AW, Saphonn V, Peiris M, Shao H, Pérez DR, Gray GC.** 2013. Evidence for avian H9N2 influenza virus infections among rural villagers in Cambodia. *Journal of Infection and Public Health* **6**:69–79.
20. **Arzey GG, Kirkland PD, Arzey KE, Frost M, Maywood P, Conaty S, Hurt AC, Deng Y-M, Iannello P, Barr I, Dwyer DE, Ratnamohan M, McPhie K, Selleck P.** 2012. Influenza Virus A (H10N7) in Chickens and Poultry Abattoir Workers, Australia. *Emerg. Infect. Dis.* **18**:814–816.
21. **To KKW, Tsang AKL, Chan JFW, Cheng VCC, Chen H, Yuen K-Y.** 2014.

- Emergence in China of human disease due to avian influenza A(H10N8) e
Cause for concern? *Journal of Infection* **68**:205–215.
22. **Olsen CW**. 2002. The emergence of novel swine influenza viruses in North America. *Virus Research* **85**:199–210.
 23. **Schultz-Cherry S, Olsen CW, Easterday BC**. 2013. History of Swine influenza 21–27.
 24. **Song D, Kang B, Lee C, Jung K, Ha G, Kang D, Park S, Park B, Oh J**. 2008. Transmission of avian influenza virus (H3N2) to dogs. *Emerg. Infect. Dis.* **14**:741.
 25. **MOON H, Hong M, KIM JK, SEON B, NA W, PARK SJ, AN DJ, JEOUNG HY, KIM DJ, KIM JM, KIM SH, Webby RJ, Webster RG, KANG BK, SONG D**. 2014. H3N2 canine influenza virus with the matrix gene from the pandemic A/H1N1 virus: infection dynamics in dogs and ferrets. *Epidemiol. Infect.* 1–9.
 26. **GH W, MB T, MM S**. 1963. A new influenza virus associated with equine respiratory disease. *Journal of American Veterinary Medical Association* **143**:587–590.
 27. **Presti RM, Zhao G, Beatty WL, Mihindukulasuriya KA, Travassos da Rosa APA, Popov VL, Tesh RB, Virgin HW, Wang D**. 2009. Quarantil, Johnston Atoll, and Lake Chad Viruses Are Novel Members of the Family Orthomyxoviridae. *Journal of Virology* **83**:11599–11606.
 28. **Krossøy B, Hordvik I, Nilsen F, Nylund A, Endresen C**. 1999. The Putative Polymerase Sequence of Infectious Salmon Anemia Virus Suggests a New Genus within the Orthomyxoviridae. *Journal of Virology* **73**:2136–2142.

29. **Fauquet CM, Mayo MA.** 2001. The 7th ICTV report. Archives of Virology.
30. **Hubálek Z, Rudolf I.** 2012. Tick-borne viruses in Europe. Parasitol Res **111**:9–36.
31. **De Graaf M, Fouchier RAM.** 2014. Role of receptor binding specificity in influenza A virus transmission and pathogenesis. The EMBO Journal **33**:823–841.
32. **Rossman JS, Leser GP, Lamb RA.** 2012. Filamentous Influenza Virus Enters Cells Via Macropinocytosis. Journal of Virology **86**:10950–10960.
33. **Rossman JS, Lamb RA.** 2011. Influenza virus assembly and budding. Virology **411**:229–236.
34. **de Vries E, de Vries RP, Wienholts MJ, Floris CE, Jacobs M-S, van den Heuvel A, Rottier PJM, de Haan CAM.** 2012. Influenza A virus entry into cells lacking sialylated N-glycans. PNAS 1–6.
35. **de Vries E, Tscherne DM, Wienholts MJ, Cobos-Jiménez V, Scholte F, Garcia-Sastre A, Rottier PJM, de Haan CAM.** 2011. Dissection of the Influenza A Virus Endocytic Routes Reveals Macropinocytosis as an Alternative Entry Pathway. PLoS Pathog **7**:e1001329.
36. **Sieczkarski SB, Whittaker GR.** 2002. Influenza Virus Can Enter and Infect Cells in the Absence of Clathrin-Mediated Endocytosis. Journal of Virology **76**:10455–10464.
37. **Rust MJ, Lakadamyali M, Zhang F, Zhuang X.** 2004. Assembly of endocytic machinery around individual influenza viruses during viral entry. Nat Struct Mol Biol **11**:567–573.

38. **Dourmashkin RR, Tyrrell DA.** 1974. Electron microscopic observations on the entry of influenza virus into susceptible cells. *J. Gen. Virol.* **24**:129–141.
39. **Patterson S, Oxford JS, Dourmashkin RR.** 1979. Studies on the mechanism of influenza virus entry into cells. *J. Gen. Virol.* **43**:223–229.
40. **Pinto LH, Holsinger LJ, Lamb RA.** 1992. Influenza virus M2 protein has ion channel activity. *Cell* **69**:517–528.
41. **Li S, Sieben C, Ludwig K, Höfer CT, Chiantia S, Herrmann A, Eghiaian F, Schaap IAT.** 2014. pH-Controlled Two-Step Uncoating of Influenza Virus. *Biophysj* **106**:1447–1456.
42. **Bui M, Whittaker G, Helenius A.** 1996. Effect of M1 protein and low pH on nuclear transport of influenza virus ribonucleoproteins. *Journal of Virology* **70**:8391–8401.
43. **Boulo S, Akarsu H, Lotteau V, Müller CW, Ruigrok RWH, Baudin F.** 2011. Human importin alpha and RNA do not compete for binding to influenza A virus nucleoprotein. *Virology* **409**:84–90.
44. **Gabriel G, Klingel K, Otte A, Thiele S, Hudjetz B, Arman-Kalcek G, Sauter M, Shmidt T, Rother F, Baumgarte S, Keiner B, Hartmann E, Bader M, Brownlee GG, Fodor E, Klenk H-D.** 2011. Differential use of importin- α isoforms governs cell tropism and host adaptation of influenza virus. *Nature Communications* **2**:156.
45. **O'Neill RE, Jaskunas R, Blobel G, Palese P, Moroianu J.** 1995. Nuclear Import of Influenza Virus RNA Can Be Mediated by Viral Nucleoprotein and Transport Factors Required for Protein Import. *Journal of Biological*

- Chemistry **270**:22701–22704.
46. **O'Neill RE, Talon J, Palese P.** 1998. The influenza virus NEP (NS2 protein) mediates the nuclear export of viral ribonucleoproteins. *The EMBO Journal* **17**:288–296.
 47. **Herz C, Stavnezer E, Krug R, Gurney T.** 1981. Influenza virus, an RNA virus, synthesizes its messenger RNA in the nucleus of infected cells. *Cell* **26**:391–400.
 48. **Jackson DA, Caton AJ, McCready SJ, Cook PR.** 1982. Influenza virus RNA is synthesized at fixed sites in the nucleus.
 49. **Ulmanen I, Broni BA, Krug RM.** 1981. Role of two of the influenza virus core P proteins in recognizing cap 1 structures (m⁷GpppNm) on RNAs and in initiating viral RNA transcription. *Proceedings of the National Academy of Sciences* **78**:7355–7359.
 50. **Plotch SJ, Bouloy M, Ulmanen I, Krug RM.** 1981. A unique cap (m⁷GpppXm)-dependent influenza virion endonuclease cleaves capped RNAs to generate the primers that initiate viral RNA transcription. *Cell* **23**:847–858.
 51. **Plotch SJ, Bouloy M, Krug RM.** 1979. Transfer of 5'-terminal cap of globin mRNA to influenza viral complementary RNA during transcription in vitro. *Proceedings of the National Academy of Sciences* **76**:1618–1622.
 52. **Bouloy M, Plotch SJ, Krug RM.** 1978. Globin mRNAs are primers for the transcription of influenza viral RNA in vitro. *Proceedings of the National Academy of Sciences* **75**:4886–4890.
 53. **Braam J, Ulmanen I, Krug RM.** 1983. Molecular model of a eucaryotic

- transcription complex: functions and movements of influenza P proteins during capped RNA-primed transcription. *Cell* **34**:609–618.
54. **Poon LL, Pritlove DC, Fodor E, Brownlee GG.** 1999. Direct evidence that the poly (A) tail of influenza A virus mRNA is synthesized by reiterative copying of a U track in the virion RNA template. *Journal of Virology* **73**:3473–3476.
55. **Brunotte L, Flies J, Bolte H, Reuther P, Vreede F, Schwemmle M.** 2014. The Nuclear Export Protein of H5N1 Influenza A Viruses Recruits Matrix 1 (M1) Protein to the Viral Ribonucleoprotein to Mediate Nuclear Export. *Journal of Biological Chemistry* **289**:20067–20077.
56. **Neumann G, Hughes MT, Kawaoka Y.** 2000. Influenza A virus NS2 protein mediates vRNP nuclear export through NES-independent interaction with hCRM1. *The EMBO Journal* **19**:6751–6758.
57. **Iwatsuki-Horimoto K, Horimoto T, Fujii Y, Kawaoka Y.** 2004. Generation of Influenza A Virus NS2 (NEP) Mutants with an Altered Nuclear Export Signal Sequence. *Journal of Virology* **78**:10149–10155.
58. **Jo S, Kawaguchi A, Takizawa N, Morikawa Y, Momose F, Nagata K.** 2010. Involvement of vesicular trafficking system in membrane targeting of the progeny influenza virus genome. *Microbes Infect.* **12**:1079–1084.
59. **Momose F, Sekimoto T, Ohkura T, Jo S, Kawaguchi A, Nagata K, Morikawa Y.** 2011. Apical Transport of Influenza A Virus Ribonucleoprotein Requires Rab11-positive Recycling Endosome. *PLoS ONE* **6**:e21123.
60. **Amorim MJ, Bruce EA, Read EKC, Foeglein A, Mahen R, Stuart AD, Digard**

- P. 2011. A Rab11- and Microtubule-Dependent Mechanism for Cytoplasmic Transport of Influenza A Virus Viral RNA. *Journal of Virology* **85**:4143–4156.
61. **Avilov SV, Moisy D, Naffakh N, Cusack S.** 2012. Influenza A virus progeny vRNP trafficking in live infected cells studied with the virus-encoded fluorescently tagged PB2 protein. *Vaccine* **30**:7411–7417.
62. **Ali A, Avalos RT, Ponimaskin E, Nayak DP.** 2000. Influenza virus assembly: effect of influenza virus glycoproteins on the membrane association of M1 protein. *Journal of Virology* **74**:8709–8719.
63. **Ohkura T, Momose F, Ichikawa R, Takeuchi K, Morikawa Y.** 2014. Influenza A Virus Hemagglutinin and Neuraminidase Mutually Accelerate Their Apical Targeting through Clustering of Lipid Rafts. *Journal of Virology* **88**:10039–10055.
64. **Scheiffele P, Roth MG, Simons K.** 1997. Interaction of influenza virus haemagglutinin with sphingolipid-cholesterol membrane domains via its transmembrane domain. *The EMBO Journal* **16**:5501–5508.
65. **Gómez-Puertas P, Albo C, Pérez-Pastrana E, Vivo A, Portela A.** 2000. Influenza virus matrix protein is the major driving force in virus budding. *Journal of Virology* **74**:11538–11547.
66. **Roberts KL, Leser GP, Ma C, Lamb RA.** 2013. The Amphipathic Helix of Influenza A Virus M2 Protein Is Required for Filamentous Bud Formation and Scission of Filamentous and Spherical Particles. *Journal of Virology* **87**:9973–9982.
67. **Rossman JS, Jing X, Leser GP, Lamb RA.** 2010. Influenza Virus M2 Protein

- Mediates ESCRT-Independent Membrane Scission. *Cell* **142**:902–913.
68. **Schmidt NW, Mishra A, Wang J, DeGrado WF, Wong GCL.** 2013. Influenza Virus A M2 Protein Generates Negative Gaussian Membrane Curvature Necessary for Budding and Scission. *J. Am. Chem. Soc.* **135**:13710–13719.
69. **Leser GP, Lamb RA.** 2005. Influenza virus assembly and budding in raft-derived microdomains: A quantitative analysis of the surface distribution of HA, NA and M2 proteins. *Virology* **342**:215–227.
70. **Zebedee SL, Richardson CD, Lamb RA.** 1985. Characterization of the influenza virus M2 integral membrane protein and expression at the infected-cell surface from cloned cDNA. *Journal of Virology* **56**:502–511.
71. **Takeda M, Leser GP, Russell CJ, Lamb RA.** 2003. Influenza virus hemagglutinin concentrates in lipid raft microdomains for efficient viral fusion. *Proceedings of the National Academy of Sciences* **100**:14610–14617.
72. **Lamb RA, Krug RM.** 2001. Orthomyxoviridae: the viruses and their replication, pp. 1487–1531. *In* Knipe, DM, Howley, PM, Griffin, DE (eds.), *Fields Virology*, 4 ed. Lippincott Williams & Wilkins, Philadelphia.
73. **Arzt S, Baudin F, Barge A, Timmins P, Burmeister WP, Ruigrok RWH.** 2001. Combined Results from Solution Studies on Intact Influenza Virus M1 Protein and from a New Crystal Form of Its N-Terminal Domain Show That M1 Is an Elongated Monomer. *Virology* **279**:439–446.
74. **Sha B, Luo M.** 1997. Structure of a bifunctional membrane-RNA binding protein, influenza virus matrix protein M1. *Nature Structural & Molecular Biology* **4**:239–244.

75. **Shtykova EV, Baratova LA, Fedorova NV, Radyukhin VA, Ksenofontov AL, Volkov VV, Shishkov AV, Dolgov AA, Shilova LA, Batishchev OV, Jeffries CM, Svergun DI.** 2013. Structural Analysis of Influenza A Virus Matrix Protein M1 and Its Self-Assemblies at Low pH. *PLoS ONE* **8**:e82431.
76. **Shishkov AV, Goldanskii VI, Baratova LA, Fedorova NV, Ksenofontov AL, Zhirnov OP, Galkin AV.** 1999. The in situ spatial arrangement of the influenza A virus matrix protein M1 assessed by tritium bombardment. *Proceedings of the National Academy of Sciences* **96**:7827–7830.
77. **Zhang K, Wang Z, Liu X, Yin C, Basit Z, Xia B, Liu W.** 2012. Dissection of Influenza A Virus M1 Protein: pH-Dependent Oligomerization of N-Terminal Domain and Dimerization of C-Terminal Domain. *PLoS ONE* **7**:e37786.
78. **Harris A, Forouhar F, Qiu S, Sha B, Luo M.** 2001. The Crystal Structure of the Influenza Matrix Protein M1 at Neutral pH: M1–M1 Protein Interfaces Can Rotate in the Oligomeric Structures of M1. *Virology* **289**:34–44.
79. **Calder LJ, Wasilewski JA, Berrimen JA, Rosenthal PB.** 2010. Structural organization of a filamentous influenza A virus. *Proceedings of the National Academy of Sciences* **107**:10685–10690.
80. **Ruigrok RWH, Barge A, Durrer P, Brunner J, Ma K, Whittaker GR.** 2000. Membrane Interaction of Influenza Virus M1 Protein. *Virology* **267**:289–298.
81. **Ye Z, Robinson D, Wagner RR.** 1995. Nucleus-targeting domain of the matrix protein (M1) of influenza virus. *Journal of Virology* **69**:1964–1970.
82. **Watanabe K, Handa H, Mizumoto K, Nagata K.** 1996. Mechanism for

- inhibition of influenza virus RNA polymerase activity by matrix protein. *Journal of Virology* **70**:241–247.
83. **Zvonarjev AY, Ghendon YZ.** 1980. Influence of membrane (M) protein on influenza A virus virion transcriptase activity in vitro and its susceptibility to rimantadine. *Journal of Virology* **33**:583–586.
84. **Ye ZP, Baylor NW, Wagner RR.** 1989. Transcription-inhibition and RNA-binding domains of influenza A virus matrix protein mapped with anti-idiotypic antibodies and synthetic peptides. *Journal of Virology* **63**:3586–3594.
85. **Noton SL, Medcalf E, Fisher D, Mullin AE, Elton D, Digard P.** 2007. Identification of the domains of the influenza A virus M1 matrix protein required for NP binding, oligomerization and incorporation into virions. *Journal of General Virology* **88**:2280–2290.
86. **Akarsu H, Burmeister WP, Petosa C, Petit I, Müller CW, Ruigrok RW, Baudin F.** 2003. Crystal structure of the M1 protein-binding domain of the influenza A virus nuclear export protein (NEP/NS2). *The EMBO Journal* **22**:4646–4655.
87. **Shimizu T, Takizawa N, Watanabe K, Nagata K, Kobayashi N.** 2011. Crucial role of the influenza virus NS2 (NEP) C-terminal domain in M1 binding and nuclear export of vRNP. *FEBS LETTERS* **585**:41–46.
88. **Zhang J, Lamb RA.** 1996. Characterization of the membrane association of the influenza virus matrix protein in living cells. *Virology* **225**:255–266.
89. **Chen BJ, Leser GP, Jackson D, Lamb RA.** 2008. The Influenza Virus M2

- Protein Cytoplasmic Tail Interacts with the M1 Protein and Influences Virus Assembly at the Site of Virus Budding. *Journal of Virology* **82**:10059–10070.
90. **Enami M, Enami K.** 1996. Influenza virus hemagglutinin and neuraminidase glycoproteins stimulate the membrane association of the matrix protein. *Journal of Virology* **70**:6653–6657.
91. **Iwatsuki-Horimoto K, Horimoto T, Noda T, Kiso M, Maeda J, Watanabe S, Muramoto Y, Fujii K, Kawaoka Y.** 2006. The Cytoplasmic Tail of the Influenza A Virus M2 Protein Plays a Role in Viral Assembly. *Journal of Virology* **80**:5233–5240.
92. **McCown MF, Pekosz A.** 2006. Distinct Domains of the Influenza A Virus M2 Protein Cytoplasmic Tail Mediate Binding to the M1 Protein and Facilitate Infectious Virus Production. *Journal of Virology* **80**:8178–8189.
93. **Garcia-Sastre A, Palese P.** 1995. The cytoplasmic tail of the neuraminidase protein of influenza A virus does not play an important role in the packaging of this protein into viral envelopes. *Virus Research* **37**:37–47.
94. **Jin H, Leser GP, Lamb RA.** 1994. The influenza virus hemagglutinin cytoplasmic tail is not essential for virus assembly or infectivity. *The EMBO Journal* **13**:5504–5515.
95. **Jin H, Leser GP, Zhang J, Lamb RA.** 1997. Influenza virus hemagglutinin and neuraminidase cytoplasmic tails control particle shape. *The EMBO Journal* **16**:1236–1247.
96. **Mitnaul LJ, Castrucci MR, Murti KG, Kawaoka Y.** 1996. The cytoplasmic tail of influenza A virus neuraminidase (NA) affects NA incorporation into

- virions, virion morphology, and virulence in mice but is not essential for virus replication. *Journal of Virology* **70**:873–879.
97. **Zhang J, Leser GP, Pekosz A, Lamb RA.** 2000. The Cytoplasmic Tails of the Influenza Virus Spike Glycoproteins Are Required for Normal Genome Packaging. *Virology* **269**:325–334.
98. **Chen BJ, Leser GP, Morita E, Lamb RA.** 2007. Influenza Virus Hemagglutinin and Neuraminidase, but Not the Matrix Protein, Are Required for Assembly and Budding of Plasmid-Derived Virus-Like Particles. *Journal of Virology* **81**:7111–7123.
99. **Bialas KM, Desmet EA, Takimoto T.** 2012. Specific Residues in the 2009 H1N1 Swine-Origin Influenza Matrix Protein Influence Virion Morphology and Efficiency of Viral Spread In Vitro. *PLoS ONE* **7**:e50595.
100. **Latham T, Galarza JM.** 2001. Formation of Wild-Type and Chimeric Influenza Virus-Like Particles following Simultaneous Expression of Only Four Structural Proteins. *Journal of Virology* **75**:6154–6165.
101. **Lai JCC, Chan WWL, Kien F, Nicholls JM, Peiris JSM, Garcia JM.** 2010. Formation of virus-like particles from human cell lines exclusively expressing influenza neuraminidase. *Journal of General Virology* **91**:2322–2330.
102. **Cheung CY, Poon LLM, Lau AS, Luk W, Lau YL, Shortridge KF, Gordon S, Guan Y, Peiris JSM.** 2002. Induction of proinflammatory cytokines in human macrophages by influenza A (H5N1) viruses: a mechanism for the unusual severity of human disease? *The Lancet* **360**:1831–1837.

103. **Chan MC, Chan RWY, Chan L, Mok C, Hui K, Fong J, Tao KP, Poon LLM, Nicholls JM, Guan Y, Peiris JSM.** 2013. Tropism and innate host responses of a novel avian influenza A H7N9 virus: an analysis of ex-vivo and in-vitro cultures of the human respiratory tract. *The Lancet Respiratory Medicine* **1**:534–542.
104. **de Jong MD, Simmons CP, Thanh TT, Hien VM, Smith GJD, Chau TNB, Hoang DM, Van Vinh Chau N, Khanh TH, Dong VC, Qui PT, Van Cam B, Ha DQ, Guan Y, Peiris JSM, Chinh NT, Hien TT, Farrar J.** 2006. Fatal outcome of human influenza A (H5N1) is associated with high viral load and hypercytokinemia. *Nat Med* **12**:1203–1207.
105. **Centers for Disease Control and Prevention (CDC).** 2013. Prevention and control of seasonal influenza with vaccines. Recommendations of the Advisory Committee on Immunization Practices--United States, 2013-2014. *MMWR. Recommendations and reports: Morbidity and mortality weekly report. Recommendations and reports/Centers for Disease Control* **62**:1.
106. **Johnson NPAS, Mueller J.** 2002. Updating the Accounts: Global Mortality of the 1918-1920 "Spanish" Influenza Pandemic. *Bulletin of the History of Medicine* **76**:105–115.
107. **Shope RE.** 1936. THE INCIDENCE OF NEUTRALIZING ANTIBODIES FOR SWINE INFLUENZA VIRUS IN THE SERA OF HUMAN BEINGS OF DIFFERENT AGES. *J. Exp. Med.* **63**:669–684.
108. **Worobey M, Han G-Z, Rambaut A.** 2014. A synchronized global sweep of the internal genes of modern avian influenza virus. *Nature* 1–16.

109. **Doherty PC, Turner SJ, Webby RG, Thomas PG.** 2006. Influenza and the challenge for immunology. *Nat Immunol* **7**:449–455.
110. **Kash JC, Tumpey TM, Proll SC, Carter V, Perwitasari O, Thomas MJ, Basler CF, Palese P, Taubenberger JK, Garcia-Sastre A, Swayne DE, Katze MG.** 2006. Genomic analysis of increased host immune and cell death responses induced by 1918 influenza virus. *Nature*.
111. **Kobasa D, Jones SM, Shinya K, Kash JC, Copps J, Ebihara H, Hatta Y, Hyun Kim J, Halfmann P, Hatta M, Feldmann F, Alimonti JB, Fernando L, Li Y, Katze MG, Feldmann H, Kawaoka Y.** 2007. Aberrant innate immune response in lethal infection of macaques with the 1918 influenza virus. *Nature* **445**:319–323.
112. **Shanks GD, Brundage JF.** 2012. Pathogenic Responses among Young Adults during the 1918 Influenza Pandemic. *Emerg. Infect. Dis.* **18**:201–207.
113. **Morens DM, Fauci AS.** 2007. The 1918 Influenza Pandemic: Insights for the 21st Century. *J INFECT DIS* **195**:1018–1028.
114. **Taubenberger JK, Morens DM.** 2006. 1918 Influenza: the mother of all pandemics. *Emerg. Infect. Dis.* **12**:15–22.
115. **Cox NJ, Subbarao K.** 2000. Global epidemiology of influenza: past and present. *Annu. Rev. Med.* **51**:407–421.
116. **Kawaoka Y, Krauss S, Webster RG.** 1989. Avian-to-human transmission of the PB1 gene of influenza A viruses in the 1957 and 1968 pandemics. *Journal of Virology* **63**:4603–4608.
117. **Scholtissek C, Rohde WV, Hoyningen Von V, Rott R.** 1978. On the origin of

- the human influenza virus subtypes H2N2 and H3N2. *Virology* **87**:13–20.
118. 2009. Emergence of a Novel Swine-Origin Influenza A (H1N1) Virus in Humans. *N Engl J Med* **360**:2605–2615.
119. 2010. CDC Estimates of 2009 H1N1 Cases and Related Hospitalizations and Deaths from April 2009 through April 10, 2010, By Age Group. CDC Report 1–1.
120. **Smith GJD, Vijaykrishna D, Bahl J, Lycett SJ, Worobey M, Pybus OG, Ma SK, Cheung CL, Raghwani J, Bhatt S, Peiris JSM, Guan Y, Rambaut A.** 2009. Origins and evolutionary genomics of the 2009 swine-origin H1N1 influenza A epidemic. *Nature* **459**:1122–1125.
121. **Komadina N, Roque V, Thawatsupha P, Rimando-Magalong J, Waicharoen S, Bomasang E, Sawanpanyalert P, Rivera M, Iannello P, Hurt AC, Barr IG.** 2007. Genetic analysis of two influenza A (H1) swine viruses isolated from humans in Thailand and the Philippines. *Virus Genes* **35**:161–165.
122. **Myers KP, Olsen CW, Gray GC.** 2007. Cases of swine influenza in humans: a review of the literature. *Clinical Infectious Diseases* **44**:1084–1088.
123. **Shinde V, Bridges CB, Uyeki TM, Shu B, Balish A, Xu X, Lindstrom S, Gubareva LV, Deyde V, Garten RJ, Harris M, Gerber S, Vagasky S, Smith F, Pascoe N, Martin K, Dufficy D, Ritger K, Conover C, Quinlisk P, Klimov A, Bresee JS, Finelli L.** 2009. Triple-Reassortant Swine Influenza A (H1) in Humans in the United States, 2005–2009. *N Engl J Med* **360**:2616–2625.
124. **Koen JS.** 1919. A practical method for field diagnosis of swine diseases.

- Journal of the American Veterinary Medical Association **14**:468–470.
125. **J C.** 1919. Influenza including its infection among pigs. National Medical Journal of China **5**:34–44.
126. **M D, CN M, WB N.** 1922. Remarks on hog flu **62**:162–171.
127. **CN M.** 1927. Some observations on “hog flu” and its seasonal prevalence in Iowa. Journal of the American Veterinary Medical Association **71**:368–377.
128. **Shope RE.** 1931. Swine influenza III. Filtration experiments and etiology. J. Exp. Med. **54**:373–385.
129. **Shope RE.** 1934. THE INFECTION OF FERRETS WITH SWINE INFLUENZA VIRUS. J. Exp. Med. **60**:49–61.
130. **BC E.** Swine Influenza, pp. 244–255. *In* AD, L (ed.), Diseases of Swine, 6 ed. Iowa State University Press, Ames.
131. **Gaydos JC, Top FH, Hodder RA, Russell PK.** 2006. Swine influenza a outbreak, Fort Dix, New Jersey, 1976. Emerg. Infect. Dis. **12**:23–28.
132. **Gorman OT, Bean WJ, Kawaoka Y, Donatelli I, Guo YJ, Webster RG.** 1991. Evolution of influenza A virus nucleoprotein genes: implications for the origins of H1N1 human and classical swine viruses. Journal of Virology **65**:3704–3714.
133. **Kanegae Y, Sugita S, Shortridge KF, Yoshioka Y, Nerome K.** 1994. Origin and evolutionary pathways of the H1 hemagglutinin gene of avian, swine and human influenza viruses: cocirculation of two distinct lineages of swine virus. Archives of Virology **134**:17–28.
134. **Sheerar MG, Easterday BC, Hinshaw VS.** 1989. Antigenic conservation of

- H1N1 swine influenza viruses. *J. Gen. Virol.* **70 (Pt 12)**:3297–3303.
135. **Luoh SM, McGregor MW, Hinshaw VS.** 1992. Hemagglutinin mutations related to antigenic variation in H1 swine influenza viruses. *Journal of Virology* **66**:1066–1073.
136. **Noble S, McGregor MS, Wentworth DE, Hinshaw VS.** 1993. Antigenic and genetic conservation of the haemagglutinin in H1N1 swine influenza viruses. *J. Gen. Virol.* **74**:1197–1200.
137. **CW O, MW M, AJ C, B S, B H, VS H.** 1993. Antigenic and genetic analysis of a recently isolated H1N1 swine influenza virus. *American Journal of Veterinary Research* **54**:1630–1636.
138. **Olsen CW, Carey S, Hinshaw L, Karasin AI.** 2000. Virologic and serologic surveillance for human, swine and avian influenza virus infections among pigs in the north-central United States. *Archives of Virology* **145**:1399–1419.
139. **S D, R B, R S, C M, GP M.** 1992. Antigenic variant of swine influenza virus causing proliferative and necrotizing pneumonia in pigs. *Journal of Veterinary Diagnostic Investigation* **4**:380–392.
140. **Karasin AI, West K, Carman S, Olsen CW.** 2004. Characterization of Avian H3N3 and H1N1 Influenza A Viruses Isolated from Pigs in Canada. *J. Clin. Microbiol.* **42**:4349–4354.
141. **Karasin AI, Brown IH, Carman S, Olsen CW.** 2000. Isolation and Characterization of H4N6 Avian Influenza Viruses from Pigs with Pneumonia in Canada. *Journal of Virology* **74**:9322–9327.

142. **Zhou NN, Senne DA, Landgraf JS, Swenson SL, Erickson G, Rossow K, Liu L, Yoon KJ, Krauss S, Webster RG.** 1999. Genetic reassortment of avian, swine, and human influenza A viruses in American pigs. *Journal of Virology* **73**:8851–8856.
143. **Karasin AI, Schutten MM, Cooper LA, Smith CB, Subbarao K, Anderson GA, Carman S, Olsen CW.** 2000. Genetic characterization of H3N2 influenza viruses isolated from pigs in North America, 1977-1999: evidence for wholly human and reassortant virus genotypes. *Virus Research* **68**:71–85.
144. **Webby RJ, Swenson SL, Krauss SL, Gerrish PJ, Goyal SM, Webster RG.** 2000. Evolution of Swine H3N2 Influenza Viruses in the United States. *Journal of Virology* **74**:8243–8251.
145. **Karasin AI, Olsen CW, Anderson GA.** 2000. Genetic characterization of an H1N2 influenza virus isolated from a pig in Indiana. *J. Clin. Microbiol.* **38**:2453–2456.
146. **Karasin AI, Landgraf J, Swenson S, Erickson G, Goyal S, Woodruff M, Scherba G, Anderson G, Olsen CW.** 2002. Genetic Characterization of H1N2 Influenza A Viruses Isolated from Pigs throughout the United States. *J. Clin. Microbiol.* **40**:1073–1079.
147. **Corzo CA, Culhane M, Juleen K, Stigger-Rosser E, Ducatez MF, Webby RJ, Lowe JF.** 2013. Active Surveillance for Influenza A Virus among Swine, Midwestern United States, 2009–2011. *Emerg. Infect. Dis.* **19**:954–960.
148. **Epperson S, Jhung M, Richards S, Quinlisk P, Ball L, Moll M, Boulton R, Haddy L, Biggerstaff M, Brammer L, Trock S, Burns E, Gomez T, Wong**

- KK, Katz J, Lindstrom S, Klimov A, Bresee JS, Jernigan DB, Cox N, Finelli L, for the Influenza A (H3N2)v Virus Investigation Team.** 2013. Human Infections With Influenza A(H3N2) Variant Virus in the United States, 2011-2012. *Clinical Infectious Diseases* **57**:S4–S11.
149. **Biggerstaff M, Reed C, Epperson S, Jhung MA, Gambhir M, Bresee JS, Jernigan DB, Swerdlow DL, Finelli L.** 2013. Estimates of the Number of Human Infections With Influenza A(H3N2) Variant Virus, United States, August 2011-April 2012. *Clinical Infectious Diseases* **57**:S12–S15.
150. **Blanton L, Brammer L, Smith S, Mustaquim D, Steffens C, Abd Elal AI, Gubareva L, Hall H, Wallis T, Villanueva J, Xu X, Bresee J, Cox N, Finelli L.** 2014. Update: influenza activity - United States and worldwide, may 18-september 20, 2014. *MMWR Morb. Mortal. Wkly. Rep.* **63**:861–864.
151. Case Count: Detected U.S. Human Infections with H3N2v by State since August 2011. Centers for Disease Control and Prevention.
152. **KK.** 1933. Die Aetiologie der Ferkelgrippe (enzootische Pneumonie des Ferkels). *Zentralbl Bakt* **129**:161–176.
153. **HG L.** 1938. The problems of the practitioner in connection with the differential diagnosis and treatment of diseases of young pigs. *Veterinary Record* **50**:1377.
154. **F B, AW G.** 1941. Discussion on Swine Influenza in the British Isles. *Proceedings of the Royal Society of Medicine* **34**:611–615.
155. **RE G.** 1941. Discussion on swine influenza in the British Isles. *Proceedings of the Royal Society of Medicine* **34**:615–617.

156. **Neumeier E, Meier-Ewert H, Cox NJ.** 1994. Genetic relatedness between influenza A (H1N1) viruses isolated from humans and pigs. *J. Gen. Virol.* **75 (Pt 8)**:2103–2107.
157. **Neumeier E, Meier-Ewert H.** 1992. Nucleotide sequence analysis of the HA1 coding portion of the haemagglutinin gene of swine H1N1 influenza viruses. *Virus Research* **23**:107–117.
158. **Brown IH, Ludwig S, Olsen CW, Hannoun C, Scholtissek C, Hinshaw VS, Harris PA, McCauley JW, Strong I, Alexander DJ.** 1997. Antigenic and genetic analyses of H1N1 influenza A viruses from European pigs. *J. Gen. Virol.* **78 (Pt 3)**:553–562.
159. **Zell R, Scholtissek C, Ludwig S.** 2013. Genetics, evolution, and the zoonotic capacity of European Swine influenza viruses. *Curr. Top. Microbiol. Immunol.* **370**:29–55.
160. **R H, R H, O C.** 1950. Isolation of influenza virus in Czechoslovakia. *Cas Cesk Vet* **5**:289.
161. **Pensaert M, Ottis K, Vandeputte J, Kaplan MM, Bachmann PA.** 1981. Evidence for the natural transmission of influenza A virus from wild ducts to swine and its potential importance for man. *Bull. World Health Organ.* **59**:75–78.
162. **Scholtissek C, Bürger H, Bachmann PA, Hannoun C.** 1983. Genetic relatedness of hemagglutinins of the H1 subtype of influenza A viruses isolated from swine and birds. *Virology* **129**:521–523.
163. **Krumbholz A, Lange J, Sauerbrei A, Groth M, Platzer M, Kanrai P,**

- Pleschka S, Scholtissek C, Buttner M, Durrwald R, Zell R.** 2014. Origin of the European avian-like swine influenza viruses. *Journal of General Virology* **95**:2372–2376.
164. **Van Reeth K, Brown IH, Dürrwald R, Foni E, Labarque G, Lenihan P, Maldonado J, Markowska-Daniel I, Pensaert M, Pospisil Z, Koch G.** 2008. Seroprevalence of H1N1, H3N2 and H1N2 influenza viruses in pigs in seven European countries in 2002–2003. *Influenza and Other Respiratory Viruses* **2**:99–105.
165. **Schrader C, S uuml ss J.** 2004. Molecular Epidemiology of Porcine H3N2 Influenza A Viruses Isolated in Germany between 1982 and 2001. *Intervirology* **47**:72–77.
166. **Krumbholz A, Philipps A, Oehring H, Schwarzer K, Eitner A, Wutzler P, Zell R.** 2010. Current knowledge on PB1-F2 of influenza A viruses. *Med Microbiol Immunol* **200**:69–75.
167. **Krumbholz A, Schmidtke M, Bergmann S, Motzke S, Bauer K, Stech J, Durrwald R, Wutzler P, Zell R.** 2009. High prevalence of amantadine resistance among circulating European porcine influenza A viruses. *Journal of General Virology* **90**:900–908.
168. **Campitelli L, Donatelli I, Foni E, Castrucci MR, Fabiani C, Kawaoka Y, Krauss S, Webster RG.** 1997. Continued evolution of H1N1 and H3N2 influenza viruses in pigs in Italy. *Virology* **232**:310–318.
169. **Marozin S, Gregory V, Cameron K, Bennett M, Valette M, Aymard M, Foni E, Barigazzi G, Lin Y, Hay A.** 2002. Antigenic and genetic diversity among

- swine influenza A H1N1 and H1N2 viruses in Europe. *J. Gen. Virol.* **83**:735–745.
170. **Simon-Grif  M, Mart n-Valls GE, Vilar MJ, Garc a-Bocanegra I, Mora M, Mart n M, Mateu E, Casal J.** 2011. *Veterinary Microbiology. Vet. Microbiol.* **149**:56–63.
171. **de Jong JC, van Nieuwstadt AP, Kimman TG, Loeffen WL, Bestebroer TM, Bijlsma K, Verweij C, Osterhaus AD, Class EC.** 1999. Antigenic drift in swine influenza H3 haemagglutinins with implications for vaccination policy. *Vaccine* **17**:1321–1328.
172. **Kyriakis CS, Brown IH, Foni E, Kuntz-Simon G, Maldonado J, Madec F, Essen SC, Chiapponi C, Van Reeth K.** 2011. *Virological Surveillance and Preliminary Antigenic Characterization of Influenza Viruses in Pigs in Five European Countries from 2006 to 2008. Zoonoses and Public Health* **58**:93–101.
173. **IH B, P C, PA H, DJ A.** 1995. Disease outbreaks in pigs in Great Britain due to an influenza A virus of H1N2 subtype. *Veterinary Record* **136**:328–329.
174. **Brown IH, Harris PA, McCauley JW, Alexander DJ.** 1998. Multiple genetic reassortment of avian and human influenza A viruses in European pigs, resulting in the emergence of an H1N2 virus of novel genotype. *J. Gen. Virol.* **79 (Pt 12)**:2947–2955.
175. **Zell R, Bergmann S, Krumbholz A, Wutzler P, D rrwald R.** 2008. Ongoing evolution of swine influenza viruses: a novel reassortant. *Archives of Virology* **153**:2085–2092.

176. **Gourreau JM, Kaiser C, Valette M, Douglas AR, Labie J, Aymard M.** 1994. Isolation of two H1N2 influenza viruses from swine in France. *Archives of Virology* **135**:365–382.
177. **Moreno A, Chiapponi C, Boniotti MB, Sozzi E, Foni E, Barbieri I, Zanoni MG, Faccini S, Lelli D, Cordioli P.** 2012. *Veterinary Microbiology. Vet. Microbiol.* **156**:265–276.
178. **Brown IH, Alexander DJ, Chakraverty P, Harris PA, Manvell RJ.** 1994. Isolation of an influenza A virus of unusual subtype (H1N7) from pigs in England, and the subsequent experimental transmission from pig to pig. *Vet. Microbiol.* **39**:125–134.
179. **Itoh Y, Shinya K, Kiso M, Watanabe T, Sakoda Y, Hatta M, Muramoto Y, Tamura D, Sakai-Tagawa Y, Noda T, Sakabe S, Imai M, Hatta Y, Watanabe S, Li C, Yamada S, Fujii K, Murakami S, Imai H, Kakugawa S, Ito M, Takano R, Iwatsuki-Horimoto K, Shimojima M, Horimoto T, Goto H, Takahashi K, Makino A, Ishigaki H, Nakayama M, Okamatsu M, Takahashi K, Warshauer D, Shult PA, Saito R, Suzuki H, Furuta Y, Yamashita M, Mitamura K, Nakano K, Nakamura M, Brockman-Schneider R, Mitamura H, Yamazaki M, Sugaya N, Suresh M, Ozawa M, Neumann G, Gern J, Kida H, Ogasawara K, Kawaoka Y.** 2009. In vitro and in vivo characterization of new swine-origin H1N1 influenza viruses. *Nature* **460**:1021–1025.
180. **CHU CM, DAWSON IM, ELFORD WJ.** 1949. Filamentous forms associated with newly isolated influenza virus. *The Lancet* **1**:602.

181. **Elleman CJ, Barclay WS.** 2004. The M1 matrix protein controls the filamentous phenotype of influenza A virus. *Virology* **321**:144–153.
182. **Seladi-Schulman J, Steel J, Lowen AC.** 2013. Spherical influenza viruses have a fitness advantage in embryonated eggs, while filament-producing strains are selected in vivo. *Journal of Virology* **87**:13343–13353.
183. **Roberts PC, Lamb RA, Compans RW.** 1998. The M1 and M2 proteins of influenza A virus are important determinants in filamentous particle formation. *Virology* **240**:127–137.
184. **Bourmakina SV.** 2003. Reverse genetics studies on the filamentous morphology of influenza A virus. *Journal of General Virology* **84**:517–527.
185. **Burleigh LM, Calder LJ, Skehel JJ, Steinhauer DA.** 2004. Influenza A Viruses with Mutations in the M1 Helix Six Domain Display a Wide Variety of Morphological Phenotypes. *Journal of Virology* **79**:1262–1270.
186. **Rossman JS, Jing X, Leser GP, Balannik V, Pinto LH, Lamb RA.** 2010. Influenza Virus M2 Ion Channel Protein Is Necessary for Filamentous Virion Formation. *Journal of Virology* **84**:5078–5088.
187. **Bialas KM, Bussey KA, Stone RL, Takimoto T.** 2014. Specific Nucleoprotein Residues Affect Influenza Virus Morphology. *Journal of Virology* **88**:2227–2234.
188. **Roberts PC, Compans RW.** 1998. Host cell dependence of viral morphology. *Proceedings of the National Academy of Sciences* **95**:5746–5751.
189. **Griffin JA, Basak S, Compans RW.** 1983. Effects of hexose starvation and the role of sialic acid in influenza virus release. *Virology* **125**:324–334.

190. **Salas PJ, Misek DE, Vega-Salas DE, Gundersen D, Cereijido M, Rodriguez-Boulan E.** 1986. Microtubules and actin filaments are not critically involved in the biogenesis of epithelial cell surface polarity. *The Journal of cell biology* **102**:1853–1867.
191. **Simpson-Holley M, Ellis D, Fisher D, Elton D, McCauley J, Digard P.** 2002. A Functional Link between the Actin Cytoskeleton and Lipid Rafts during Budding of Filamentous Influenza Virions. *Virology* **301**:212–225.
192. **Bruce EA, Digard P, Stuart AD.** 2010. The Rab11 Pathway Is Required for Influenza A Virus Budding and Filament Formation. *Journal of Virology* **84**:5848–5859.
193. **Allerson MW, Cardona CJ, Torremorell M.** 2013. Indirect Transmission of Influenza A Virus between Pig Populations under Two Different Biosecurity Settings. *PLoS ONE* **8**:e67293.
194. **Mubareka S, Lowen AC, Steel J, Coates AL, Garcia-Sastre A, Palese P.** 2009. Transmission of Influenza Virus via Aerosols and Fomites in the Guinea Pig Model. *J INFECT DIS* **199**:858–865.
195. **Gralton J, Tovey ER, McLaws M-L, Rawlinson WD.** 2013. Respiratory virus RNA is detectable in airborne and droplet particles. *J. Med. Virol.* n/a–n/a.
196. **Fabian P, McDevitt JJ, DeHaan WH, Fung ROP, Cowling BJ, Chan KH, Leung GM, Milton DK.** 2008. Influenza Virus in Human Exhaled Breath: An Observational Study. *PLoS ONE* **3**:e2691.
197. **Siegel JD, Rhinehart E, Jackson M, Chiarello L.** 2007. 2007 Guideline for Isolation Precautions: Preventing Transmission of Infectious Agents in

- Health Care Settings. American Journal of Infection Control **35**:S65–S164.
198. **Lowen AC, Steel J, Mubareka S, Palese P.** 2008. High Temperature (30 C) Blocks Aerosol but Not Contact Transmission of Influenza Virus. Journal of Virology **82**:5650–5652.
199. **Lowen AC, Mubareka S, Steel J, Palese P.** 2007. Influenza virus transmission is dependent on relative humidity and temperature. PLoS Pathog **3**:1470–1476.
200. **Lowen AC, Steel J.** 2014. Roles of Humidity and Temperature in Shaping Influenza Seasonality. Journal of Virology **88**:7692–7695.
201. **Glaser L, Stevens J, Zamarin D, Wilson IA, Garcia-Sastre A, Tumpey TM, Basler CF, Taubenberger JK, Palese P.** 2005. A Single Amino Acid Substitution in 1918 Influenza Virus Hemagglutinin Changes Receptor Binding Specificity. Journal of Virology **79**:11533–11536.
202. **Ito T, Couceiro JNS, Kelm S, Baum LG, Krauss S, Castrucci MR, Donatelli I, Kida H, Paulson JC, Webster RG.** 1998. Molecular basis for the generation in pigs of influenza A viruses with pandemic potential. Journal of Virology **72**:7367–7373.
203. **Scholtissek C, Bürger H, Kistner O, Shortridge KF.** 1985. The nucleoprotein as a possible major factor in determining host specificity of influenza H3N2 viruses. Virology **147**:287–294.
204. **Ma W, Kahn RE, Richt JA.** 2008. The pig as a mixing vessel for influenza viruses: Human and veterinary implications. J Mol Genet Med **3**:158–166.
205. **Herfst S, Schrauwen EJA, Linster M, Chutinimitkul S, de Wit E, Munster**

- VJ, Sorrell EM, Bestebroer TM, Burke DF, Smith DJ, Rimmelzwaan GF, Osterhaus ADME, Fouchier RAM.** 2012. Airborne Transmission of Influenza A/H5N1 Virus Between Ferrets. *Science* **336**:1534–1541.
206. **Imai M, Herfst S, Sorrell EM, Schrauwen EJA, Linster M, De Graaf M, Fouchier RAM, Kawaoka Y.** 2013. ARTICLE IN PRESS. *Virus Research* **178**:15–20.
207. **Tumpey TM, Maines TR, Van Hoeven N, Glaser L, Solorzano A, Pappas C, Cox NJ, Swayne DE, Palese P, Katz JM, Garcia-Sastre A.** 2007. A Two-Amino Acid Change in the Hemagglutinin of the 1918 Influenza Virus Abolishes Transmission. *Science* **315**:655–659.
208. **Jayaraman A, Pappas C, Raman R, Belser JA, Viswanathan K, Shriver Z, Tumpey TM, Sasisekharan R.** 2011. A Single Base-Pair Change in 2009 H1N1 Hemagglutinin Increases Human Receptor Affinity and Leads to Efficient Airborne Viral Transmission in Ferrets. *PLoS ONE* **6**:e17616.
209. **Galloway SE, Reed ML, Russell CJ, Steinhauer DA.** 2013. Influenza HA Subtypes Demonstrate Divergent Phenotypes for Cleavage Activation and pH of Fusion: Implications for Host Range and Adaptation. *PLoS Pathog* **9**:e1003151.
210. **Mair CM, Ludwig K, Herrmann A, Sieben C.** 2014. Receptor binding and pH stability - How influenza A virus hemagglutinin affects host-specific virus infection. *Biochimica et Biophysica Acta. BBA - Biomembranes* **1838**:1153–1168.
211. **Zaraket H, Bridges OA, Duan S, Baranovich T, Yoon SW, Reed ML,**

- Salomon R, Webby RJ, Webster RG, Russell CJ.** 2013. Increased Acid Stability of the Hemagglutinin Protein Enhances H5N1 Influenza Virus Growth in the Upper Respiratory Tract but Is Insufficient for Transmission in Ferrets. *Journal of Virology* **87**:9911–9922.
212. **Reed ML, Bridges OA, Seiler P, KIM JK, Yen HL, Salomon R, Govorkova EA, Webster RG, Russell CJ.** 2010. The pH of Activation of the Hemagglutinin Protein Regulates H5N1 Influenza Virus Pathogenicity and Transmissibility in Ducks. *Journal of Virology* **84**:1527–1535.
213. **de Wit E, Kawaoka Y, de Jong MD, Fouchier RAM.** 2008. Pathogenicity of highly pathogenic avian influenza virus in mammals. *Vaccine* **26**:D54–D58.
214. **Gabriel G, Abram M, Keiner B, Wagner R, Klenk HD, Stech J.** 2007. Differential Polymerase Activity in Avian and Mammalian Cells Determines Host Range of Influenza Virus. *Journal of Virology* **81**:9601–9604.
215. **Gabriel G, Dauber B, Wolff T, Planz O, Klenk HD, Stech J.** 2005. The viral polymerase mediates adaptation of an avian influenza virus to a mammalian host. *Proceedings of the National Academy of Sciences* **102**:18590–18595.
216. **Gao Y, Zhang Y, Shinya K, Deng G, Jiang Y, Li Z, Guan Y, Tian G, Li Y, Shi J, Liu L, Zeng X, Bu Z, Xia X, Kawaoka Y, Chen H.** 2009. Identification of Amino Acids in HA and PB2 Critical for the Transmission of H5N1 Avian Influenza Viruses in a Mammalian Host. *PLoS Pathog* **5**:e1000709.
217. **Subbarao EK, London W, Murphy BR.** 1993. A single amino acid in the PB2 gene of influenza A virus is a determinant of host range. *Journal of Virology* **67**:1761–1764.

218. **Li Z, Chen H, Jiao P, Deng G, Tian G, Li Y, Hoffmann E, Webster RG, Matsuoka Y, Yu K.** 2005. Molecular Basis of Replication of Duck H5N1 Influenza Viruses in a Mammalian Mouse Model. *Journal of Virology* **79**:12058–12064.
219. **Gabriel G, Herwig A, Klenk H-D.** 2008. Interaction of Polymerase Subunit PB2 and NP with Importin α 1 Is a Determinant of Host Range of Influenza A Virus. *PLoS Pathog* **4**:e11.
220. **Yen HL, Liang CH, Wu CY, Forrest HL, Ferguson A, Choy KT, Jones J, Wong DDY, Cheung PPH, Hsu CH, Li OT, Yuen KM, Chan RWY, Poon LLM, Chan MCW, Nicholls JM, Krauss S, Wong CH, Guan Y, Webster RG, Webby RJ, Peiris M.** 2011. Hemagglutinin-neuraminidase balance confers respiratory-droplet transmissibility of the pandemic H1N1 influenza virus in ferrets. *Proceedings of the National Academy of Sciences* **108**:14264–14269.
221. **Xu R, Zhu X, McBride R, Nycholat CM, Yu W, Paulson JC, Wilson IA.** 2012. Functional Balance of the Hemagglutinin and Neuraminidase Activities Accompanies the Emergence of the 2009 H1N1 Influenza Pandemic. *Journal of Virology* **86**:9221–9232.
222. **Chou YY, Albrecht RA, Pica N, Lowen AC, Richt JA, Garcia-Sastre A, Palese P, Hai R.** 2011. The M Segment of the 2009 New Pandemic H1N1 Influenza Virus Is Critical for Its High Transmission Efficiency in the Guinea Pig Model. *Journal of Virology* **85**:11235–11241.
223. **Ma W, Liu Q, Bawa B, Qiao C, Qi W, Shen H, Chen Y, Ma J, Li X, Webby RJ, Garcia-Sastre A, Richt JA.** 2012. The neuraminidase and matrix genes of the

- 2009 pandemic influenza H1N1 virus cooperate functionally to facilitate efficient replication and transmissibility in pigs. *Journal of General Virology* **93**:1261–1268.
224. **Lakdawala SS, Lamirande EW, Suguitan AL, Wang W, Santos CP, Vogel L, Matsuoka Y, Lindsley WG, Jin H, Subbarao K.** 2011. Eurasian-Origin Gene Segments Contribute to the Transmissibility, Aerosol Release, and Morphology of the 2009 Pandemic H1N1 Influenza Virus. *PLoS Pathog* **7**:e1002443.
225. **Zitzow LA, Rowe T, Morken T, Shieh WJ, Zaki S, Katz JM.** 2002. Pathogenesis of Avian Influenza A (H5N1) Viruses in Ferrets. *Journal of Virology* **76**:4420–4429.
226. **Herlocher ML, Elias S, Truscon R, Harrison S, Mindell D, Simon C, Monto AS.** 2001. Ferrets as a transmission model for influenza: sequence changes in HA1 of type A (H3N2) virus. *Journal of Infectious Diseases* **184**:542–546.
227. **Barber WH, Small PA.** 1978. Local and systemic immunity to influenza infections in ferrets. *Infect. Immun.* **21**:221–228.
228. **Campbell D, Sweet C, Smith H.** 1979. Comparisons of virulence of influenza virus recombinants in ferrets in relation to their behaviour in man and their genetic constitution. *J. Gen. Virol.* **44**:37–44.
229. **Sweet C, Bird RA, Coates DM, Overton HA, Smith H.** 1985. Recent H1N1 viruses (A/USSR/90/77, A/Fiji/15899/83, A/Firenze/13/83) replicate poorly in ferret bronchial epithelium. Brief report. *Archives of Virology* **85**:305–311.

230. **Coates DM, Sweet C, Smith H.** 1986. Severity of fever in influenza: differential pyrogenicity in ferrets exhibited by H1N1 and H3N2 strains of differing virulence. *J. Gen. Virol.* **67**:419–425.
231. **Jackson S, Van Hoeven N, Chen LM, Maines TR, Cox NJ, Katz JM, Donis RO.** 2009. Reassortment between Avian H5N1 and Human H3N2 Influenza Viruses in Ferrets: a Public Health Risk Assessment. *Journal of Virology* **83**:8131–8140.
232. **Boltz DA, Rehg JE, McClaren J, Webster RG, Govorkova EA.** 2008. Oseltamivir Prophylactic Regimens Prevent H5N1 Influenza Morbidity and Mortality in a Ferret Model. *J INFECT DIS* **197**:1315–1323.
233. **Belser JA, Blixt O, Chen L-M, Pappas C, Maines TR, Van Hoeven N, Donis R, Busch J, McBride R, Paulson JC, Katz JM, Tumpey TM.** 2008. Contemporary North American influenza H7 viruses possess human receptor specificity: Implications for virus transmissibility. *PNAS* **105**:7558–7563.
234. **Wan H, Sorrell EM, Song H, Hossain MJ, Ramirez-Nieto G, Monne I, Stevens J, Cattoli G, Capua I, Chen L-M, Donis RO, Busch J, Paulson JC, Brockwell C, Webby R, Blanco J, Al-Natour MQ, Pérez DR.** 2008. Replication and Transmission of H9N2 Influenza Viruses in Ferrets: Evaluation of Pandemic Potential. *PLoS ONE* **3**:e2923.
235. **Zhu H, Wang D, Kelvin DJ, Li L, Zheng Z, Yoon SW, Wong SS, Farooqui A, Wang J, Banner D, Chen R, Zheng R, Zhou J, Zhang Y, Hong W, Dong W, Cai Q, Roehrl MHA, Huang SSH, Kelvin AA, Yao T, Zhou B, Chen X, Leung**

- GM, Poon LLM, Webster RG, Webby RJ, Peiris JSM, Guan Y, Shu Y.** 2013. Infectivity, Transmission, and Pathology of Human-Isolated H7N9 Influenza Virus in Ferrets and Pigs. *Science* **341**:183–186.
236. **Kim YH, Kim HS, Cho SH, Seo SH.** 2009. Influenza B virus causes milder pathogenesis and weaker inflammatory responses in ferrets than influenza A virus. *Viral Immunology* **22**:423–430.
237. **van Riel D.** 2006. H5N1 Virus Attachment to Lower Respiratory Tract. *Science* **312**:399–399.
238. **van Riel D, Munster VJ, de Wit E, Rimmelzwaan GF, Fouchier RAM, Osterhaus ADME, Kuiken T.** 2010. Human and Avian Influenza Viruses Target Different Cells in the Lower Respiratory Tract of Humans and Other Mammals. *The American Journal of Pathology* **171**:1215–1223.
239. **Van Hoeven N, Belser JA, Szretter KJ, Zeng H, Staeheli P, Swayne DE, Katz JM, Tumpey TM.** 2009. Pathogenesis of 1918 Pandemic and H5N1 Influenza Virus Infections in a Guinea Pig Model: Antiviral Potential of Exogenous Alpha Interferon To Reduce Virus Shedding. *Journal of Virology* **83**:2851–2861.
240. **Gabbard JD, Dlugolenski D, van Riel D, Marshall N, Galloway SE, Howerth EW, Campbell PJ, Jones C, Johnson S, Byrd-Leotis L, Steinhauer DA, Kuiken T, Tompkins SM, Tripp R, Lowen AC, Steel J.** 2014. Novel H7N9 Influenza Virus Shows Low Infectious Dose, High Growth Rate, and Efficient Contact Transmission in the Guinea Pig Model. *Journal of Virology* **88**:1502–1512.

241. **Steel J, Staeheli P, Mubareka S, Garcia-Sastre A, Palese P, Lowen AC.** 2010. Transmission of Pandemic H1N1 Influenza Virus and Impact of Prior Exposure to Seasonal Strains or Interferon Treatment. *Journal of Virology* **84**:21–26.
242. **Tang X, Chong KT.** 2009. Histopathology and growth kinetics of influenza viruses (H1N1 and H3N2) in the upper and lower airways of guinea pigs. *Journal of General Virology* **90**:386–391.
243. **Bouvier NM, Lowen AC, Palese P.** 2008. Oseltamivir-Resistant Influenza A Viruses Are Transmitted Efficiently among Guinea Pigs by Direct Contact but Not by Aerosol. *Journal of Virology* **82**:10052–10058.
244. **Kwon YK, Lipatov AS, Swayne DE.** 2009. Bronchointerstitial Pneumonia in Guinea Pigs Following Inoculation with H5N1 High Pathogenicity Avian Influenza Virus. *Veterinary Pathology* **46**:138–141.
245. **Azoulay-Dupuis E, Lambre CR, Soler P, Moreau J, Thibon M.** 1984. Lung alterations in guinea-pigs infected with influenza virus. *J. Comp. Pathol.* **94**:273–283.
246. **Steel J, Lowen AC, Mubareka S, Palese P.** 2009. Transmission of influenza virus in a mammalian host is increased by PB2 amino acids 627K or 627E/701N. *PLoS Pathog* **5**:e1000252.
247. **CH A, Laidlaw PP, W S.** 1934. The susceptibility of mice to the viruses of human and swine influenza. *The Lancet* **222**:66–68.
248. **Schulman JL, KILBOURNE ED.** 1963. EXPERIMENTAL TRANSMISSION OF INFLUENZA VIRUS INFECTION IN MICE. I. THE PERIOD OF

- TRANSMISSIBILITY. *J. Exp. Med.* **118**:257–266.
249. **Schulman JL, Kilbourne ED.** 1963. EXPERIMENTAL TRANSMISSION OF INFLUENZA VIRUS INFECTION IN MICE. II. SOME FACTORS AFFECTING THE INCIDENCE OF TRANSMITTED INFECTION. *J. Exp. Med.* **118**:267–275.
250. **Schulman JL.** 1968. The use of an animal model to study transmission of influenza virus infection. *Am J Public Health Nations Health* **58**:2092–2096.
251. **Glaser L, Conenello G, Paulson J, Palese P.** 2007. Effective replication of human influenza viruses in mice lacking a major α 2,6 sialyltransferase. *Virus Research* **126**:9–18.
252. **Ibricevic A, Pekosz A, Walter MJ, Newby C, Battaile JT, Brown EG, Holtzman MJ, Brody SL.** 2006. Influenza Virus Receptor Specificity and Cell Tropism in Mouse and Human Airway Epithelial Cells. *Journal of Virology* **80**:7469–7480.
253. **Yang YT, Evans CA.** 1961. Hypothermia in Mice Due to Influenza Virus Infection. *Experimental Biology and Medicine* **108**:776–780.
254. **Belser JA, Wadford DA, Pappas C, Gustin KM, Maines TR, Pearce MB, Zeng H, Swayne DE, Pantin-Jackwood M, Katz JM, Tumpey TM.** 2010. Pathogenesis of Pandemic Influenza A (H1N1) and Triple-Reassortant Swine Influenza A (H1) Viruses in Mice. *Journal of Virology* **84**:4194–4203.
255. **Davies WL, Gunert RR, Haff RF, McGahen JW, Neumayer EM, Paulshock M, Watts JC, Wood TR, Hermann EC, Hoffman CE.** 1964. Antiviral activity of 1-adamantanamine (Amantadine). *Science* **144**:862–863.
256. **Sidwell RW, Huffman JH, Barnard DL, Bailey KW, Wong MH, Morrison A,**

- Syndergaard T, Kim CU.** 1998. Inhibition of influenza virus infections in mice by GS4104, an orally effective influenza virus neuraminidase inhibitor. *ANTIVIRAL RESEARCH* **37**:107–120.
257. **Rabinovich S.** 1972. Rimantadine therapy of influenza A infection in mice. *Antimicrob. Agents Chemother.* **1**:408–411.
258. **Van Kerkhove MD, Hirve S, Koukounari A, Mounts AW, for the H1N1pdm serology working group.** 2013. Estimating age-specific cumulative incidence for the 2009 influenza pandemic: a meta-analysis of A(H1N1)pdm09 serological studies from 19 countries. *Influenza and Other Respiratory Viruses* **7**:872–886.
259. **Campbell PJ, Danzy S, Kyriakis CS, Deymier MJ, Lowen AC, Steel J.** 2014. The m segment of the 2009 pandemic influenza virus confers increased neuraminidase activity, filamentous morphology, and efficient contact transmissibility to a/puerto rico/8/1934-based reassortant viruses. *Journal of Virology* **88**:3802–3814.
260. **Ward AC.** 1995. Specific changes in the M1 protein during adaptation of influenza virus to mouse. *Archives of Virology* **140**:383–389.
261. **Kamal RP, Katz JM, York IA.** 2014. Molecular Determinants of Influenza Virus Pathogenesis in Mice, pp. 243–274. *In Current Topics in Microbiology and Immunology.* Springer International Publishing, Cham.
262. **Vijaykrishna D, Poon LLM, Zhu HC, Ma SK, Li OTW, Cheung CL, Smith GJD, Peiris JSM, Guan Y.** 2010. Reassortment of Pandemic H1N1/2009 Influenza A Virus in Swine. *Science* **328**:1529–1529.

263. **Moreno A, Di Trani L, Faccini S, Vaccari G, Nigrelli D, Boniotti MB, Falcone E, Boni A, Chiapponi C, Sozzi E, Cordioli P.** 2011. Veterinary Microbiology. *Vet. Microbiol.* **149**:472–477.
264. **Starick E, Lange E, Fereidouni S, Bunzenthall C, Hoveler R, Kuczka A, grosse Beilage E, Hamann HP, Klingelhofer I, Steinhauer D, Vahlenkamp T, Beer M, Harder T.** 2011. Reassorted pandemic (H1N1) 2009 influenza A virus discovered from pigs in Germany. *Journal of General Virology* **92**:1184–1188.
265. **Sreta D, Tantawet S, Ayudhya SNN, Thontiravong A, Wongphatcharachai M, Lapkuntod J, Bunpapong N, Tuanudom R, Suradhat S, Vimolket L, Poovorawan Y, Thanawongnuwech R, Amonsin A, Kitikoon P.** 2010. Pandemic (H1N1) 2009 Virus on Commercial Swine Farm, Thailand. *Emerg. Infect. Dis.* **16**:1587–1590.
266. **Howard W.** 2011. Reassortant Pandemic (H1N1) 2009 Virus in Pigs, United Kingdom. *Emerg. Infect. Dis.* **17**:1049–1052.
267. **Ali A, Khatri M, Wang L, Saif YM, Lee C-W.** 2012. Veterinary Microbiology. *Vet. Microbiol.* **158**:60–68.
268. **Liu Q, Ma J, Liu H, Qi W, Anderson J, Henry SC, Hesse RA, Richt JA, Ma W.** 2011. Emergence of novel reassortant H3N2 swine influenza viruses with the 2009 pandemic H1N1 genes in the United States. *Archives of Virology* **157**:555–562.
269. **Bowman AS, Nelson SW, Page SL, Nolting JM, Killian ML, Sreevatsan S, Slemons RD.** 2014. Swine-to-Human Transmission of Influenza A(H3N2)

- Virus at Agricultural Fairs, Ohio, USA, 2012. *Emerg. Infect. Dis.* **20**:1472–1480.
270. **Jhung MA, Epperson S, Biggerstaff M, Allen D, Balish A, Barnes N, Beaudoin A, Berman L, Bidol S, Blanton L, Blythe D, Brammer L, D'Mello T, Danila R, Davis W, de Fijter S, DiOrio M, Durand LO, Emery S, Fowler B, Garten R, Grant Y, Greenbaum A, Gubareva L, Havers F, Haupt T, House J, Ibrahim S, Jiang V, Jain S, Jernigan D, Kazmierczak J, Klimov A, Lindstrom S, Longenberger A, Lucas P, Lynfield R, McMorrow M, Moll M, Morin C, Ostroff S, Page SL, Park SY, Peters S, Quinn C, Reed C, Richards S, Scheftel J, Simwale O, Shu B, Soyemi K, Stauffer J, Steffens C, Su S, Torso L, Uyeki TM, Vetter S, Villanueva J, Wong KK, Shaw M, Bresee JS, Cox N, Finelli L.** 2013. Outbreak of Variant Influenza A(H3N2) Virus in the United States. *Clinical Infectious Diseases* **57**:1703–1712.
271. **Centers for Disease Control and Prevention (CDC.** 2011. Swine-origin influenza A (H3N2) virus infection in two children--Indiana and Pennsylvania, July-August 2011. *MMWR Morb. Mortal. Wkly. Rep.* **60**:1213–1215.
272. **Centers for Disease Control and Prevention (CDC.** 2011. Limited human-to-human transmission of novel influenza A (H3N2) virus--Iowa, November 2011. *MMWR Morb. Mortal. Wkly. Rep.* **60**:1615.
273. **Ma J, Shen H, Liu Q, Bawa B, Qi W, Duff M, Lang Y, Lee J, Yu H, Bai J, Tong G, Hesse RA, Richt JA, Ma W.** 2015. Pathogenicity and Transmissibility of Novel Reassortant H3N2 Influenza Viruses with 2009 Pandemic H1N1 Genes

in Pigs. *Journal of Virology* **89**:2831–2841.

274. **Pearce MB, Jayaraman A, Pappas C, Belser JA, Zeng H, Gustin KM, Maines TR, Sun X, Raman R, Cox NJ.** 2012. Pathogenesis and transmission of swine origin A (H3N2) v influenza viruses in ferrets. *Proceedings of the National Academy of Sciences* **109**:3944–3949.